

The role of SHIP in intestinal tuft cells

by

Ada Yu-Jie Zhang

B.Sc., The University of British Columbia, 2019

A THESIS SUBMITTED IN PARTIAL FULFILLMENT OF
THE REQUIREMENTS FOR THE DEGREE OF

MASTER OF SCIENCE

in

THE FACULTY OF GRADUATE AND POSTDOCTORAL STUDIES
(Experimental Medicine)

THE UNIVERSITY OF BRITISH COLUMBIA
(Vancouver)

July 2021

© Ada Yu-Jie Zhang, 2021

The following individuals certify that they have read, and recommend to the Faculty of Graduate and Postdoctoral Studies for acceptance, a thesis entitled:

The role of SHIP in intestinal tuft cells

submitted by Ada Yu-Jie Zhang in partial fulfillment of the requirements for

the degree of Master of Science

in Experimental Medicine

Examining Committee:

Dr. Laura Sly, Associate Professor, Pediatrics, UBC

Supervisor

Dr. Bruce Vallance, Professor, Pediatrics, UBC

Supervisory Committee Member

Dr. Marc Horwitz, Professor, Microbiology and Immunology, UBC

Additional Examiner

Additional Supervisory Committee Members:

Dr. Pauline Johnson, Professor, Microbiology and Immunology, UBC

Supervisory Committee Member

Abstract

Inflammatory bowel disease (IBD) is characterized by inflammation along the gastrointestinal tract, which may develop from disruptions in mucosal homeostasis. Intestinal epithelial cells are central in maintaining homeostasis by recognizing and responding to extracellular signals. One of these cell types, tuft cells, has been proposed to have a role in secretion, absorption, and/or reception. However, their role in the intestine remains understudied. We found that tuft cells express SH2 domain-containing inositol 5'-phosphatase (SHIP), which is thought to be hematopoietic-specific. SHIP is a negative regulator of the PI3-kinase pathway, so SHIP deficiency increases PI3K-mediated cell growth, proliferation, and activation. Tuft cells secrete IL-25, which activates group 2 innate lymphoid cells (ILC2s), inducing type 2 immune responses that can promote inflammation and tissue repair. Tuft cells also express cyclooxygenase (COX)1 and COX2, which produce prostaglandins that regulate inflammation and repair. I hypothesized that SHIP deficiency in tuft cells increases their activity, promoting inflammation and/or healing via activation of type 2 immunity and prostaglandin synthesis.

We created a mouse deficient in SHIP only in intestinal tuft cells to examine tuft cell functions in DSS-induced colitis, a mouse model of colonic inflammation. I found that mice with SHIP-deficient tuft cells have exacerbated DSS-induced colitis that is accompanied by elevated IL-25 concentrations and reduced COX activity. IL-5 and IL-13 concentrations were not increased, suggesting that these type 2 cytokines did not worsen disease and the tuft cell-ILC2 circuit may not function in the colon. Pro-inflammatory mediators, eosinophils, IL-1 β , IL-6, and TNF- α , did not appear to exacerbate disease. Rather, my results suggest that endogenous IL-25 plays a pro-inflammatory role, whereas COX is protective in DSS-induced colitis. I evaluated the potential protective function of COX during recovery from DSS-induced colitis. I found that

mice with SHIP-deficient tuft cells have increased disease activity early in recovery and may have some histological features that are consistent with increased type 2-mediated healing. Investigating the role of tuft cell-derived IL-25 and COX in DSS-induced colitis and recovery may provide insight into the biological processes that occur in the development of intestinal inflammation that is pertinent to IBD.

Lay Summary

My research aims to characterize the role of a rare cell type in the gut, the tuft cell, in inflammation that is associated with IBD. Tuft cells have important functions in promoting immune responses during challenges and tissue repair after injury. However, their role remains understudied. Tuft cells express a protein called SHIP, which inhibits cell activation. We have created a mouse that lacks SHIP only in intestinal tuft cells. I found that loss of SHIP in tuft cells leads to worsened DSS-induced colitis, a mouse model of human IBD. Disease development may be affected by changes in the amount of tuft cell products in the gut that are induced by loss of SHIP. In future studies, these products can be targeted to treat DSS-induced colitis, which may lead to new therapeutic strategies that are especially important for the subset of people with IBD who have low SHIP activity.

Preface

This work was conducted at the BC Children's Hospital Research Institute as part of the requirements for the Master of Science degree in Experimental Medicine. Animal studies were reviewed and approved by the University of British Columbia according to guidelines provided by the Canadian Council on Animal Care under the protocol numbers A21-0035 and A21-0028.

In Chapter 1, Figures 1.2-1.4 and 1.6 were created in BioRender.com. Figure 1.2 was modified and used with permission from Bischoff SC *et al.* Intestinal permeability--a new target for disease prevention and therapy. BMC Gastroenterology 2014. Figure 1.5 was reproduced from Sauv e JP. COX-expressing tuft cells initiate Crohn's disease-like intestinal inflammation in SHIP^{-/-} mice. University of British Columbia 2019. Figure 1.6 was modified and used with permission from Ting H-A and von Moltke J. The immune function of tuft cells at gut mucosal surfaces and beyond. The Journal of Immunology 2019. Figure 1.7 was modified and used with permission from Dobranowski P and Sly LM. SHIP negatively regulates type 2 immune responses in mast cells and macrophages. Journal of Leukocyte Biology 2018. For Figure 1.8, tissues were stained and imaged by Hayley Brugger. Figures in Chapter 3 were assembled by me.

Susan C. Menzies completed genotyping for mice. I conducted all experimental work described in Chapters 2-5 with the assistance of Hoyoung Jung, who contributed to immunofluorescence staining and imaging, brightfield imaging, and assays of cytokines, COX activity, and cysteinyl leukotrienes. Data from previous work done by Yvonne Pang is included in Figures 3.1B and 3.4. I completed all data analysis described in Chapters 2-5.

Table of Contents

Abstract.....	iii
Lay Summary	v
Preface.....	vi
Table of Contents	vii
List of Tables	x
List of Figures.....	xi
List of Abbreviations	xiv
Acknowledgements	xvii
Dedication	xviii
Chapter 1: Introduction	1
1.1 Inflammatory bowel disease	1
1.1.1 Disease presentation.....	2
1.1.2 Treatment	2
1.1.3 Disease pathogenesis	3
1.2 Intestinal epithelium.....	10
1.2.1 Anatomy of the intestinal epithelium.....	11
1.2.2 Tuft cells	14
1.2.3 Tuft cells and eicosanoids.....	18
1.2.4 Tuft cell-ILC2 circuit.....	19
1.2.5 Tuft cells in disease.....	23
1.3 Mouse models of IBD.....	25

1.4	Src homology 2 domain-containing inositol 5'-phosphatase (SHIP).....	27
1.4.1	Description.....	27
1.4.2	PI3K pathway.....	28
1.4.3	SHIP enzymatic activity	29
1.4.4	SHIP deficiency	30
1.4.5	Tuft cells in SHIP ^{-/-} mice	31
1.4.6	Tuft cell-specific SHIP-deficient mice	32
1.5	Thesis objectives and hypothesis	33
1.5.1	Summary of rationale.....	33
1.5.2	Aims	34
1.5.3	Significance.....	35
Chapter 2: Materials and methods.....		36
2.1	Mice	36
2.2	DSS experiments.....	36
2.3	Hematoxylin and eosin (H&E) and Congo Red staining.....	37
2.4	Histological analyses	38
2.5	Immunofluorescence staining.....	39
2.6	Tissue homogenization and cytokine assays.....	40
2.7	Cysteinyl leukotrienes assay	41
2.8	COX activity assay	41
2.9	Statistical analyses	42
Chapter 3: Results.....		43
3.1	SHIP deficiency in tuft cells exacerbates DSS-induced colitis	43

3.2	SHIP deficiency causes increased IL-25 concentrations during DSS-induced colitis..	53
3.3	SHIP deficiency causes reduced COX activity during DSS-induced colitis	59
3.4	Comparison of SHIP WT and SHIP def mice after 5 days of DSS treatment	63
3.5	Examining a potential role for SHIP deficiency in tuft cells during recovery from DSS-induced colitis	72
Chapter 4: Discussion		83
Chapter 5: Concluding remarks.....		96
5.1	Conclusions.....	96
5.2	Future directions	99
References		102

List of Tables

Table 2.1	Disease scoring criteria	37
Table 2.2	Histological damage scoring	38

List of Figures

Figure 1.1	Pathogenesis of IBD	4
Figure 1.2	Epithelial and immune cells within the intestinal mucosa.....	8
Figure 1.3	Anatomy of the small intestinal epithelium	13
Figure 1.4	Tuft cell structure.....	15
Figure 1.5	Tuft cells are the only intestinal epithelial cells that express SHIP	16
Figure 1.6	Tuft cell activity leads to prostaglandin synthesis and type 2 immune responses....	21
Figure 1.7	SHIP is a negative regulator of the PI3K pathway	30
Figure 1.8	Cre-recombinase efficiency and resulting SHIP deficiency in the colon	33
Figure 3.1	SHIP deficiency in tuft cells exacerbates colon shortening after DSS treatment	44
Figure 3.2	SHIP deficiency in tuft cells exacerbates weight loss during DSS-induced colitis..	46
Figure 3.3	DSS-induced histological damage does not significantly differ across the length of the colon due to SHIP deficiency in tuft cells.....	48
Figure 3.4	SHIP deficiency in tuft cells exacerbates histological damage after DSS treatment	49
Figure 3.5	Eosinophil numbers are similar between DSS-treated SHIP WT and SHIP def mice	52
Figure 3.6	SHIP deficiency in tuft cells leads to higher IL-25 concentrations after DSS treatment	54
Figure 3.7	Colonic IL-5, IL-13, and IL-33 concentrations are not higher in tuft cell-specific SHIP-deficient mice.....	55
Figure 3.8	Type 1 pro-inflammatory cytokine concentrations are not higher due to tuft cell-specific SHIP deficiency after DSS treatment	57

Figure 3.9 Cysteinyl leukotrienes concentrations are not higher due to tuft cell-specific SHIP deficiency	58
Figure 3.10 COX activity is reduced in mice with SHIP-deficient tuft cells after DSS treatment	59
Figure 3.11 SHIP deficiency in tuft cells does not change colonic tuft cell percentage after DSS treatment	61
Figure 3.12 COX activity is lower after DSS treatment when normalized to tuft cell percentage in mice with SHIP-deficient tuft cells.....	62
Figure 3.13 SHIP deficiency in tuft cells causes minimal colon shortening and thickening after 5 days of DSS treatment	64
Figure 3.14 SHIP deficiency in tuft cells does not exacerbate weight loss within 5 days of DSS treatment	64
Figure 3.15 SHIP deficiency in tuft cells does not exacerbate disease activity within 5 days of DSS treatment	65
Figure 3.16 Histological damage after 5 days of DSS treatment does not significantly differ across the length of the colon due to SHIP deficiency in tuft cells	67
Figure 3.17 SHIP deficiency in tuft cells does not exacerbate histological damage after 5 days of DSS treatment	68
Figure 3.18 IL-25 and IL-4 concentrations are not higher in mice with SHIP-deficient tuft cells after 5 days of DSS treatment	69
Figure 3.19 IL-5, IL-13, and IL-33 concentrations are not significantly higher due to SHIP deficiency in tuft cells in mice treated with DSS for 5 days.....	70

Figure 3.20 Type 1 pro-inflammatory cytokines are not higher due to SHIP deficiency in tuft cells after 5 days of DSS treatment.....	71
Figure 3.21 SHIP deficiency in tuft cells does not affect COX activity after 5 days of DSS treatment	72
Figure 3.22 SHIP deficiency in tuft cells does not cause differences in colon length and thickness 5 days of recovery from DSS-induced colitis	73
Figure 3.23 SHIP deficiency in tuft cells does not improve weight gain during recovery from DSS-induced colitis	74
Figure 3.24 SHIP deficiency in tuft cells worsens stool consistency and rectal bleeding during recovery from DSS-induced colitis.....	75
Figure 3.25 SHIP deficiency in tuft cells does not improve histological damage during DSS-induced colitis recovery	77
Figure 3.26 SHIP deficiency in tuft cells may lead to reduced immune cell infiltration and increased muscle thickness after 5 days of recovery from DSS-induced colitis	78
Figure 3.27 IL-25 and IL-4 concentrations are not higher in mice with SHIP-deficient tuft cells after 5 days of recovery from DSS-induced colitis.....	79
Figure 3.28 IL-5, IL-13, and IL-33 concentrations are not higher due to SHIP deficiency after 5 days of recovery from DSS-induced colitis	80
Figure 3.29 Type 1 pro-inflammatory cytokines are not higher due to SHIP deficiency after 5 days of recovery from DSS-induced colitis	81
Figure 3.30 SHIP deficiency does not affect COX activity after 5 days of recovery from DSS-induced colitis	82

List of Abbreviations

AA	Arachidonic acid
AKT	Protein kinase B
ALOX5	Arachidonate 5-Lipoxygenase
ATG16L1	Autophagy related 16-like 1
ATOH1	Atonal homologue 1
BSA	Bovine serum albumin
CCL2	Chemokine ligand 2
CD	Crohn's disease
CD4	Cluster of differentiation 4
CD8	Cluster of differentiation 8
COX	Cyclooxygenase
DAI	Disease activity index
DAPI	4',6-diamidino-2-phenylindole
DC	Dendritic cell
DCLK1	Doublecortin-like kinase 1
DSS	Dextran sodium sulfate
ELISA	Enzyme-linked immunosorbent assay
FITC	Fluorescein isothiocyanate
GALT	Gut-associated lymphoid tissue
GFI1	Growth factor independence 1
GTP	Guanosine triphosphate

GWAS	Genome-wide association studies
HPGDS	Hematopoietic prostaglandin-D synthase
IBD	Inflammatory bowel disease
IEC	Intestinal epithelial cell
IFN	Interferon
Ig	Immunoglobulin
IL	Interleukin
ILC2	Group 2 innate lymphoid cells
IRGM	Immunity-related GTPase family 5 protein
ITLN1	Intelectin-1
LGR5	Leucine Rich Repeat Containing G Protein-Coupled Receptor 5
MUC	Mucin
Neurog3	Neurogenin 3
NF- κ B	Nuclear factor-kappa B
NOD2	Nucleotide-binding oligomerization domain containing 2
NSAID	Nonsteroidal anti-inflammatory drugs
PBS	Phosphate-buffered saline
PCNA	Proliferating cell nuclear antigen
PDK1	Phosphoinositide-dependent kinase-1
PG	Prostaglandin
PG-PS	Peptidoglycan-polysaccharide
PH	Pleckstrin homology

PI3K	Phosphatidylinositol 3-kinase
POU2F3	POU domain class 2, transcription factor 3
PTEN	Phosphatase and tensin homolog protein
PTGS	Prostaglandin-endoperoxide synthase
SHIP	Src 2 homology 2 domain-containing inositol 5'-phosphatase
SNP	Single nucleotide polymorphism
SOX9	SRY-box transcription factor 9
SPDEF	SAM pointed domain-containing ETS transcription factor
SUCNR1	Succinate receptor 1
TA	Transit amplifying
TBS	Tris-buffered saline
TGF	Transforming growth factor
TLR	Toll-like receptor
TNBS	Trinitrobenzene sulfonic acid
TNF	Tumor necrosis factor
TNFAIP3	Tumor necrosis factor alpha-induced protein 3
TNFR1	TNF receptor 1
TRPM5	Transient receptor potential cation channel subfamily M member 5
TSLP	Thymic stromal lymphopietin
TUNEL	Terminal deoxynucleotidyl transferase dUTP nick end labeling
TXA ₂	Thromboxane A
UC	Ulcerative colitis

Acknowledgements

This work was funded by a research grant and Canada Graduate Scholarships Award from the Natural Sciences and Engineering Research Council (NSERC).

I would like to thank my supervisor Dr. Laura Sly for being such an amazing mentor over the past two years. You provided me invaluable support and guidance for my project and future goals while always being understanding and patient. Through your supervision, I have learned how to be an effective researcher and communicator. Your passion for science has made me excited to continue a lifelong career in science myself. I am grateful for all the opportunities you provided me in the lab. I would also like to thank the past and present members of the Sly lab for their help, support, and friendship. This includes Dr. Mahdis Monajemi, Jean Phillippe Sauvé, Yvonne Pang, Kwestan Safari, Matthew Luzentales-Simpson, James Sousa, and Chanel Ghesquiere. I would like to give special thanks to Hoyoung Jung for his help on my experiments and Susan Menzies for her kind support in the lab and personally.

I would also like to thank my committee members, Dr. Pauline Johnson and Dr. Bruce Vallance, who have provided me excellent suggestions throughout my studies and supported my goals. I am also grateful to Dr. Joannie Allaire of the Vallance laboratory and Dr. Bill Rees of the Steiner laboratory at BC Children's Hospital Research Institute for helping me with microscopy and organoid experiments.

To mom and dad,

You made sacrifices for my future, believed in me, and supported my dreams.

You are my role models, who shaped me into the person I am today.

Thank you for your unconditional love,

I love you!

To my sister,

Believe in yourself, have confidence, and push to reach your potential.

I know you will have a bright future and success in anything you decide to pursue.

We love you and will support all your goals!

Chapter 1: Introduction

1.1 Inflammatory bowel disease

Inflammatory bowel disease (IBD) is a group of disorders that are characterized by chronic, relapsing and remitting, or progressive inflammation along the gastrointestinal (GI) tract. People with IBD suffer from intestinal inflammation, leading to symptoms such as weight loss, rectal bleeding, pain, nausea, and diarrhea^{1, 2}. IBD can occur at any age, affecting both sexes equally². The highest incidence is reported in adolescents and people who are 20-30 years of age³. The incidence of IBD in developed and high-income nations, including North American and European countries, grew throughout the 20th century but has stabilized in the 21st century with high burden and prevalence⁴. The incidence of IBD is now rising in newly industrialized countries⁴. There were 6.8 million cases of IBD globally in 2017, with approximately 1.5 million in North America^{4, 5}. Canada has among the highest prevalence of IBD globally with 1 in 140 people affected³. This number is expected to rise to 1 in 100 by the year 2030³. The chronic symptoms of IBD cause long-term morbidity and require lifelong treatment, creating significant economic and disease burden for individuals and society⁴. Park *et al.* (2020) estimated that the annual mean health care cost for people with IBD is over 3-fold higher than for people without IBD, driven by costs for therapeutics, hospitalization, and physician visits⁶. People with IBD also experience indirect costs related to loss of workplace productivity, time taken off work, premature retirement, and long-term disability^{6, 7}. In Canada, the estimated direct costs of IBD were \$1.28 billion (and possibly higher than \$2 billion) in 2018⁸. Indirect costs were estimated to be \$1.29 billion in 2018 and may be significantly greater in reality due to limitations in measuring costs related to presenteeism, reduced achievement, and caregiver burden⁷.

1.1.1 Disease presentation

IBD encompasses ulcerative colitis (UC) and Crohn's disease (CD). Both conditions are associated with intestinal and extraintestinal symptoms⁹. UC describes a condition of continuous inflammation that is limited to the mucosal layer of the colon and rectum⁹. It is often complicated by ulceration and edema, which is swelling due to fluid retention⁹⁻¹¹. Additionally, UC is associated with rectal bleeding, severe abdominal pain, diarrhea, and iron deficiency². Characteristic histological features of UC include acute and chronic immune cell infiltration, cryptitis, crypt abscesses, loss of crypt architecture, distortion of mucosal glands, and goblet cell depletion⁹. CD causes inflammation that can occur anywhere along the digestive tract¹¹. It most commonly affects the ileocecal region and terminal ileum⁹. CD involves discontinuous inflammation, where diseased sections (termed "skip lesions") are frequently separated by normal tissue⁹. Additionally, inflammation in CD is transmural, affecting all layers of the intestine¹¹. CD is often accompanied by fistulas, abnormal channels connecting the intestine to adjacent organs, and fibrosis that can contribute to stricture formation⁹. Histologically, it is associated with immune cell infiltration and granulomas¹². Along with weight loss and delayed growth in children that result from inadequate nutrient absorption in CD, extraintestinal manifestations include fever, arthritis, and bone abnormalities⁹.

1.1.2 Treatment

There is no standard treatment for IBD, but options include non-specific anti-inflammatories: aminosalicylates, corticosteroids and other immunosuppressants, and biological therapies². Direct costs of IBD have shifted from being driven by hospitalization to prescription medication due to the use of expensive biological therapies⁸. The use of anti-tumor necrosis factor (TNF)- α therapy (including infliximab and adalimumab), which blocks TNF- α activity,

has revolutionized IBD treatment by improving response and remission rates in people with IBD¹³. However, efficacy is limited by a lack of primary response, secondary loss of response, and adverse side effects; approximately 30% of people with IBD are primarily unresponsive to anti-TNF antibodies, and up to 10% will lose their response each year^{14, 15}. The wide variation in disease presentation and treatment efficacy may reflect the complexity of IBD and an incomplete understanding of its pathogenesis¹⁶. Thus, new therapeutic approaches are crucial. New biological therapies are gut-specific and have shown to minimize side effects and increase responsiveness¹⁵. These drugs include anti-integrin antibodies such as natalizumab and vedolizumab, which target leukocyte trafficking to the gut to reduce immune cell infiltration and the resulting inflammation¹⁵.

1.1.3 Disease pathogenesis

The etiology of IBD is largely unknown; however, research suggests that it involves genetic susceptibility, environmental influences (including abnormal gut microbiota composition), inappropriate immune activity, and barrier dysfunction (Fig 1.1)¹⁷. It is generally thought that IBD occurs in genetically susceptible people with environmental influences that result in a dysregulated immune response to commensal intestinal microbiota¹.

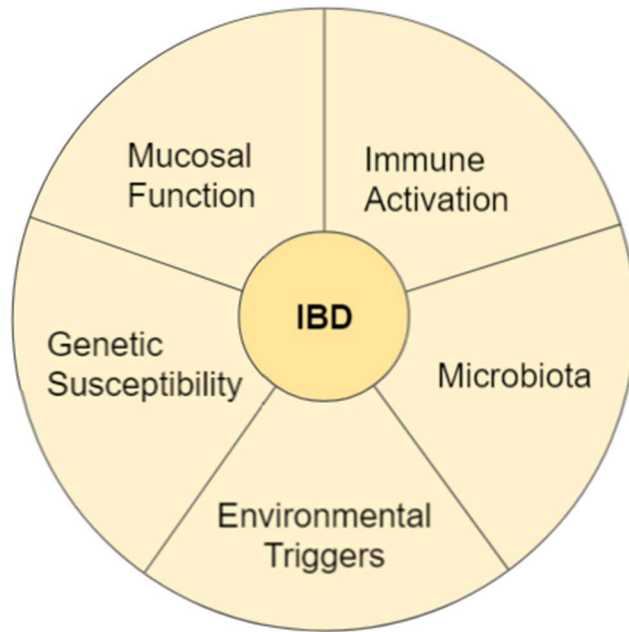


Fig 1.1. Pathogenesis of IBD.

IBD is complex and multifactorial, resulting from genetic susceptibility, environmental changes, abnormal gut microbiota composition, immunological dysregulation, and mucosal barrier dysfunction¹⁷.

Genetic factors

Genetic studies of IBD include family and twin studies that have shown a 26-fold and 9-fold increased risk for developing CD and UC, respectively, when a sibling has the disease¹⁸. Genome-wide association studies (GWAS) in the past few decades have made significant advances in describing the role of genetics in IBD by identifying single nucleotide polymorphisms (SNPs) and genes that may influence disease susceptibility¹⁹. A meta-analysis in 2015 identified 201 loci associated with IBD, which included 41 CD-specific and 30 UC-specific loci^{20, 21}. For example, nucleotide-binding oligomerization domain containing 2 (*NOD2*) was the first gene to be associated with increased susceptibility for CD¹⁹. *NOD2* is a receptor for muramyl dipeptides that activates nuclear factor- κ B (NF- κ B)-driven transcription, thereby regulating innate and subsequent adaptive immune responses²². A *NOD2* loss of function variant

leads to increased production of pro-inflammatory cytokines²³. Additionally, *NOD2*, autophagy related 16-like 1 (*ATG16L1*), and immunity-related GTPase family M protein (*IRGM*) polymorphisms disrupt autophagy^{11, 24}, which leads to increased bacterial persistence and potential intestinal inflammation²⁵. Other genes that have been implicated are the interleukin (IL)-23 receptor (*IL-23R*), *IL-10*, and the IL-10 receptor (*IL-10R*)¹⁹, which encode proteins that regulate inflammation, and intelectin-1 (*ITLN1*) and mucin (*MUC*)^{19, 26}, which are involved in barrier function²⁷. Identifying genes and loci associated with IBD is crucial to understanding the biological processes relevant to intestinal inflammation and thus the development of new therapies²¹. The majority of the loci identified in GWAS are non-coding variations that are implicated in pathogenesis at the gene expression level^{21, 28}. Thus, more recent studies have identified epigenetic markers that can broadly regulate gene expression, including noncoding RNAs and microRNAs²¹. Since the concordance rates of CD and UC in identical twins are approximately 50% and 16%, respectively, other factors such as environmental triggers must be involved in pathogenesis^{19, 28, 29}.

Environmental factors

Environmental factors that influence the incidence of IBD include smoking, hygiene, diet, geography, pollution, and social status³⁰. For example, diets rich in saturated fatty acids and processed meats (termed the “Western diet”) are reported to increase risk for IBD^{21, 31}. This may explain the geographical differences observed in the incidence of IBD. Another factor reported to increase the risk of IBD is the use of medications, especially antibiotics, nonsteroidal anti-inflammatory drugs (NSAIDs), oral contraceptives, and statins^{21, 32, 33}. The major environmental driver of IBD that has been studied extensively is the microbiota, which is also influenced by genetics, immune responses, and the environment^{11, 34, 35}. The GI tract is colonized at birth by

1000-5000 different species of microbes¹¹. The gut microbiota is crucial for intestinal homeostasis; microbial dysbiosis, the imbalance in gut microbial composition, influences intestinal function, health, and disease and has been reported in people with IBD^{11, 21, 36}. The most common changes in microbiota composition that are associated with disease are a decrease in *Firmicutes* and an increase in *Proteobacteria* and *Bacteroidetes*^{21, 37}. *Proteobacteria* adhere to the intestinal epithelium, affecting permeability, altering microbiota composition, and inducing inflammation^{21, 38}. Additionally, commensal microbes in the gut are necessary for the development of the immune system and protect from pathogens via colonization resistance¹¹. The microbiota stimulates immune cells to produce cytokines like the precursor of IL-1 β and IL-22, which are important in pathogen defense³⁹. Studies have also demonstrated that bacterial colonization in the gut is necessary for the development of intestinal inflammation in IBD in several ways; for example, IBD typically occurs in the regions with the highest abundance of microbes, and antibiotics can ameliorate symptoms in some cases of IBD^{34, 40}.

Immunological factors

The intestine comprises the largest compartment of the immune system, which is constantly exposed to antigens and the microbiota⁴¹. The intestinal immune system is composed of organized lymphoid tissue and populations of innate and adaptive effector cells^{11, 41}. Innate immunity includes barrier function of the intestinal mucosa, antibacterial proteins, stomach acidity that limits microbial growth, and innate immune cells and their products^{11, 42}. The mucus layer on the surface of epithelial cells is the first line of defense⁴³. Epithelial cells are the second physical barrier, which coordinate with immune cells to maintain homeostasis⁴³. Immune cells that are present include dendritic cells (DCs), macrophages, and innate lymphoid cells. DCs are

antigen-presenting cells that sample antigen in the luminal contents via microfold (M) cells, extending dendrites through the epithelium, and breaches in the epithelial barrier^{11, 44}. They can activate naïve T cells¹¹ by transporting antigens to gut-associated lymphoid tissue (GALT), which consists of Peyer's patches, mesenteric lymph nodes, and lymphoid follicles⁴⁵.

Macrophages similarly maintain close proximity to the luminal contents, lying just underneath the single-cell epithelial layer, to clear microbes and stimuli that cross the barrier⁴⁶. In addition to DCs and macrophages, GALT contains populations of intraepithelial lymphocytes, B cells, plasma cells, and T cells, which induce an adaptive immune response to microbial infection⁴⁷.

The main hypotheses explaining the role of inappropriate innate immune responses in IBD suggest that there is a reduced response to gut microbes that allows accumulation of commensals and recruitment of inflammatory lymphocytes, or that defects in innate immune cells causes a loss of tolerance to the microbiota, initiating inappropriate inflammation⁴⁸. For example, DCs accumulate in the inflammatory sites of the mucosa in murine models of colitis and people with IBD^{11, 21, 49}. Furthermore, in murine colitis and people with IBD, defects in macrophages lead to an inflammatory phenotype that produces large amounts of pro-inflammatory cytokines²¹. There is elevated production of non-specific pro-inflammatory mediators in the inflammatory sites of people with IBD, including free radicals, leukotrienes, and pro-inflammatory cytokines (e.g. IL-1 β , TNF- α , and the IL-6 family of cytokines: IL-12, IL-23, IL-17, IL-18, and transforming growth factor (TGF)- β)¹¹. Another immune cell involved in IBD is the eosinophil^{50, 51}. Eosinophils have pro-inflammatory and promotility activity, producing mediators that interact with cells of the innate and adaptive immune response^{50, 51}. In IBD, they are associated with an array of effects, including inflammation, tissue damage, tissue repair, and formation of fibrosis and strictures^{51, 52}.

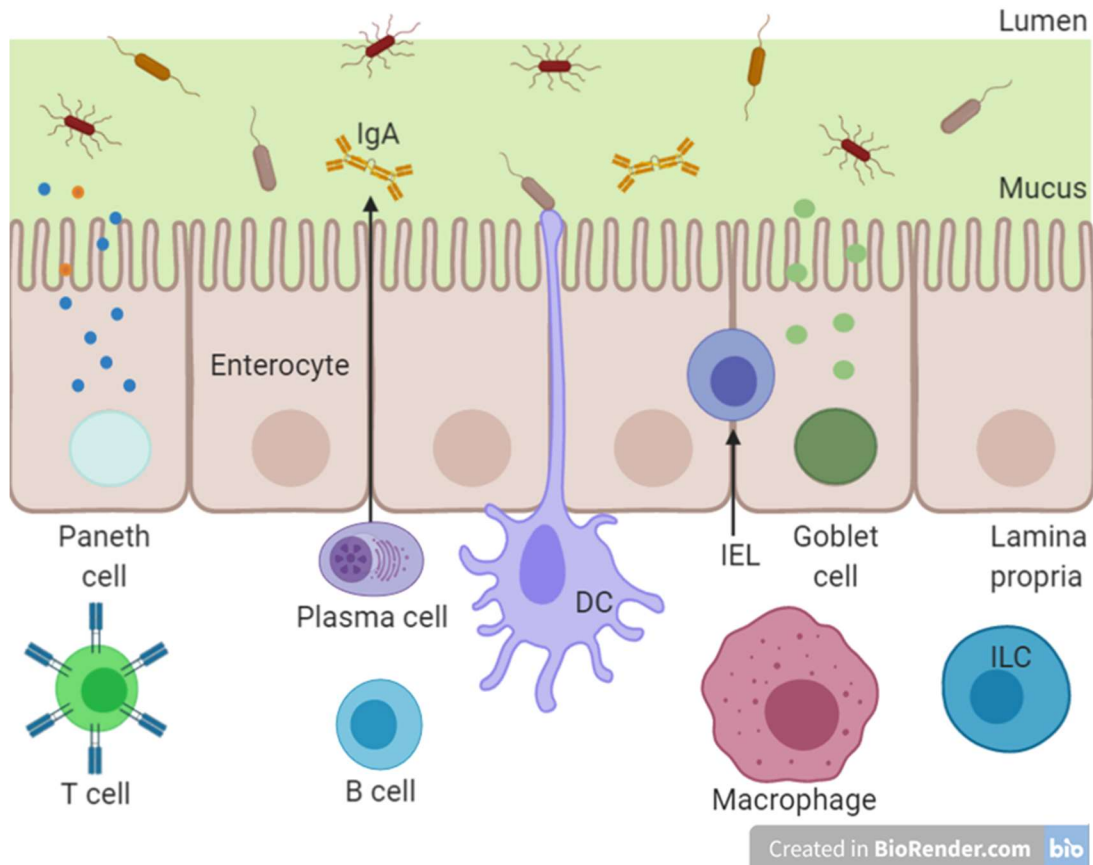


Fig 1.2. Epithelial and immune cells within the intestinal mucosa.

The intestinal epithelium consists of a single layer of cells that separates luminal contents containing gut microbiota from underlying immune cells in the lamina propria. Created in BioRender.com. Modified and used with permission from BioMed Central Ltd: Bischoff *et al.* BMC Gastroenterol. 2014⁵³.

When activated, antigen-presenting cells (e.g. DCs and macrophages) release various signals, including cytokines and chemokines, to induce migration of local and circulating lymphocytes to inflammatory sites²¹. Lymphocytes enter inflamed tissue via the binding of their integrin molecules to cellular adhesion molecules on endothelial cells⁵⁴. An imbalance of signals leads to lymphocyte infiltration into the mucosa, causing excessive T cell responses²¹. Cluster of differentiation 4 (CD4⁺) Th cells have a key role in adaptive immunity, differentiating upon activation into the different Th cell subsets, including Th1, Th2, Th17, and Treg cells¹¹. Naïve

CD4⁺ T cells differentiate into Th1 and Th17 cells with IL-12, IL-18, IL-23, and TGF- β stimulation, producing interferon (IFN)- γ and TNF- α ^{11, 21}. These cells drive the immune response against intracellular viral and bacterial infections^{11, 55}. IL-4 stimulates Th2 cell differentiation, which produces IL-4, IL-5, IL-13, and IL-25⁵⁶. Th2 cells are key players in the immune response against helminth infections^{11, 56}. Finally, Treg cells differentiate under TGF- β stimulation and are crucial for intestinal homeostasis by maintaining immune tolerance and regulating lymphocyte activity; they restrain effector T cells and control the innate inflammatory response^{11, 55, 57}.

The different regions of the intestine have distinct immunological components⁴¹. The small intestinal immune system primarily involves IL-17 and IL-22-producing T cells and innate lymphoid cells, antimicrobial peptide production by Paneth cells, intraepithelial lymphocytes, and regulatory T cells⁴¹. The colon is a reservoir for large numbers of commensal microbes; thus, the colonic immune system must monitor the microbiota without expelling them, which involves production of a thick mucus layer, immunoglobulin A (IgA) production, and regulatory T cells⁴¹. Furthermore, it is thought that the T cell subsets involved in UC and CD are different. CD involves an excessive Th1 and Th17 response that is mediated by IL-12, IFN- γ , and TNF, while UC involves a Th2 response that is mediated by IL-4, IL-5, IL-10, and IL-13^{21, 58, 59}. However, there is increasing evidence suggesting that UC is a Th2 atypical response due to low IL-4 concentrations in tissue from people with UC and UC-specific Th cells^{21, 60, 61}. Furthermore, UC is also associated with a Th1 and Th17 immune response^{62, 63}. Additionally, while CD is thought to be Th1-mediated, one of its major complications, fibrosis, is also mediated by some type 2 cytokines (i.e. IL-13 and IL-33)⁶⁴. In summary, immunological dysregulation in IBD is characterized by epithelial barrier damage; excessive inflammation that is driven by commensal

microbes and infiltration of T cells, B cells, DCs, macrophages, neutrophils, mast cells, and eosinophils; and a failure to regulate the inflammatory response^{11, 42, 65}.

Intestinal mucosal barrier dysfunctions

Dysfunctions of the intestinal barrier, including abnormal permeability, downregulation of proteins forming the tight junctions of the barrier, and epithelial regeneration defects have been reported in in people with IBD^{21, 66-70}. Functional defects in specialized intestinal epithelial cells (IECs) such as Paneth cells and goblet cells, which produce the protective mucus layer of the mucosa, have been shown to cause colitis in mice^{21, 71, 72}. Pro-inflammatory cytokines, including TNF- α and IFN- γ , are secreted during intestinal inflammation in response to microbiota and can increase epithelial permeability, further exacerbating inflammation^{11, 73}.

1.2 Intestinal epithelium

Homeostasis in the intestine is preserved by interactions of the intestinal mucosa, which includes epithelial cells, immune cells, and the microbiota. Their balanced interactions prevent mounting of inappropriate immune responses to the microbiota that would otherwise cause intestinal inflammation²¹. Intestinal mucosal barrier dysfunction allows gut microbes to invade the mucosa, causing inappropriate inflammation⁴⁷.

The intestinal epithelium consists of a 400 mm² single layer of epithelial cells that forms a barrier with several functions: absorption of nutrients, sampling of intestinal contents, and regulation of immune responses^{11, 57}. It physically separates the lumen, containing the microbiota, from the lamina propria, containing immune cells. Tight junctions between epithelial cells allow the epithelium to act as a selective barrier¹¹. IECs produce mucins and anti-microbial defensins to prevent pathogen entry³⁹. In addition to creating a mucosal barrier that physically separates gut microbiota from immune cells, epithelial cells also modulate immune responses by

delivering antigens and secreting immunological mediators. IECs express toll-like receptors (TLRs), which are innate immune receptors that recognize microbial structures³⁹. IECs can also respond to and produce chemokines and cytokines to recruit immune cells^{39, 47}.

1.2.1 Anatomy of the intestinal epithelium

The epithelium of the small intestine is organized into large numbers of self-renewing crypt-villus units (Fig 1.3). Villi are finger-like protrusions of the gut wall that project into the lumen to maximize absorptive surface area. The small intestine consists of three sections: duodenum, jejunum, and ileum⁷⁴. The duodenum is the shortest segment, connecting to the stomach. The jejunum is the middle segment, containing circular folds and villi. The third segment of the small intestine is the ileum, which contains villi but no circular folds. At the base of the villi are crypts that invaginate into the underlying mesenchyme and house proliferating epithelial cells that carry out self-renewal of the epithelium⁷⁵. IECs are replaced every 4-5 days by intestinal stem cells, which are multipotent stem cells that continuously divide, migrating upwards and differentiating into the specialized cells of the epithelium⁷⁴. Cells are eventually shed at the villus tip by apoptosis (anoikis)⁷⁴. Adjacent to intestinal stem cells are Paneth cells, which are long-lived cells that migrate downwards after differentiation^{74, 76}. Paneth cells secrete antimicrobial peptides and proteins into the mucus layer, maintaining the intestinal stem cell niche and homeostatic balance with microbiota^{21, 72}. Defects in *NOD2* and *ATG16L1* impair Paneth cell autophagy and α -defensins production, disrupting anti-microbial activity^{21, 77}. These variants are associated with increased risk for CD^{21, 72}. The mucosa of the colon does not contain villi or Paneth cells⁴⁷. Enterocytes are simple columnar epithelial cells that are the major cell type of the intestinal epithelium, lining the inner surface of the small and large intestines⁷⁴. They absorb nutrients from the lumen and secrete immunoglobulins (e.g. IgA)⁷⁴. Enteroendocrine

cells, which exist as single cells spread throughout the intestinal tract, secrete hormones and peptides into the bloodstream in response to metabolites from the microbiota to coordinate the intestinal innate immune response⁷⁴. Moreover, goblet cells are found throughout the intestinal tract secreting mucins to maintain the mucus layer covering the epithelium, which is crucial for mucosal defense and repair^{21, 78}. Goblet cell numbers are higher in the large intestine, which contains significantly greater numbers of microbes, compared to the small intestine⁴⁷. This results in the formation of a thick mucus layer⁴⁷. In contrast, the mucus layer of the small intestine consists of abundant chemical barriers, including anti-microbial peptides secreted by Paneth cells⁴⁷. Deletion of the goblet cell-derived MUC2 causes spontaneous murine colitis^{21, 71}. Thus, goblet cells are protective against colitis development⁴⁷. An additional specialized epithelial cell type exists in Peyer's patches - villous M cells that deliver antigen for sampling by immune cells^{47, 76}. Finally, tuft cells are a rare chemosensory epithelial cell type that are located throughout the intestinal tract⁵⁶. Tuft cells are the focus of this thesis and will be described in detail.

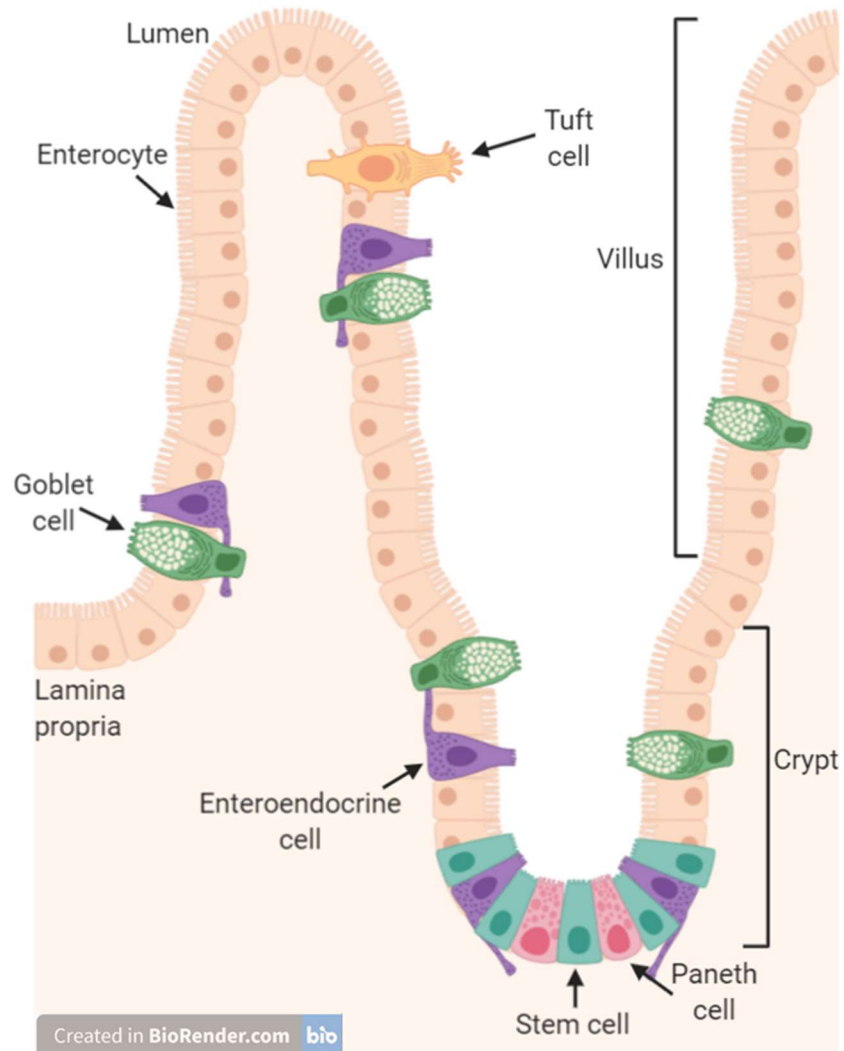


Fig 1.3. Anatomy of the small intestinal epithelium.

The intestinal epithelium of the small intestine is organized into crypt-villus units. The IEC population consists of specialized cell types including enterocytes, goblet cells, enteroendocrine cells, Paneth cells, and tuft cells that differentiate from intestinal stem cells⁷⁹. Created in BioRender.com.

1.2.2 Tuft cells

Tuft cells (also known as brush cells in the airways, or caveolated, multivesicular, and fibrillovesicular cells) were identified in 1955 as a rare type of IEC based on their distinctive morphology⁸⁰. They range from pear to barrel-shaped and extend from the basal lamina to the intestinal lumen⁸¹. Their most prominent features include apical vesicles and a bundle of microfilaments connected to a tuft of microvilli that extend 1.2 μm in length from their apical surface to form a tubulovesicular system (Fig 1.4)^{79, 81, 82}. Tuft cells are primarily found in endodermal derived epithelium in the hollow organs of the respiratory and GI tract⁸³. In the lungs, they are thought to promote protective respiratory reflexes and neurogenic inflammation of the mucosa⁸⁴. In the GI tract, tuft cells are found in the stomach, throughout the small and large intestine, and in the pancreato-biliary system⁸⁵. They make up 0.4 – 2 % of the IEC population under homeostatic conditions^{56, 80, 86}. Based on their morphology, distribution, gene expression, and histochemical and cytochemical analyses, their proposed functions include apocrine secretion, absorption, and reception⁸⁵. Tuft cells have recently emerged as key players in the intestine that regulate immune responses to injury and pathogens such as helminths, promoting inflammation and epithelial repair⁸⁵. However, their role in the intestine is not well-studied.

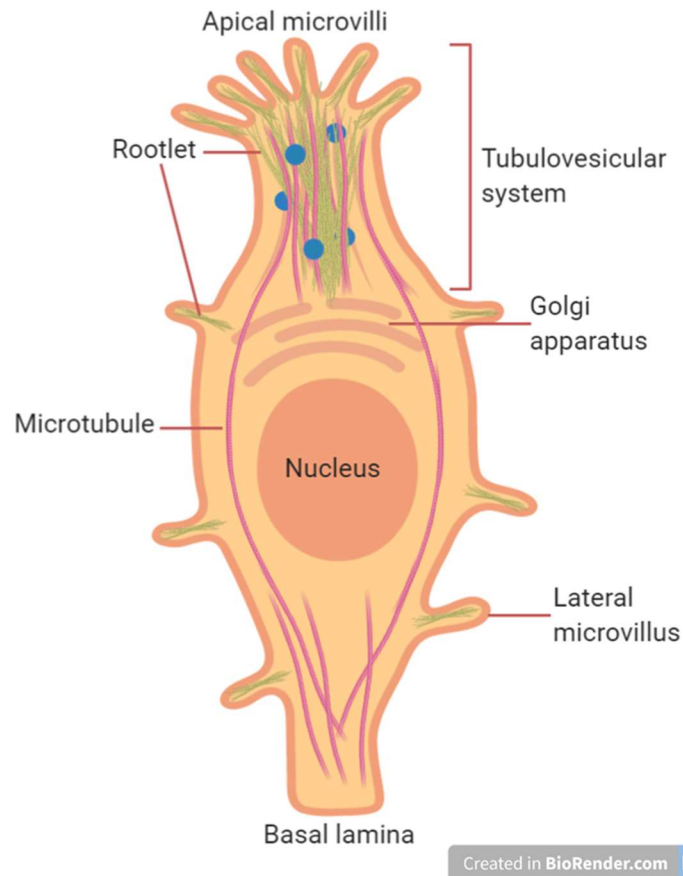


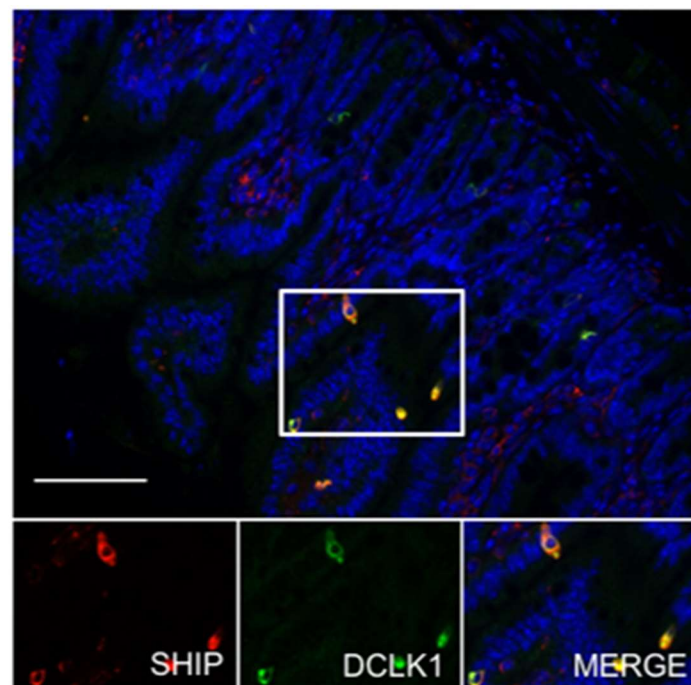
Fig 1.4. Tuft cell structure.

Tuft cells have a distinct pear or barrel shape with a bulge around the nucleus. They extend from the basal lamina with long microvilli that protrude into the lumen and associate with rootlets to form the tubulovesicular system⁷⁵. Created in BioRender.com.

Markers for tuft cells include doublecortin-like kinase 1 (*DCLK1*) and POU domain class 2, transcription factor 3 (*POU2F3*)^{80, 85}. *DCLK1* was initially proposed as a marker of quiescent intestinal stem cells, but it was later determined that *DCLK1*⁺ cells in the small intestine and colon are mostly long-lived, post-mitotic tuft cells that can regulate the stem cell niche and are critical for intestinal homeostasis⁸⁷. The combination of cytokeratin 18 filaments, neurofilaments, actin filaments, acetylated tubulin, and *DCLK1* is restricted to tuft cells⁷⁵. *POU2F3* is required for the development of taste receptor cells; *POU2F3* knockout mice cannot develop tuft cells and display metabolic defects such as lower weight and energy^{80, 88}. Using

DCLK1 as a tuft cell marker (Fig 1.5), our research team previously found that tuft cells are the only intestinal epithelial cells that express the Src homology 2 domain-containing inositol 5'-phosphatase (SHIP), which was thought to be hematopoietic-specific^{89,90}. SHIP is one of foci of this work and will be described further in Section 1.4.

The appearance of tuft cells is late in embryonic development, but the exact timing of their differentiation in the gut is unknown⁷⁵. In humans, tuft cells have been identified morphologically in the small intestine of a 5-month old fetus^{75,91}. In mice, DCLK1 expression is first detected in intestinal tuft cells 1 week after birth^{75,92}. However, tuft cell numbers remain very low, reaching a stable density that is similar in the small intestine and colon after weaning at around 3-4 weeks of age^{79,83,93}.



Scale bars = 100 μ m

Fig 1.5. Tuft cells are the only intestinal epithelial cells that express SHIP.

Ileal cross-section from a wild-type mouse that was co-stained for SHIP (red) and DCLK1 (green). SHIP is localized in DCLK1⁺ (tuft) cells. Reproduced with permission from Sauv e (2019)⁹⁰.

Tuft cells were proposed to be secretory in function after the discovery that the transcription factor atonal homologue 1 (*ATOH1*), which is required for development of secretory cells in the gut, is necessary for their differentiation^{92, 94}. Their differentiation is distinct from that of other IECs, in that it does not require neurogenin 3 (*Neurog3*), SRY-box transcription factor 9 (*SOX9*), or growth factor independence 1 (*GFI1*) and SAM pointed domain-containing ETS transcription factor (*SPDEF*), which promote the differentiation of enteroendocrine, Paneth, and goblet cells, respectively⁹². A hallmark of tuft cells is their expression of taste receptors and related proteins, including the G protein α -gustducin, which relays signals from taste receptors, and transient receptor potential cation channel subfamily M member 5 (TRPM5), which transduces signals from sweet, bitter, and umami stimuli⁸⁰. The expression of these proteins suggests that tuft cells have a role in chemo-sensing. Furthermore, tuft cells may have a more specialized function in sensing helminths and protists, as they have selective expression of other G protein-coupled receptors such as the succinate receptor 1 (*SUCRNI*)⁷⁹. Additionally, the presence of microvesicles within the tubulovesicular system and granules in the cytoplasm suggest a role in apocrine secretion⁷⁵. Another function of tuft cells is promoting IEC proliferation and enhancing epithelial barrier integrity^{80, 87}. Depleting DCLK1⁺ IECs in mice reduces the number of replicating cells in the colon^{80, 87}. The mechanism of how tuft cells regulate cell division is unknown, but DCLK1 expression downregulates microRNAs associated with tumor suppression and decreased cell proliferation in pancreatic cancer^{80, 95}. Furthermore, they have been described as a reserve stem cell population with the ability to reconstitute entire intestinal crypts^{80, 87}.

1.2.3 Tuft cells and eicosanoids

Tuft cells express markers of the eicosanoid biosynthesis pathway. In all tissues, tuft cells express arachidonate 5-lipoxygenase (ALOX5), ALOX5 activating protein, and leukotriene C4 synthase, which are required for leukotriene synthesis⁸⁵. Furthermore, under normal conditions, tuft cells constitutively express all enzymes required for prostaglandin-D₂ (PGD₂) synthesis, including hematopoietic prostaglandin-D synthase (HPGDS) and prostaglandin-endoperoxide synthases (PTGS)/cyclooxygenases (COX) 1 and 2^{75, 92}. The regulation of eicosanoid biosynthesis in tuft cells and the physiologic function of tuft cell-derived eicosanoids are unclear⁷⁹. While their ability to produce cysteinyl leukotrienes and prostaglandins is understudied, they have been reported to respond to eicosanoids⁸⁵. For example, elevated PGE₂ levels are associated with decreased tuft cell frequency in the colon^{85, 96}. Additionally, in the airways, tracheal tuft cell expansion and type 2 inflammation are reported in response to leukotriene E₄, which is dependent on IL-25 and the leukotriene E₄ receptor^{84, 85, 97}.

Tuft cells are the only epithelial cells in the uninflamed intestine that express the opioid β -endorphin, COX1, and COX2⁹². Opioids are critical in homeostatic gut function, regulating gastric emptying, gut motility, intestinal secretion, and pain⁹⁸. COX1 and COX2 are the rate limiting enzymes in the synthesis of prostaglandins that play a role in epithelial barrier integrity, intestinal tissue repair, and inflammation^{99, 100}. COX metabolizes arachidonic acid that is released from the plasma membrane into PGH₂¹⁰¹. PGH₂ is the common substrate for enzymes that produce prostanoids, a subclass of eicosanoids comprising of PGE₂, PGD₂, PGI₂, and thromboxane A₂ (TXA₂)¹⁰¹. PGE₂ is one of the most abundant prostaglandins produced and has a wide range of biological effects¹⁰². It is well-established as an inflammatory mediator but also has immunosuppressive functions that contribute to the resolution of inflammation and return to

homeostasis through tissue regeneration^{101, 102}. The physiological activity of PGE₂ and other prostanoids is mediated by downstream signaling of G-protein coupled receptors that are selective for individual substrates¹⁰². For example, PGE₂ binds members of the EP family of receptors, which exists in four isoforms (EP1-4) and activates processes such as cell proliferation, apoptosis, angiogenesis, inflammation, and immune surveillance¹⁰².

The relative contributions of COX1 and COX2 to the biologic activities of prostaglandins in the GI mucosa are unclear¹⁰³. It is thought that COX1 is responsible for basal production of prostaglandins under normal conditions, while COX2 expression is induced during inflammation¹⁰³. In mice, COX1 plays a protective role against small intestinal and mucosal injury through prostaglandin synthesis that promotes epithelial regeneration¹⁰³. COX2 gene and protein expression is stimulated by pro-inflammatory cytokines, including IL-1 β ¹⁰⁴ and TNF- α ¹⁰⁵. Thus, inducible COX2 may drive pro-inflammatory actions of prostaglandins during mucosal injury, whereas COX1 may synthesize cytoprotective prostaglandins^{103, 106}. However, COX1 is also reported to be induced in intestinal epithelial cells during inflammation¹⁰⁷. Furthermore, these observations suggest that the anti-inflammatory and harmful actions of NSAIDs, which target COX activity, may be due to inhibition of COX2 and COX1, respectively¹⁰³. Yet, selective COX2 inhibitors have been shown to be harmful in mice with preexisting intestinal inflammation, suggesting that COX2 may also have protective functions in the GI mucosa^{103, 108}. Thus, further characterization of COX activity is necessary.

1.2.4 Tuft cell-ILC2 circuit

Intestinal tuft cells express the G-protein coupled receptor SUCNR1, which detects succinate, a metabolite produced by bacteria and helminths⁸⁵. Succinate accumulation is also associated with IBD; for example, fecal succinate concentrations are 3 to 4-fold higher in people

with IBD compared to healthy individuals¹⁰⁹. Similarly, succinate levels are increased in inflammatory lesions compared to healthy tissue¹⁰⁹. Moreover, mouse models of colitis cause an increase in fecal succinate that corresponds with disease severity¹⁰⁹. Tuft cells can be activated by sensing succinate in the lumen via their SUCNR1, implicating them in helminth infections and IBD^{79, 110}. They induce type 2 immune responses by producing IL-25 (also known as IL-17E), which activates group 2 innate lymphoid cells (ILC2s) via the IL-17 receptor (composed of IL-17RA and IL-17RB)⁸⁵. ILC2s produce IL-5 and IL-13, which recruit eosinophils and promote inflammation and post-injury adaptive remodeling and repair⁸⁵. Type 2 cytokines promote tissue repair and fibrosis directly and by targeting cells including macrophages, fibroblasts, epithelial cells, and endothelial cells¹¹¹. For example, IL-13 induces tissue fibrosis via activation of TGF- β ¹¹². Moreover, IL-13 increases the expression of angiogenin-4, which is an antimicrobial peptide secreted by Paneth and goblet cells that inhibits the growth of certain bacterial species such as *Listeria monocytogenes* and *Enterococcus faecalis*^{80, 113, 114}. Thus, tuft cells may have the ability to influence the composition of the microbiota⁸⁰. IL-13 induces tuft and goblet cell lineage amplification by acting on intestinal stem cells, which are leucine rich repeat containing G protein-coupled receptor 5 (LGR5⁺) cells in the crypt niche⁷⁹. ILC2s also produce IL-4, which similarly promotes tuft cell lineage amplification, leading to tuft cell hyperplasia⁷⁹. This creates a feedforward loop referred to as the tuft cell-ILC2 circuit (Fig 1.6), which can be activated exogenously with recombinant IL-13 (rIL-13) or by stimulating ILC2s with rIL-25⁸⁵.

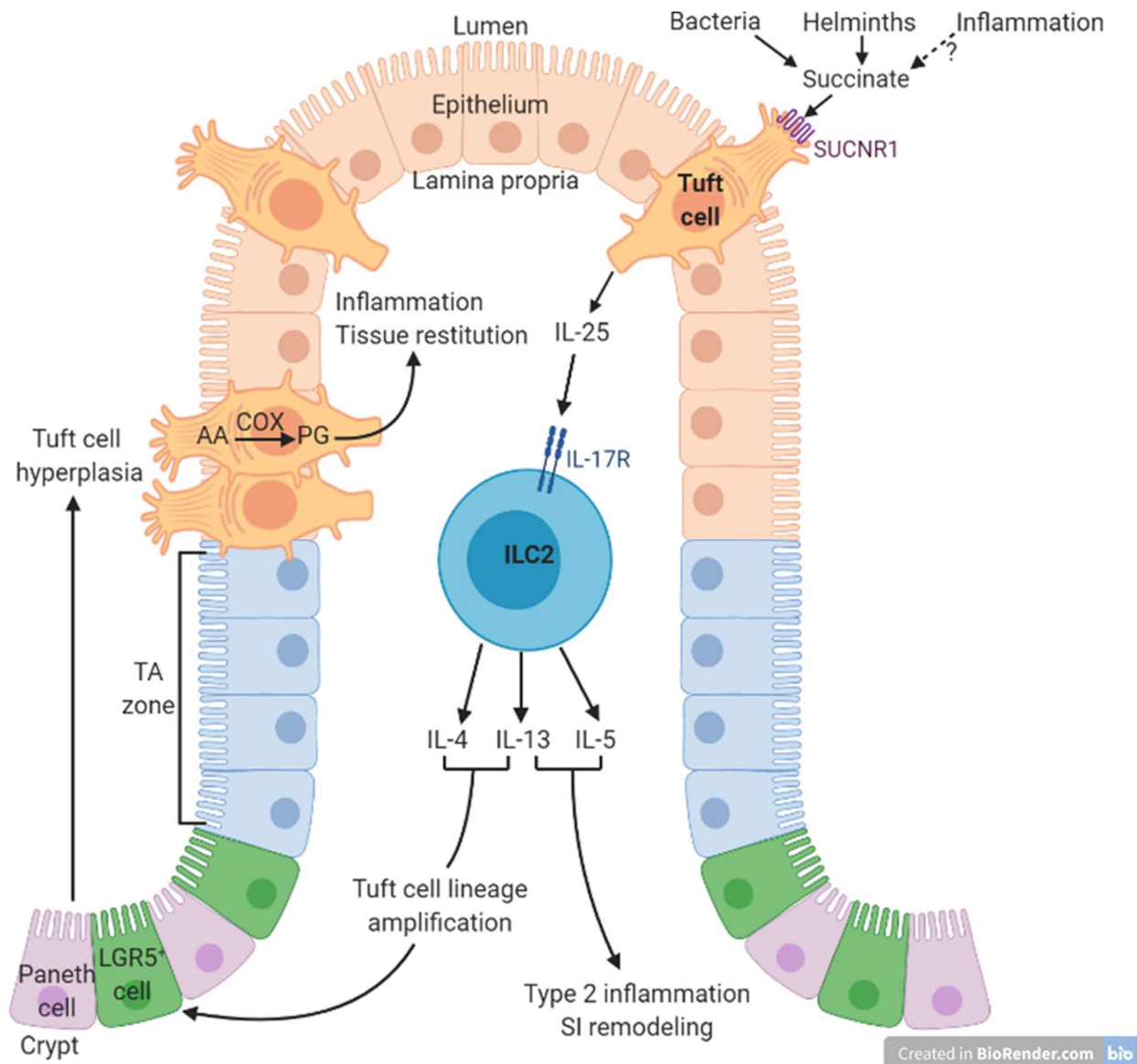


Fig 1.6. Tuft cell activity leads to prostaglandin synthesis and type 2 immune responses^{79, 85}. Succinate is produced by bacteria and helminths in the intestinal lumen. Higher levels of succinate are also associated with inflammation. Tuft cells detect succinate via SUCNR1 and produce IL-25, which activates ILC2s via the IL-17 receptor, leading to IL-4, IL-5, and IL-13 production. IL-5 and IL-13 promote type 2 inflammation and intestine remodeling. In intestinal crypts, LGR5⁺ cells are multipotent stem cells that continuously divide to carry out self-renewal of the epithelium. Cells migrate upward into the transit amplifying (TA) zone, a population of cells that divide multiple times before undergoing terminal differentiation into mature epithelial cells, including tuft cells. IL-4 and IL-13 promote tuft cell lineage amplification, leading to tuft cell hyperplasia. Tuft cells also express COX1 and COX2, which convert arachidonic acid (AA) to prostaglandins (PG). Prostaglandins regulate inflammation and intestinal repair. Modified and used with permission from The American Association of Immunologists, Inc: Ting and von Moltke. *J. Immunol.* 2019⁷⁹.

New molecules that are involved in the tuft cell-ILC2 circuit continue to be discovered. ILC2s are responsive to signals produced in the local environment, so context-specific regulation of tuft cell-ILC2 circuits may exist in the intestine¹¹⁵. Thus, molecules in addition to IL-25 may be required to activate ILC2s¹¹⁵. Type 2-promoting factors include thymic stromal lymphopoietin (TSLP) and IL-33¹¹⁶. IL-33 is in the IL-1 family of cytokines and localizes to IECs to produce two functions in response to epithelial injury: acting as an alarmin that alerts immune cells and triggering wound healing in the mucosa¹¹⁶. The pro-inflammatory role of IL-33 has been demonstrated in murine colitis models, where neutralization of IL-33 or its receptor ST2 ameliorates colitis^{117, 118}. Furthermore, exogenous IL-33 increases concentrations of type 2 cytokines IL-4 and IL-13, exacerbating dextran sodium sulfate (DSS)-induced colitis in mice by impairing epithelial barrier integrity¹¹⁶. IL-33 activity is also associated with impaired tissue repair, delaying healing and prolonging colitis¹¹⁶. Conversely, IL-33 has protective effects, such as promoting epithelial restitution/repair and the resolution of inflammation¹¹⁹. Other mediators involved in the tuft cell-ILC2 circuit are cysteinyl leukotrienes. Leukotrienes are lipid signaling molecules that act as inflammatory mediators¹¹⁵. Tuft cells are capable of leukotriene synthesis, which was thought to be restricted to hematopoietic cells¹¹⁵. Tuft cells have been reported to express cysteinyl leukotrienes for optimal activation of ILC2s and rapid induction of type 2 immunity during helminth infections¹¹⁵.

1.2.5 Tuft cells in disease

Tuft cell-derived IL-25 has been implicated in allergic disease, airway viral responses, and parasitic infections through overactivation of type 2 immune responses^{79, 86, 120}. Additionally, tuft cells have been proposed to be protective in *Clostridium difficile* infections; IL-25 is suppressed in a mouse model of *C. difficile*-mediated colitis and people infected with *C. difficile*¹²¹. Restoration of IL-25 reduces mortality and pathology in *C. difficile* infection, which is mediated by recruitment of eosinophils that protect the gut barrier^{80, 121}. Conversely, the ability of tuft cells to enhance IEC regeneration may exacerbate colorectal cancer⁸⁰. Tuft cell hyperplasia is associated with gastric inflammation and metaplasia in the intestine⁹³. DCLK1⁺ cells are overrepresented in 75% of human primary colorectal cancers and colorectal adenocarcinomas^{80, 122}. Furthermore, they are associated with lower patient survival following cancer resection^{80, 122}. Ablation of DCLK1⁺ cells can halt tumor growth¹²³. Moreover, as the reserve stem cell population, tuft cells could proliferate and become cancer-initiating cells with genetic insult^{80, 87}.

As the dominant source of IL-25 in the intestinal epithelium, tuft cells are central to intestinal type 2 immune responses that respond to pathogens and cause allergic inflammation, especially in helminth infections^{79, 85}. IL-25 induces type 2 immunity to promote worm expulsion^{79, 124}. There is dramatic IL-4/IL-13-mediated tuft cell hyperplasia during infections by helminths such as *Trichinella spiralis*¹²⁵. Mice lacking α -gustducin, POU2F3, or TRPM5 have a dysfunctional immune response against helminth infections^{56, 80, 120}. Additionally, deletion of components of the tuft cell-ILC2 circuit such as IL-25 and IL-4 receptor (IL-4R) leads to delayed clearance of *Nippostrongylus brasiliensis*^{79, 126}.

Type 2 immune responses contribute to intestinal homeostasis, conferring protection against infections by maintaining barrier defence and repairing injury, while suppressing type 1 inflammation¹¹¹. Previously, epithelial-specific ablation of DCLK1 has been shown to impair epithelial repair responses and worsen IBD, suggesting that tuft cells play an important role in inflammation-driven epithelial restitution^{127, 128}. Additionally, depleting DCLK1⁺ IECs in mice reduces the number of epithelial cells in the colon, increases gut permeability, and leads to higher IL-1 β and IL-17 levels during DSS-induced colitis^{80, 87}. Furthermore, patients with IBD have fewer tuft cells and IL-25 levels than healthy controls during active disease compared to remission⁸⁰. Taken together, this suggests that tuft cells have a role as immune sentinels that can monitor the lumen and relay signals to immune cells within the lamina propria⁷⁹. Thus, they are critical for intestinal homeostasis and protection during infections and inflammation⁸⁰.

Conversely, excessive tuft cell-mediated activation of type 2 immunity may promote inflammation and cause pathological wound healing that leads to fibrosis¹²⁹. Dysregulated type 2 immunity may lead to persistent inflammation that contributes to UC, or excessive tissue repair that causes fibrosis and stricture formation, which occurs primarily in CD¹¹⁶. Elevation of type 2 cytokines are noted in the lamina propria of the gut in animal models and people with UC^{111, 130}. The mechanisms that determine how type 2-mediated tissue regeneration leads to fibrotic complications are unclear¹¹¹. Tuft cells may also impact epithelial wound healing through their ability to promote IEC proliferation, further suggesting that they may impact recovery in IBD¹²⁹.

131.

1.3 Mouse models of IBD

Animal models of intestinal inflammation that resemble features of human IBD have provided valuable insight into the development of IBD¹³². While no model completely reflects the complexity of IBD, they have allowed study of the major components of disease¹³². The models can be separated into four general categories: spontaneous, adoptive transfer, genetically engineered, and chemically induced models.

The SAMP1/YitFc mouse strain is a spontaneous model of CD-like ileitis used to study chronic intestinal inflammation¹³³. It occurs without genetic, chemical, or immunological manipulation¹³³. SAMP1/YitFc mice display CD-like disease location, histological features, extra-intestinal manifestations, and response to conventional therapies¹³³. In particular, mice have high IFN- γ production preceding ileitis, severe transmural and discontinuous inflammation in the terminal ileum that is acute and chronic, perianal disease, and strictures¹³⁴. This model is suitable for understanding mechanisms that precede the onset of disease, leading to discovery of preventive therapies¹³³. Another model is the C3H/HeJBir strain, which displays spontaneous colitis^{134, 135}. C3H/HeJBir mice have increased B and T cell reactivity to antigens of commensal bacteria¹³⁶. Disadvantages of spontaneous models include poor breeding, increased costs for colony maintenance, and unknown specific etiology¹³⁴.

Adoptive transfer colitis involves transfer of naïve CD4⁺ CD45RB^{hi} T cells that are depleted of Tregs from wild-type (WT) mice into immunodeficient mice (i.e. severe combined immunodeficient, or SCID, mice) that lack T and B cells¹³⁷. These studies have demonstrated that this T cell subset is involved in the development of intestinal inflammation, since mice that receive cell transfer develop chronic pancolitis¹³⁴. This model is relevant for investigating the

chronic features of intestinal inflammation, role of specific T cell subsets (i.e. Tregs), and immunoregulation in IBD¹³².

Genetically engineered models are developed by genetic manipulation targeting cytokine function, T cell function, or epithelial barrier function¹³². Models can target cytokines (e.g. IL10^{-/-}, IL2^{-/-}, and TGF- β ^{-/-}), signaling pathways (e.g. JAK3^{-/-} and STAT3^{-/-}), immune cell function (e.g. T-cell receptor- α ^{-/-}), and barrier function (e.g. MUC2^{-/-})¹³⁴. Each model leads to colitis, enterocolitis, ileitis, or systemic inflammation¹³⁸. These models allow investigation of specific genetic variants and cell types but have limited applicability because few single-gene deletions are associated with human IBD¹³⁴. I will describe the SHIP-deficient mouse, a genetic model pertinent to my studies, in Section 1.4.4.

Finally, chemically induced models are those that administer noxious chemicals to induce intestinal inflammation¹³². These include DSS, trinitrobenzene sulfonic acid (TNBS), acetic acid, oxazolone, and peptidoglycan-polysaccharide (PG-PS)¹³². Each model displays unique inflammation features and mimics different aspects of human IBD¹³⁹. For example, DSS can be used to induce acute or chronic colitis, with the acute model being especially useful for studying colonic tissue/epithelial injury and repair¹³⁴. Oxazolone colitis is considered an experimental analogue of UC, as both involve Th2-mediated colitis¹³⁴. These models are commonly used because they are easy to induce and inexpensive, but disadvantages include lack of reproducibility and reduced pathogenic relevance to human IBD¹³⁴.

In my work, I used the DSS-induced colitis model. DSS is a water-soluble, negatively charged sulfated polysaccharide that causes damage to the epithelial layer in the large intestine, allowing luminal contents to interact with immune cells in the lamina propria¹⁴⁰. The high negative charge is toxic to colonic epithelia, creating erosions that increase permeability¹⁴⁰. It is

thought that the specificity of DSS to the colon is a result of the abundant bacterial populations in the colon that promote water and electrolyte absorption¹⁴⁰. DSS induces changes in expression of tight junction proteins and increased expression of pro-inflammatory cytokines (TNF- α , IL-1 β , IFN- γ , IL-10, and IL-12) as early as 1 day of challenge, with development of additional clinical symptoms of disease including weight loss, diarrhea, rectal bleeding, stool loosening, and eventually, mortality^{140, 141}. Acute histological changes in the colon are seen 4-7 days after the start of DSS challenge and include mucin and goblet cell depletion, ulceration, and neutrophil infiltration¹⁴⁰. Th1, Th17, and Th2-like responses are associated with DSS-induced colitis, but it most closely mimics the clinical and histopathological features of acute UC¹⁴⁰. However, unlike in human IBD, DSS-induced colitis is T and B cell-independent, limiting its applicability¹⁴⁰. Instead, this model is useful for studying the contribution of the innate immune system to the development of inflammation¹⁴⁰. It is widely used due to its rapidity, controllability, and reproducibility¹⁴⁰. The model can also be used to study recovery from colitis by administering DSS for 5 days and normal drinking water afterwards¹¹⁹. This allows study of defective or delayed tissue repair and healing, which are implicated in IBD¹¹⁹.

1.4 Src homology 2 domain-containing inositol 5'-phosphatase (SHIP)

1.4.1 Description

SHIP is a hematopoietic-specific lipid phosphatase that negative regulates the class I phosphatidylinositol 3-kinase (PI3K) pathway. The human gene encoding the 145kDa SHIP protein (*INPP5D*) is located at chromosome 2q37.1¹⁴². In the mouse, SHIP is located on chromosome 1. The SHIP 5-phosphatase family consists of two major isoforms: SHIP1 (or SHIP) and SHIP2¹⁴³. They share a high level of amino acid conservation, both containing SH2-domains and being ~140 kDa proteins¹⁴³. However, their tissue distribution differs significantly.

SHIP1 is thought to be restricted to hematopoietic cells, spermatocytes, osteoblasts, and mesenchymal stem cells, functioning in myeloid homeostasis^{142, 143}. SHIP2 is ubiquitously expressed, and its role is more tissue-dependent, with tumor suppressing or oncogenic activity¹⁴³.

1.4.2 PI3K pathway

PI3Ks are a family of enzymes that promote biological processes such as cell growth, differentiation, proliferation, and immune activation^{89, 144}. PI3Ks are divided into three classes: class I, II, and III, based on their substrate specificity, sequence homology, and regulation¹⁴⁵. Class I PI3Ks are heterodimeric enzymes that are further categorized into IA and IB. Class IA PI3Ks are composed of one of three catalytic p110 subunits (p110 α , β , or δ). The regulatory subunit is composed of one of p85 α (or its splice variants, p55 α and p50 α), p85 β , or p55 γ ¹⁴⁶. Class IB is composed of one of two regulatory subunits (p87 or p101) and the catalytic subunit p110 γ ¹⁴⁷. The catalytic subunits p110 α and p110 β are ubiquitously expressed, while p110 γ and p110 δ are thought to be hematopoietic-specific¹⁴⁸. Class II PI3Ks are monomeric kinases that act downstream of receptor tyrosine kinases and G-protein coupled receptors¹⁴⁷. Finally, Class III PI3K consists of a single catalytic subunit Vps34 and regulatory subunit Vps15¹⁴⁹.

Upon activation of receptor tyrosine kinases, G-protein coupled receptors, growth factor, and TLRs, Class I PI3Ks are recruited to the cell membrane¹⁵⁰. They phosphorylate the 3' position of phosphatidylinositol-4,5-bisphosphate PI(4,5)P₂, generating PI(3,4,5)P₃^{151, 152}. PI(3,4,5)P₃ recruits proteins with pleckstrin homology (PH) domains to the plasma membrane¹⁴². This includes serine-threonine kinases, such as protein kinase B (AKT) and phosphoinositide-dependent kinase-1 (PDK1); protein tyrosine kinases, such as the Tec family; exchange factors for guanosine triphosphate (GTP)-binding proteins; and adaptor proteins¹⁴². Upon activation, these proteins initiate further signaling pathways that drive cellular processes such as molecular

trafficking, vesicle mediated transport, regulation of the actin cytoskeleton, GTPase function, development, movement, organization, growth, and proliferation¹⁴². Inositol phosphatases influence PI(3,4,5)P₃ levels and include phosphatase and tensin homolog protein (PTEN) and SHIP¹⁴². PTEN is a tumor suppressor enzyme that prevents AKT hyperactivation; PTEN deficiency leads to prolonged cell survival that causes abnormal tissue growth^{142, 153, 154}. Dysregulation of the PI3K pathway is implicated in many altered human metabolic states; thus, its enzymatic components are important targets for therapeutic interventions¹⁴².

1.4.3 SHIP enzymatic activity

SHIP exerts its enzymatic activity by translocating from the cytoplasm to the cell membrane, where it binds PI(3,4,5)P₃¹⁴². This occurs through association with an adaptor and scaffold proteins and/or direct binding via its SH2 domain¹⁴². Whereas PTEN converts PI(3,4,5)P₃ to PI(4,5)P₂, SHIP dephosphorylates the 5' position of PI(3,4,5)P₃ to generate PI(3,4)P₂, inhibiting PI3K-mediated cell growth, proliferation, and activation by preventing further recruitment of downstream effectors of PI3K⁸⁹. SHIP is critical for immune homeostasis, as loss of SHIP leads to increased PI3K-mediated immune activation¹⁵⁵. However, SHIP may have dual functions, as its product PI(3,4)P₂ can also activate downstream effectors of PI3K, including IRGM1 or AKT due to its increased affinity for the AKT PH domain^{142, 156-158}.

SHIP and SHIP2 have varying roles in cell signaling. SHIP functions as a negative regulator of immunoreceptor signaling (e.g. inflammatory signaling)¹⁵⁴ and hematopoietic progenitor cell proliferation/survival¹⁵⁹, and as an inducer of cellular apoptosis^{142, 160}. It has been implicated as a hematopoietic tumor activator and suppressor, the latter only being described in a murine B cell lymphoma mouse model^{142, 161, 162}. SHIP2 is a negative regulator of the insulin-

signaling pathway; SHIP2 knockout mice have reduced body weight and are resistant to weight gain due to insulin-stimulated AKT^{142, 163}.

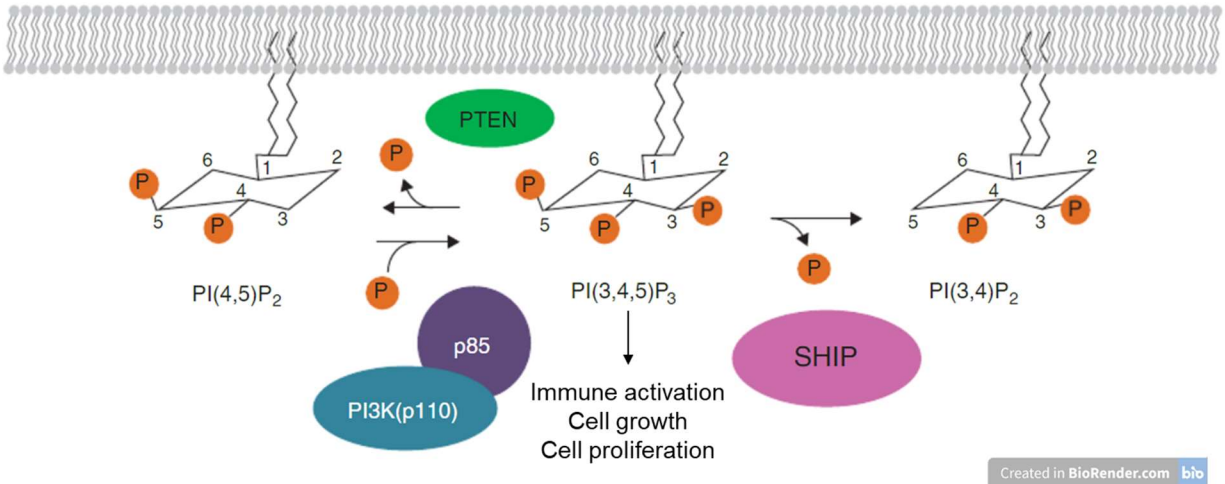


Fig 1.7. SHIP is a negative regulator of the PI3K pathway.

In the PI3K pathway, activated receptors stimulate class I PI3Ks, composed of a heterodimer between a p110 catalytic subunit bound by the regulatory subunit p85. Activated PI3Ks phosphorylate PI(4,5)P₂ to PI(3,4,5)P₃. PI(3,4,5)P₃ is a second messenger that activates downstream signaling pathways that lead to immune activation, cell growth, and proliferation. PI3K activity is reversed by PTEN. SHIP negatively regulates PI3Ks by dephosphorylating the 5' position of PI(3,4,5)P₃, therefore inhibiting PI3K-mediated immune activation, cell growth, and proliferation. Modified and used with permission from Society for Leukocyte Biology: Dobranowski and Sly. *J. Leukoc. Biol.* 2018¹⁵⁵.

1.4.4 SHIP deficiency

By disrupting the regulation of cell activity, SHIP deficiency may disrupt homeostasis and consequently processes such as nutrient absorption and growth. SHIP deficiency is reported in 15% of people with CD¹⁶⁴. There are SNPs in the human *SHIP/INPP5D* gene that are enriched in people with CD or UC^{142, 165}. Furthermore, levels of SHIP mRNA, protein, and activity are reduced in immune cells isolated from inflamed ileal tissue in pediatric patients with CD¹⁶⁶⁻¹⁶⁸. Mice with germ-line SHIP deficiency (*SHIP*^{-/-} mice) were first developed by replacing the entire first exon of the gene with a neomycin resistance cassette¹⁶⁹. They have lower body weights,

systemic mast cell hyperplasia, progressive splenomegaly, massive macrophage infiltration in the lungs, a myeloproliferative disorder, and a shortened lifespan^{142, 160, 169, 170}. Furthermore, they have increased serum levels of IL-6, TNF, and IL-5^{142, 170}. Importantly, they develop spontaneous discontinuous inflammation in the distal ileum starting at 4 weeks of age with several key features resembling human CD, including fibrosis^{171, 172}. All SHIP^{-/-} mice develop ileal inflammation by 6 weeks of age¹⁷¹. There is a paucity of T cells (CD4⁺ and CD8⁺) in the inflamed mucosa of SHIP^{-/-} mice, suggesting that inflammation is not attributed to excessive T effector cell activity^{142, 172}. Instead, inflammation is characterized by neutrophil infiltration, granuloma-like aggregates, goblet cell hyperplasia, and a mixed Th2 and Th17 cytokine profile¹⁷². Additionally, the inflamed intestinal tissue and intestinal macrophages from SHIP^{-/-} mice have higher concentrations of IL-1 β and IL-18 than their wild-type counterparts¹⁶⁷. Inflammation can be cured by bone marrow transplantation, suggesting that it is caused by bone marrow-derived hematopoietic cells and not tuft cells¹⁷².

1.4.5 Tuft cells in SHIP^{-/-} mice

The onset of inflammation coincides with the developmental appearance of tuft cells, at 4 weeks of age, in SHIP^{-/-} mice⁹⁰. Previously, our research team found 2.6-fold more HPGDS⁺ intestinal tuft cells in SHIP^{-/-} mice compared to wild-type controls at 4 weeks of age and 7-fold more tuft cells at 8 weeks of age after the establishment of inflammation. Later, Sauv e (2019) similarly found that tuft cell numbers are increased 6-fold in the inflamed distal ileum of SHIP^{-/-} mice at 8 weeks of age⁹⁰. However, there was no tuft cell hyperplasia in non-inflamed tissues (e.g. colon) or at 4 weeks of age⁹⁰. Thus, inflammation, rather than SHIP deficiency, drives tuft cell hyperplasia in the SHIP^{-/-} mouse ileum⁹⁰.

Like previous studies, Sauv  (2019) found that tuft cells represent the majority of COX1-expressing IECs in the absence of inflammation in wild-type and SHIP^{-/-} mice⁹⁰. During inflammation in the SHIP^{-/-} mouse, there is an increase in COX1-expressing tuft cells and other COX1-expressing cells in the lamina propria, which are likely sub-epithelial immune cells⁹⁰. COX activity and prostaglandin levels (PGD₂ and PGE₂) are higher in the inflamed ileal tissues of SHIP^{-/-} mice⁹⁰. Furthermore, prophylactic treatment with the COX inhibitor piroxicam prevents the development of ileal inflammation in SHIP^{-/-} mice, while causing a reduction in ileal tuft cell numbers and IL-1  levels⁹⁰. Thus, tuft cell-derived COX may be involved in the initiation of ileal inflammation in SHIP^{-/-} mice⁹⁰.

1.4.6 Tuft cell-specific SHIP-deficient mice

To investigate the role of SHIP in tuft cells without extraneous variables introduced by spontaneous intestinal inflammation, we created a mouse deficient in SHIP only in intestinal tuft cells by crossing floxed SHIP mice with Fabp-cre mice. Fabp-cre mice express cre-recombinase in a mosaic pattern in all intestinal epithelial cell types¹⁷³. Cre-recombinase deletes loxP, or floxed sequences¹⁷³. In this mouse, the SHIP gene is flanked by loxP sites, so cre-recombinase recognizes and excises/inverts SHIP in the gut only. Since tuft cells are the only IECs that express SHIP⁹⁰, these mice are SHIP-deficient only in intestinal tuft cells. We previously determined that tuft cell-specific SHIP-deficient (SHIP def) mice do not develop spontaneous intestinal inflammation at any age. Knowing the mosaic pattern of cre-recombinase expression, we evaluated cre-recombinase efficiency and resulting SHIP deficiency throughout the intestinal tract. SHIP deficiency is only 10-20% in the ileum, whereas it is the highest in the colon at around 50% SHIP deficiency. Thus, DSS-induced colitis was chosen as an appropriate disease model to investigate the role of SHIP deficiency in intestinal tuft cells.

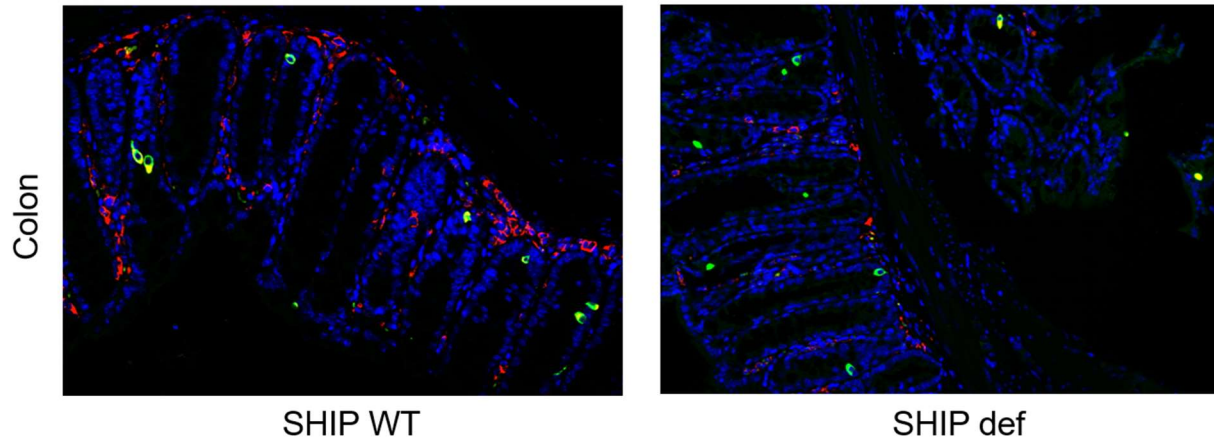


Fig 1.8. Cre-recombinase efficiency and resulting SHIP deficiency in the colon.

Pictured are colon cross-sections from SHIP wild-type (WT) and tuft cell-specific SHIP-deficient (SHIP def) mice. Cross-sections were co-stained for SHIP (red) and DCLK1 (green). SHIP is localized in 100% of DCLK1⁺ (tuft) cells in the SHIP WT cross-section. SHIP deficiency averages 50% in colon cross-sections. In this specific SHIP def example, it is 75%. Fluorescent images were acquired by Hayley Brugger from our research team.

1.5 Thesis objectives and hypothesis

1.5.1 Summary of rationale

SHIP deficiency results in increased PI3K-mediated cell growth, proliferation, and immune activation. Germ-line SHIP^{-/-} mice develop spontaneous CD-like ileitis, which is driven by increased production of macrophage-derived IL-1 β ¹⁶⁷. We previously found that tuft cells are the only IEC to express SHIP, which was thought to be hematopoietic-specific⁹⁰. Tuft cells are present in the lungs and GI tract⁷⁵, which are both locations of spontaneous inflammation in the SHIP^{-/-} mouse^{90, 171}. Additionally, the onset of inflammation coincides with the initial appearance of tuft cells at 4 weeks of age in SHIP^{-/-} mice⁹⁰. By 8 weeks of age, after the establishment of inflammation, there are 6-fold more intestinal tuft cells in the inflamed ileal tissue of SHIP^{-/-} mice⁹⁰. Tuft cells are also the only epithelial cells in the uninflamed intestine to express COX1 and COX2, which produce prostaglandins that regulate inflammation and post-injury restitution

(resealing of the epithelial barrier)⁹². Additionally, SHIP^{-/-} mice have more COX1 positive cells, COX activity, and prostaglandin levels in inflamed ileal tissue compared to wild-type controls⁹⁰. Prophylactic (and not therapeutic) treatment with the COX inhibitor piroxicam prevents the development of intestinal inflammation in SHIP^{-/-} mice⁹⁰. This suggests that tuft cell-derived COX may be involved in initiating inflammation.

Tuft cells produce IL-25, which promotes type 2 inflammation and intestinal remodeling through ILC2 activation^{79, 85}. Tuft cells have previously been found to be protective in DSS-induced colitis¹²⁸. Furthermore, tuft cell-derived IL-25 is significantly lower in the diseased intestinal mucosa of people with IBD, suggesting reduced tuft cell activity compared to healthy controls⁸⁰. However, in addition to ileal inflammation, SHIP^{-/-} mice develop muscle thickening and fibrosis¹⁷¹, which may be due to an exacerbated type 2 immune response and/or dysregulated IEC proliferation induced by tuft cells^{111, 131, 171}. These studies demonstrate the complex role of tuft cells in regulating inflammation and post-injury tissue repair. We have generated a tuft cell-specific SHIP-deficient mouse, which does not develop spontaneous intestinal inflammation, to investigate tuft cell-specific functions during intestinal inflammation and recovery.

1.5.2 Aims

Based on this, I hypothesized that tuft cell-specific SHIP-deficient mice will have exacerbated DSS-induced intestinal inflammation because SHIP blocks COX-mediated inflammation. In addition, I hypothesized that tuft cell-specific SHIP-deficient mice will have impaired recovery from DSS-induced colitis because SHIP-deficient tuft cells will activate ILC2s to produce excessive type 2 cytokines that promote inflammation and pathological healing. To characterize the role of tuft cells in intestinal homeostasis, I had three aims:

- **Aim 1.** Determine the role of SHIP in tuft cell responses to commensal microbes during DSS-induced colitis.
- **Aim 2.** Determine if ILC2s and COX-mediated inflammation contribute to pathological inflammation during DSS-induced colitis in tuft cell-specific SHIP-deficient mice.
- **Aim 3.** Determine the effect of SHIP deficiency in tuft cells on recovery after DSS-induced colitis.

1.5.3 Significance

By examining the role of SHIP in tuft cell activity, these studies will contribute to our understanding of tuft cell functions, specifically tuft cell-derived IL-25 and COX, and the tuft cell-ILC2 circuit in murine colitis and recovery. This work may help characterize the basic biological processes involved in intestinal inflammation that may occur in people with IBD. In particular, tuft cell functions may be relevant to pathology in people with IBD who also have low SHIP levels and activity. Increased tuft cell activity due to SHIP deficiency may exacerbate inflammation, while impairing recovery by promoting pathological wound healing.

Chapter 2: Materials and methods

2.1 Mice

SHIP^{fl/fl} and Fabp1^{+/-cre} mice were crossed to generate mice with SHIP deficiency in intestinal tuft cells (SHIP^{fl/fl}xFabp1^{+/-cre}) and wild-type control littermates (SHIP^{fl/fl}xFabp1^{+/-+}) on a C57BL/6 background. Tuft cell-specific SHIP-deficient are called SHIP def and their wild-type counterparts are called SHIP WT throughout this thesis. SHIP WT and SHIP def mice were co-housed after weaning. Conventional housing of mice was maintained by technicians in the Animal Care Facility at the BC Children's Hospital Research Institute (Vancouver, BC). Mice used in DSS experiments were between 8-9 weeks of age. Experimentation was performed in accordance with Canadian Council on Animal Care guidelines and with approval from the UBC Animal Care Committee (Protocols A21-0035 and A21-0028).

2.2 DSS experiments

2.5% DSS (M.W. 36-50,000 Da; MP Biomedicals, Solon, OH, USA) was dissolved in the drinking water of mice. For Chapter 3.1-3.3, mice were treated for 7 days to induce colitis. Mice were monitored daily for weight loss, stool loosening, and rectal bleeding. Scores were assigned on a scale from 0-4, as described in Table 2.2.1. Disease activity index (DAI), the composite score of weight loss, stool loosening, and rectal bleeding, was calculated for each day.

Hemocult paper was from Beckman Coulter, Mississauga, ON, Canada. Colons were excised and rinsed with phosphate-buffered saline (PBS) after 7 days of DSS treatment, and their lengths and tissue weights were measured. For Chapter 3.4, colons were excised after 5 days of DSS treatment. For Chapter 3.5, mice were treated with DSS for 5 days and subsequently received normal drinking water for 5 days to evaluate recovery from colitis. Colons were excised after 5 days of recovery, and total colon length (end of cecum to anus) was measured (in cm). Complete

Swiss rolls of full-length colons or 0.5cm sections from the distal colon were fixed for histology. Remaining colonic samples were placed in liquid nitrogen for storage at -80°C or on ice until homogenization immediately after harvest.

Table 2.1 Disease scoring criteria

Score	Stool consistency	Rectal bleeding	Weight loss
0	Normal stool	None	0%
1	Loose stool	Detectable on Hemocult paper	1-5%
2	Very loose stool	Visible blood in stool	5-10%
3	Diarrhea	Large amount of blood in stool	10-15%
4	No formed stool	Extensive blood in stool and visible at the anus	>15%

2.3 Hematoxylin and eosin (H&E) and Congo Red staining

Colonic tissue sections from untreated and DSS-treated SHIP WT and SHIP def mice were fixed in 10% formalin (Formalde-Fresh Solution, Fisher Chemical SF934, Waltham, MA, USA) for 24 hours and stored in 70% ethanol. Tissue sections were embedded in paraffin, sliced into 5 µm cross-sections, and H&E-stained by the histology core at the BC Children’s Hospital Research Institute. Paraffin-embedded colon cross-sections were Congo Red-stained by Wax-It Histology Services Inc. at the University of British Columbia. For Fig 3.3 and Fig 3.16, colons were rolled up lengthwise via the Swiss roll technique, with the distal colon in the center of the roll. Swiss rolls were similarly fixed and sent to the histology core for H&E staining.

2.4 Histological analyses

H&E staining

Images of H&E stained tissue cross-sections were acquired using a Zeiss Axio Imager, Axiocam305 camera, and Zen Blue software. White balancing was conducted prior to imaging. Histological damage scores were assigned on a 16-point scale by two individuals blinded to experimental conditions as described in Table 2.4.1. For Fig 3.26A and Fig 3.26B, immune cell infiltration scores and muscle thickening scores were each compared between groups separately from the composite histological damage score.

Table 2.2 Histological damage scoring

Damage component	Score
Loss of crypt architecture	0 = none
	1 = <25% loss
	2 = 25-50% loss
	3 = 50-75% loss
	4 = >75% loss
Immune cell infiltration	0 = none
	1 = occasional immune cell in lamina propria
	2 = increased immune cells in lamina propria
	3 = confluent immune cells in lamina propria and breaching mucosa
	4 = immune cell infiltration throughout the section
Goblet cell depletion	0 = none
	1 = <50% depletion
	2 = >50% depletion
Ulceration	0 = none
	1 = intermediate ulceration

	2 = substantial ulceration
Edema	0 = none
	1 = <50% of section
	2 = >50% of section
Muscle thickening	0 = none
	1 = intermediate thickening
	2 = substantial thickening

Images of H&E-stained full-length colon cross sections cut from Swiss rolls were acquired using an Olympus BX61, DP71 camera, and cellSens Dimension software. White balancing was done prior to imaging. A tile scanning feature was used to acquire and stitch images taken at 10× magnification to form the complete image of colons.

Congo Red staining

Images of Congo Red-stained colon cross sections were acquired using a Zeiss Axio Imager at 40× magnification, AxioCam305 camera, and Zen Blue software. White balancing was conducted prior to imaging. The number of Congo Red+ eosinophils per 100 leukocytes was counted manually and averaged from 2 representative fields at 40× magnification in 1 cross-section per mouse (3 mice per condition).

2.5 Immunofluorescence staining

Paraffin-embedded colon cross-sections were deparaffinized by heating at 60°C for 20 minutes (min) and washing with xylene, 4 ethanol washes (100% twice, 95%, 80%), 1 wash in distilled water (dH₂O), and 1 wash in Tris-buffered saline with 0.1% Tween-20 (TBS-T). Next, sections were immersed in pre-heated sodium citrate buffer, pH 6.0, at approximately 95°C for 20 min for heat-induced epitope retrieval. After cooling to room temperature, slides were

placed in dH₂O for 3 minutes. Sections were then blocked for 60 min with 2% normal goat serum in PBS containing 1% bovine serum albumin (BSA), 0.1% Triton X-100, and 0.05% Tween-20. The primary and secondary antibodies used were rabbit polyclonal anti-DCLK1 (Abcam #ab37994, Toronto, ON) and Alexa Fluor 488 goat anti-rabbit IgG (Invitrogen #A11008, Burlington, ON). VECTASHIELD Antifade Mounting Medium with 4',6-diamidino-2-phenylindole DAPI (MJS BioLynx Inc. VECTH1200, Brockville, ON) was used to mount slides and stain nuclei. Negative controls with no primary antibody incubation were performed for staining experiments. Imaging was conducted using a Zeiss Axio Imager, Axiocam305 camera, and Zen Blue software. A cell counting script with manual adjustment was used to estimate the number of epithelial cells. Crypt lengths were estimated by manual counting. DCLK1⁺ tuft cells were counted manually to determine the percentage of tuft cells in total epithelial cells in 4-6 representative fields at 20× magnification in 1 cross-section per mouse (4-7 mice per condition).

2.6 Tissue homogenization and cytokine assays

Colonic samples were homogenized in 2 mL of homogenization buffer (10 mg/mL aprotinin and 2 mg/mL leupeptin in PBS) using a Kinematica Polytron MR2100 bench top homogenizer. Homogenates were then centrifuged at 10,000 ×g for 5 min. Supernatants were collected and stored at -80°C until used in assays. Immediately prior to assays, supernatants were thawed on ice and centrifuged at 10,000 ×g to remove debris.

Cytokine concentrations were measured in enzyme-linked immunosorbent assays (ELISAs) using 50 µL samples of full thickness colon homogenates from SHIP WT and SHIP def mice. All ELISAs were performed according to manufacturer's instructions, with the exception of using 50 µL of the clarified colon homogenates instead of 100 µL. The ELISA kits

used included: IL-1 β (Cat. No. DY401), IL-13 (Cat. No. DY413), and IL-25 (Cat. No. DY1399) from R&D Systems (Minneapolis, MN, USA); IL-4 (Cat. No. 555232), IL-5 (Cat. No. 555236), IL-6 (Cat. No. 555240), and TNF (Cat. No. 558534) from BD Biosciences (Mississauga, ON, Canada); and IL-33 (Cat. No. 88-7333) from Invitrogen. Plate washes were performed with wash buffer (0.05% Tween-20 in PBS) using a Thermo Fisher Scientific Wellwash Microplate Washer. Thermo Scientific TMB Substrate Solution (N301) and stop solution (9.75% sulfuric acid in dH₂O) were used in all ELISAs. Absorbances were read at 450 nm using a Molecular Devices FilterMax F5 Multi-Mode Microplate Reader and SoftMax Pro 6.5.1 software. Cytokine concentrations in samples were determined using a standard curve and normalized to colonic tissue weights.

2.7 Cysteinyl leukotrienes assay

Cysteinyl leukotriene concentrations were determined using the CysLT Express ELISA Kit from (Cat. No. 10009291) from Cayman Chemical (Ann Arbor, MI, USA), following manufacturer's instructions. Samples were assayed at two dilutions (1:4 and 1:8) to achieve concentrations within the range of 20-500 pg/mL. Only samples with strong correlation ($\leq 20\%$ difference) in the final calculated concentrations were included in analyses. Absorbances were read at 410 nm using a Molecular Devices FilterMax F5 Multi-Mode Microplate Reader and SoftMax Pro 6.5.1 software. Concentrations were determined using a standard curve and normalized to colonic tissue weights.

2.8 COX activity assay

COX activity was measured using the COX Fluorescent Activity Assay Kit (Cat. No. 700200) from Cayman Chemical following manufacturer's instructions. Sample wells used 10 μ L of clarified colon homogenates. Background fluorescence was determined using 10 μ L of

samples that were produced by heating clarified colon homogenates at 100°C for 5 min and centrifuging at 8,000 ×g for 1 min. No COX inhibitors were used. Fluorescence was read using an excitation wavelength of 530 nm and emission wavelength of 585 nm on a Molecular Devices FilterMax F5 Multi-Mode Microplate Reader and SoftMax Pro 6.5.1 software. COX activity was determined from a standard curve of resorufin concentration between 0 and 10 μM.

2.9 Statistical analyses

Unpaired two-tailed *t*-tests and multiple unpaired *t*-tests (False Discovery Rate 1%, two-stage step-up method of Benjamini, Krieger and Yekutieli) were performed where indicated using GraphPad Prism version 9 (GraphPad Software Inc.). The ROUT method was conducted at Q=1% using GraphPad Prism version 9 to identify and remove outliers. Differences were considered significant at $p < 0.05$.

Chapter 3: Results

3.1 SHIP deficiency in tuft cells exacerbates DSS-induced colitis

To determine whether SHIP plays a role in intestinal tuft cells during intestinal inflammation, I asked whether SHIP deficiency in tuft cells exacerbates DSS-induced colitis in mice. SHIP WT and SHIP def mice were treated with 2.5% DSS in drinking water over 7 days to induce colitis. After 7 days of DSS treatment, I harvested colons and measured their lengths. Below are representative images of SHIP WT and SHIP def full-length colons from female and male mice (Fig 3.1A). No significant differences in gross pathology between female and male mice in each condition were observed. The colons of both SHIP WT and SHIP def mice that received normal drinking water were of similar lengths and appeared healthy and uninflamed. In comparison, both DSS-treated SHIP WT and SHIP def mice had shorter colons. Furthermore, DSS-treated SHIP def mice had significantly shorter colons than SHIP WT mice (Fig 3.1B). Colon shortening is a sign of disease, suggesting that SHIP deficiency in tuft cells exacerbates DSS-induced colitis.

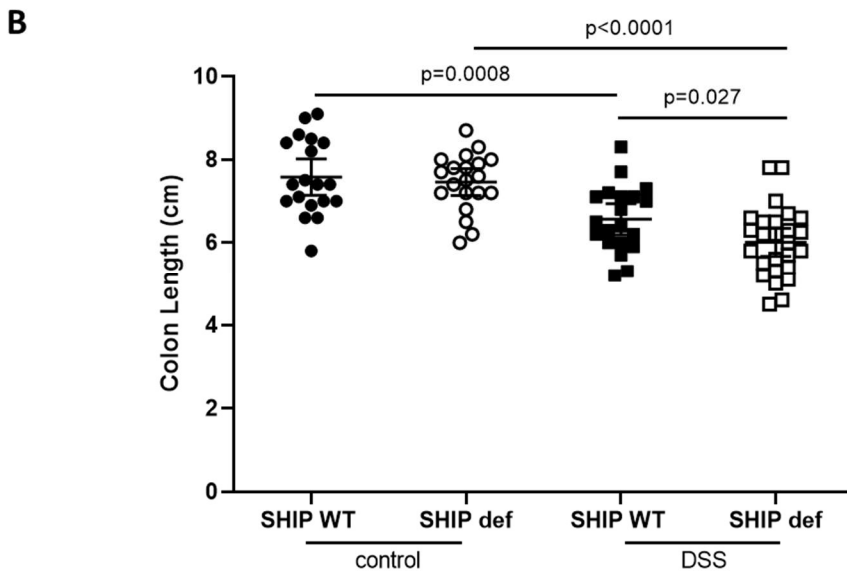
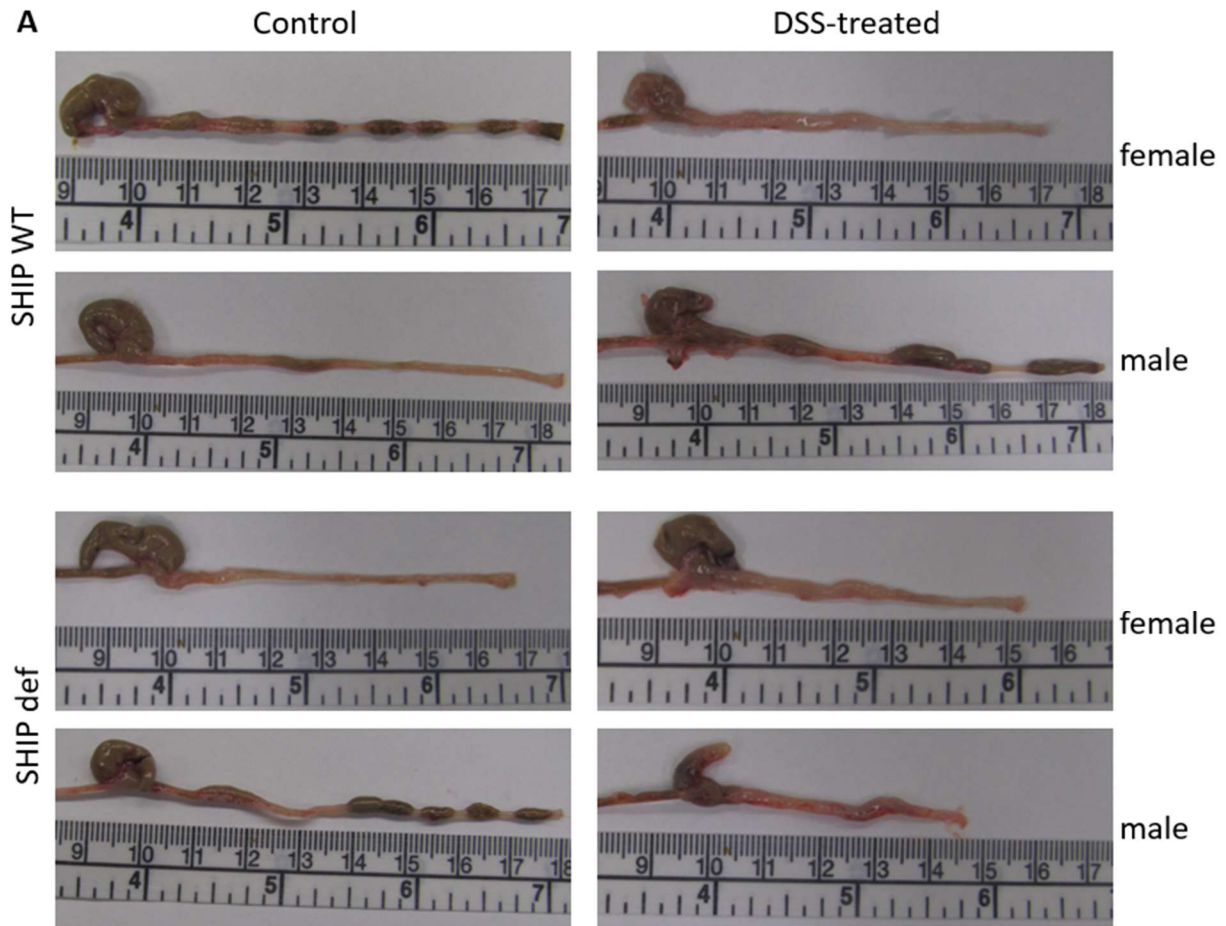


Fig 3.1. SHIP deficiency in tuft cells exacerbates colon shortening after DSS treatment. (A) Gross pathology of colons of SHIP WT and SHIP def mice after 7 days of DSS treatment. Control mice received normal drinking water; DSS-treated mice received 2.5% DSS in drinking water. Images shown are representative of 19-26 mice per group. Examples from male and

female mice are included. (B) Colon lengths for SHIP WT and SHIP def mice. Points represent individual mice and lines show mean \pm SD for each group. n = 19 SHIP WT and 20 SHIP def mice that were not treated with DSS. n = 20 SHIP WT and 26 SHIP def DSS-treated mice. Circle data points represent control mice and square data points represent DSS-treated mice. Closed and open points represent SHIP WT and SHIP def mice, respectively. p values are for comparisons indicated and were determined using an unpaired two-tailed *t*-test. Comparisons not indicated were not significantly different.

Mice were monitored daily throughout DSS treatment for signs of disease by measuring body weights and assessing stool. Stool consistency, rectal bleeding, and weight loss were assigned scores (Fig 3.2). As expected, DSS treatment caused stool loosening, rectal bleeding, and weight loss for SHIP WT and SHIP def mice (Fig 3.2). SHIP WT and SHIP def mice had similar scores for rectal bleeding and stool consistency during DSS-induced colitis (Fig 3.2A and Fig 3.2B). SHIP def mice had greater weight loss indicated by percentage of initial weight on Days 5, 6, and 7 of DSS treatment compared to SHIP WT mice (Fig 3.2C). Similarly, DSS-treated SHIP def mice had a significantly higher weight loss score on Day 7 (Fig 3.2D). As such, SHIP def mice had a higher DAI (a composite score for stool consistency, rectal bleeding, and weight loss) on Day 7, which was driven by differences in weight loss (Fig 3.2E).

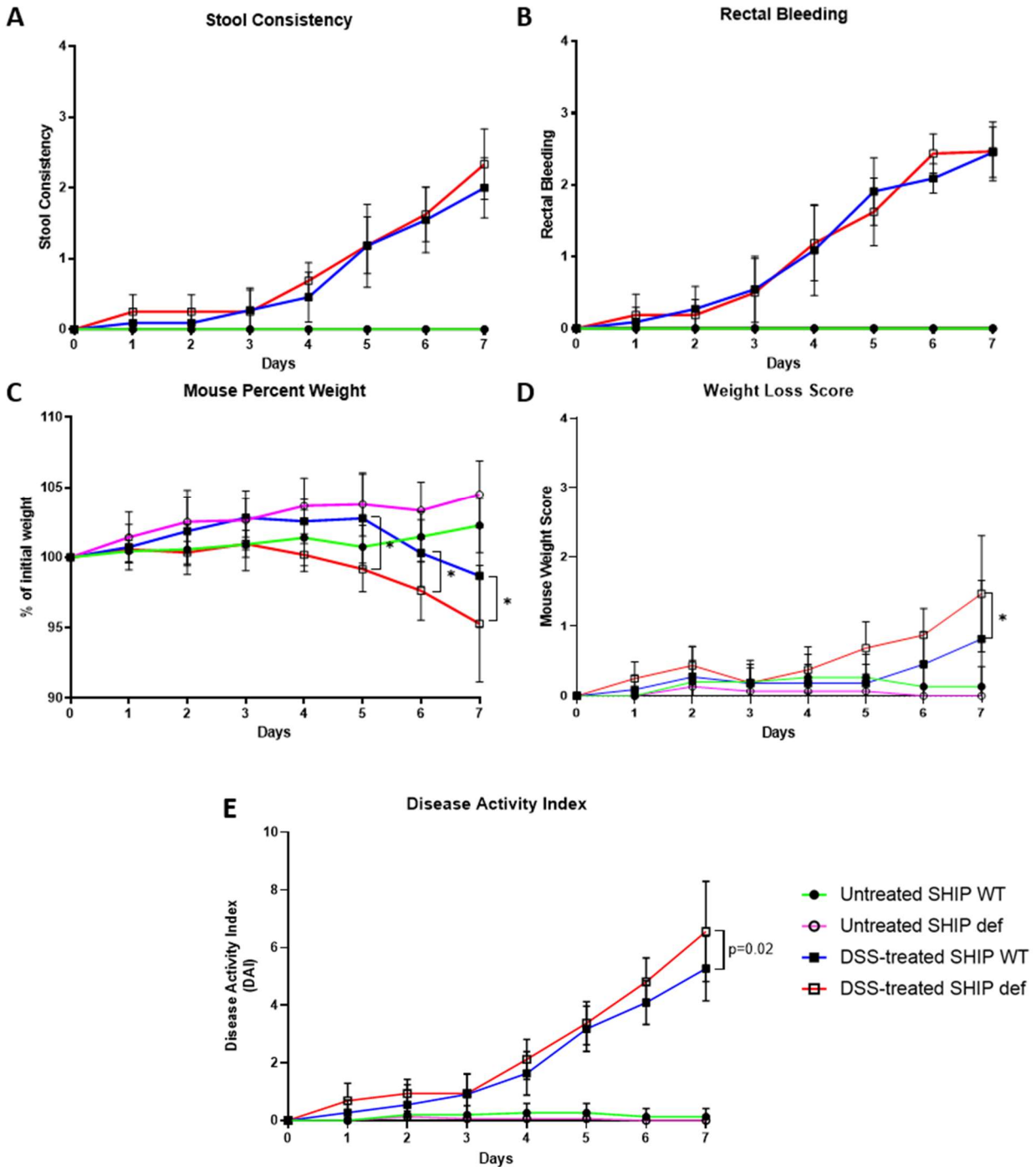


Fig 3.2. SHIP deficiency in tuft cells exacerbates weight loss during DSS-induced colitis.

Disease scores during 7 days of DSS treatment. (A) Stool consistency scores assigned on a scale of 0 - 4. 0 = normal stool in pellet form; 1 = loose stool; 2 = very loose stool; 3 = diarrhea; 4 = no formed stool. (B) Rectal bleeding scores assigned on a scale of 0 - 4. 0 = no blood in stool; 1 = blood detectable on hemocult paper; 2 = blood visible in stool; 3 = extensive blood in stool; 4 = extensive blood in stool and around anus. (C) Weight indicated by percentage of initial weight. (D) Weight loss scores assigned on a scale of 0 - 4. 0 = 0% weight loss; 1 = 1-5% weight loss; 2

= 5-10% weight loss; 3 = 10-15% weight loss; 4 = >15% weight loss. (E) DAI summing scores for stool consistency, rectal bleeding, and weight loss. Points represent the average of all mice in each group with error bars representing \pm SD. n = 15 SHIP WT and 15 SHIP def mice that were not treated with DSS. n = 11 SHIP WT and 16 SHIP def DSS-treated mice. Circle data points represent control mice and square data points represent DSS-treated mice. Closed and open points represent SHIP WT and SHIP def mice, respectively. p values are for comparisons indicated and were determined using multiple unpaired *t*-tests with correction for multiple comparisons by the two-stage step-up method of Benjamini, Krieger and Yekutieli. *p < 0.05. Comparisons not indicated were not significantly different.

To determine if differences in disease severity were location-dependent in the colons of DSS-treated SHIP WT and SHIP def mice, entire colon cross-sections were cut from Swiss rolls, H&E-stained, and assessed for histological damage after 7 days of DSS treatment (Fig 3.3). No signs of histological damage were observed in untreated SHIP WT and SHIP def mice; thus, there were no differences in histological damage across the length of the colon. No significant differences in histological damage were observed between the proximal and distal colon for DSS-treated SHIP WT and SHIP def mice. Hence, cross-sections from the distal colon were used to assign and compare histological damage scores. Additionally, homogenates of entire full thickness colons were used in cytokine assays.

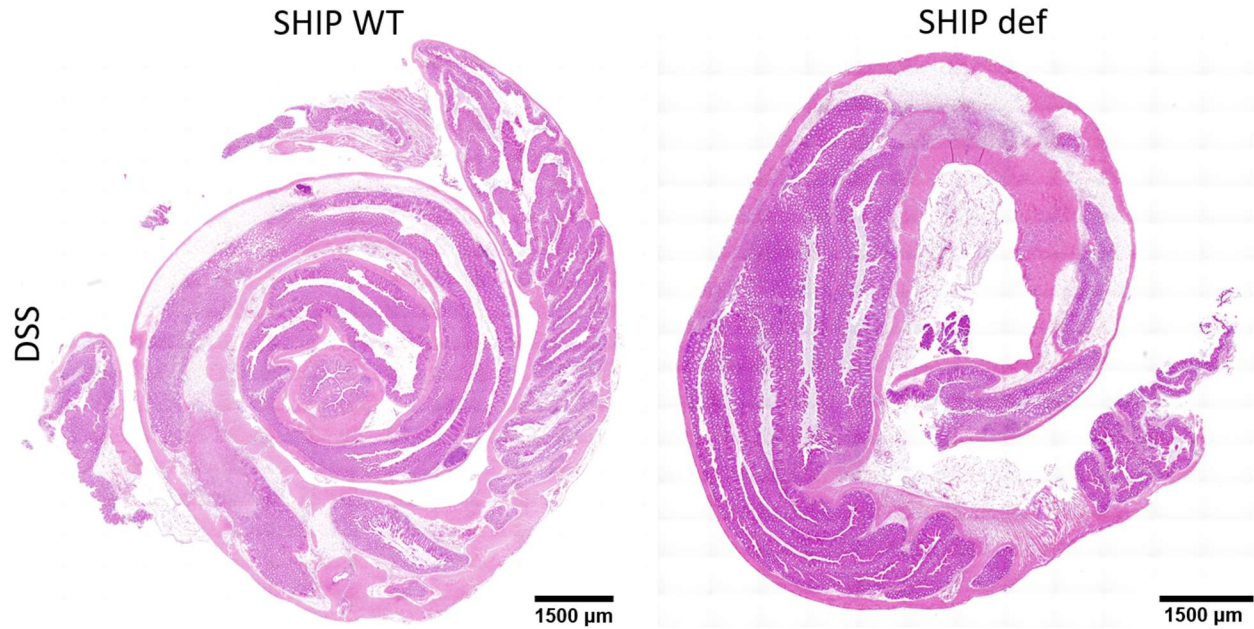


Fig 3.3. DSS-induced histological damage does not significantly differ across the length of the colon due to SHIP deficiency in tuft cells.
 H&E-stained colonic tissue cross-sections of Swiss rolls from SHIP WT and SHIP def mice that were treated with DSS for 7 days. The distal end of the colon is in the center of the roll. Photographs were taken at 10× magnification and stitched in a tile scan. Scale bars = 1500 μm.

After 7 days of DSS treatment, cross-sections of the colons of SHIP WT and SHIP def mice were collected and H&E-stained (Fig 3.4A). DSS treatment causes loss of crypt architecture, goblet cell loss, muscle thickening, edema, ulceration, and immune cell infiltration. The composite score was used to quantify histological damage. SHIP def mice have more histological damage, including loss of crypt architecture, goblet cell loss, muscle thickening, edema, ulceration, and immune cell infiltration (Fig 3.4B), suggesting increased disease severity in DSS-induced colitis due to SHIP deficiency in tuft cells.

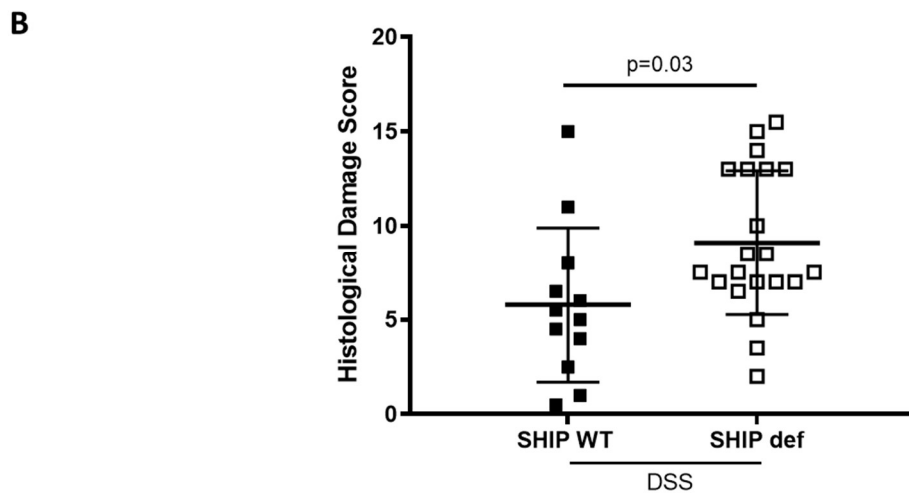
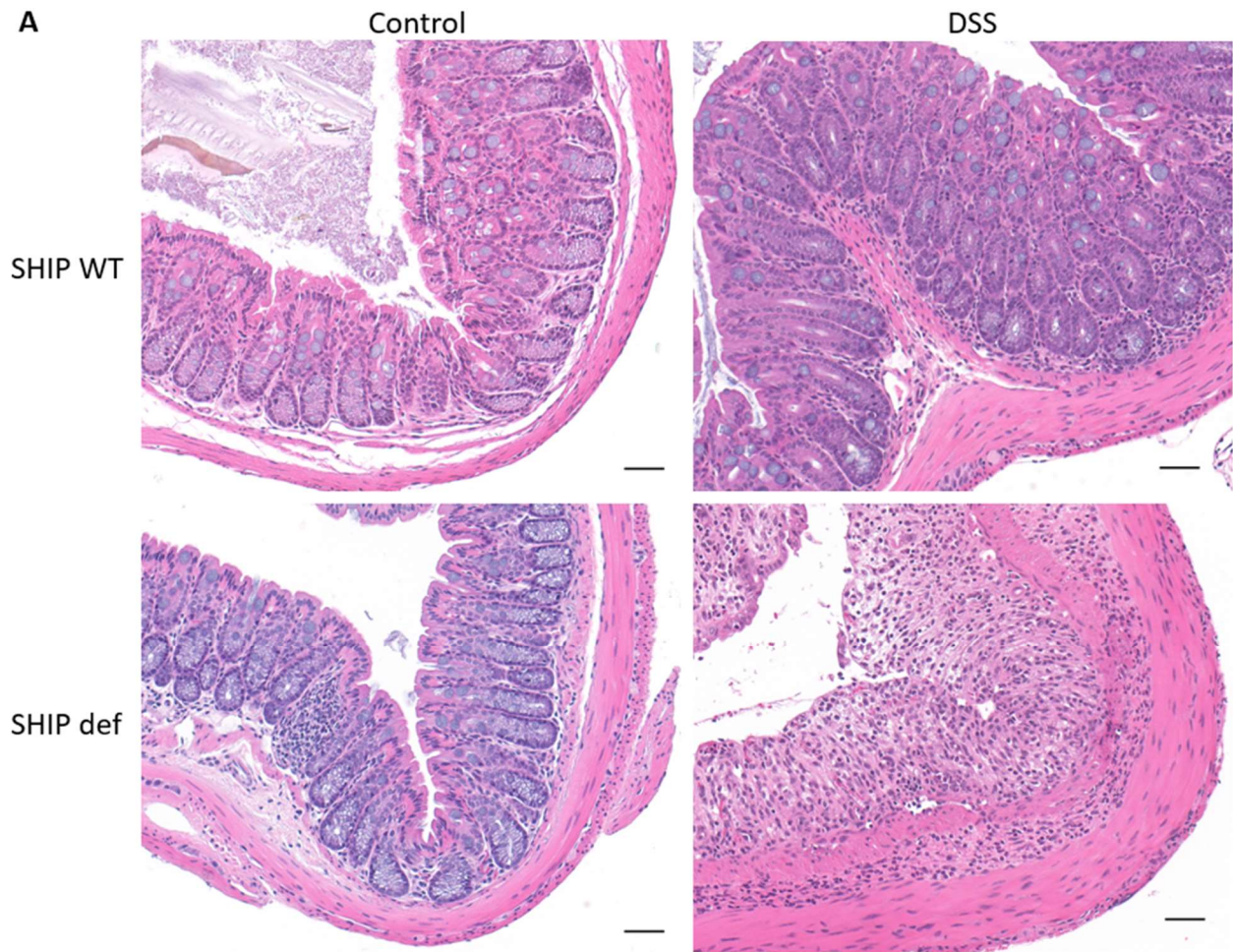


Fig 3.4. SHIP deficiency in tuft cells exacerbates histological damage after DSS treatment. (A) H&E-stained colon cross-sections of control and DSS-treated SHIP WT and SHIP def mice. Photographs were taken at 20× magnification. Scale bars = 50 μm. (B) Histological damage scores summing scores for crypt architecture loss, ulceration, goblet cell loss, immune cell

infiltration, edema, and muscle thickening for DSS-treated SHIP WT and SHIP def mice. Points represent individual mice and lines show mean \pm SD for each group. $n = 12$ SHIP WT and 21 SHIP def mice. Circle data points represent control mice and square data points represent DSS-treated mice. Closed and open points represent SHIP WT and SHIP def mice, respectively. $p = 0.03$ was determined using an unpaired two-tailed t -test.

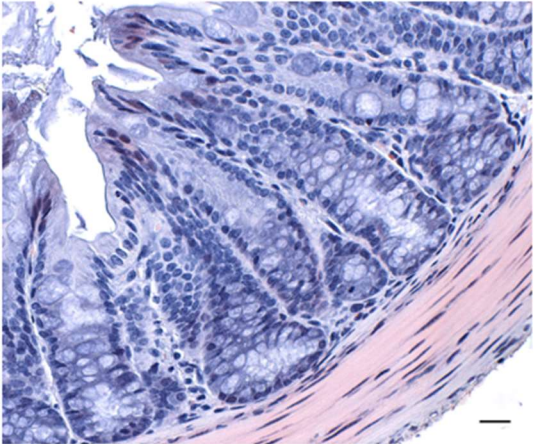
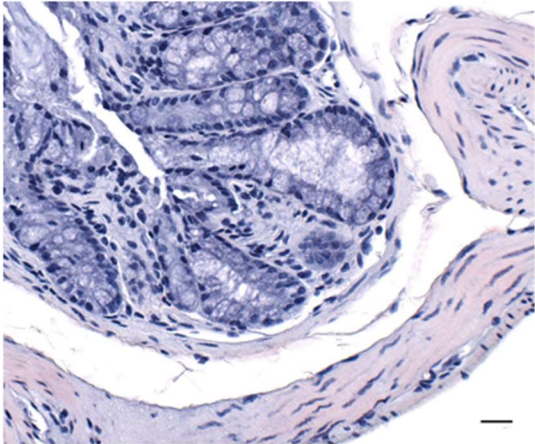
Tuft cell-derived IL-25 can recruit eosinophils by activating ILC2s to produce abundant levels of type 2 cytokines, IL-5 and IL-13, which promote eosinophil trafficking to the gut⁵⁰. Eosinophils are pro-inflammatory cells known to contribute to type 1 and type 2 immune responses, secreting type 1 cytokines (e.g. IFN- γ and IL-12), type 2 cytokines (e.g. IL-4), and the pro-fibrotic cytokine TGF- β ⁵⁰. To determine whether changes in eosinophil populations were driving increased disease severity in DSS-treated SHIP def mice, eosinophil numbers were determined by Congo Red staining of colon cross-sections from SHIP WT and SHIP def mice at baseline and after 7 days of DSS treatment (Fig 3.5). Colon cross-sections from both SHIP WT and SHIP def mice have few or no eosinophils at baseline. Colon cross-sections from SHIP WT and SHIP def mice have eosinophilia after DSS treatment. No significant differences in eosinophil numbers were observed between DSS-treated SHIP WT and SHIP def mice (Fig 3.5C), suggesting that differences in eosinophil populations were not driving increased disease activity in SHIP def mice.

A

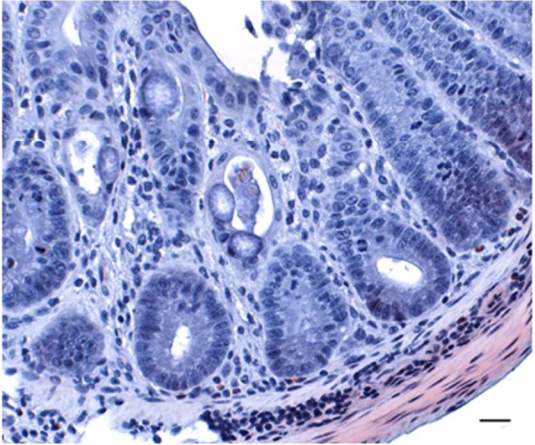
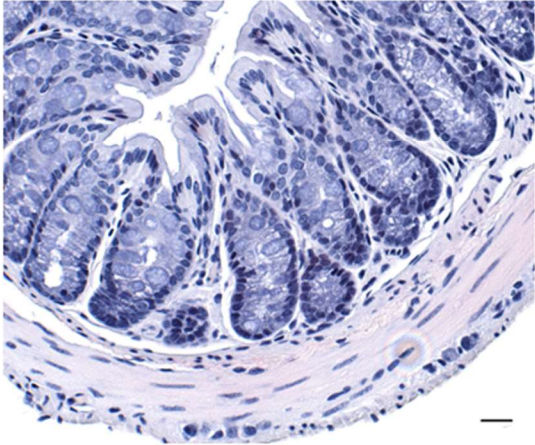
Control

DSS

SHIP WT



SHIP def



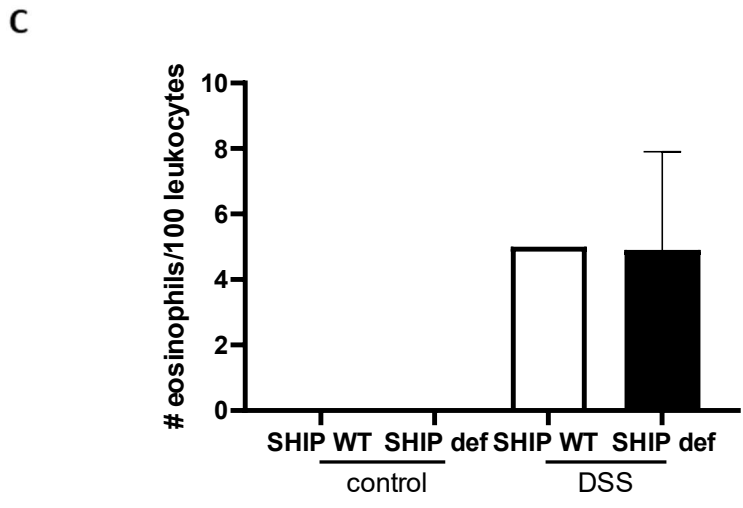
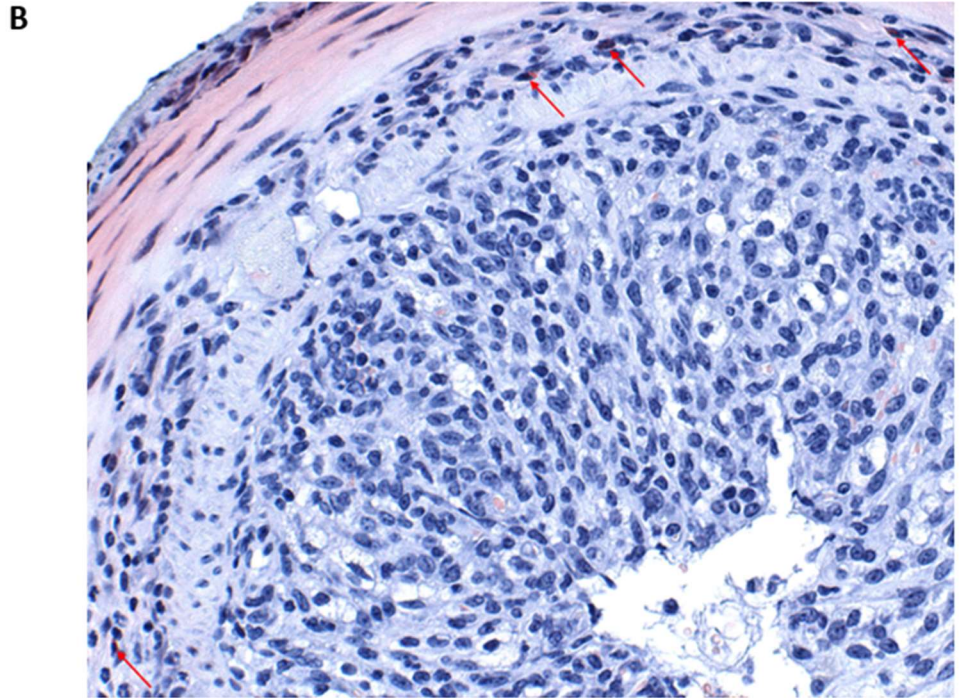


Fig 3.5. Eosinophil numbers are similar between DSS-treated SHIP WT and SHIP def mice.

(A) Congo Red-stained colon cross sections of control and DSS-treated SHIP WT and SHIP def mice. Negative (counter) staining is blue, while positive staining appears red. Photographs were taken at 40× magnification. Scale bars = 20 μm. (B) A Congo Red-stained colon cross section from a DSS-treated SHIP def mouse is shown to identify eosinophils that were counted as positive for quantitation (red arrows). Eosinophils have multilobed nuclei that appear purple or blue and cytoplasm that appears pink. Photograph taken at 40× magnification. (C) Number of eosinophils for 100 leukocytes. n = 3 for all groups. Counts were conducted manually and averaged from 2 representative fields at 40× magnification in 1 cross-section per mouse (3 mice per condition).

3.2 SHIP deficiency causes increased IL-25 concentrations during DSS-induced colitis

To determine whether SHIP deficiency caused increased tuft cell activity, as indicated by concentrations of IL-25 and type 2 cytokines, I performed ELISAs on full thickness colon tissue homogenates from control and DSS-treated SHIP WT and SHIP def mice. SHIP WT and SHIP def mice had similar concentrations of IL-25 at baseline (Fig 3.6A). DSS treatment led to a trend to lower IL-25 concentrations in SHIP WT mice. In contrast, IL-25 concentrations were not significantly lower in SHIP def mice after DSS treatment. As such, full thickness colon homogenates from SHIP def mice had higher IL-25 concentrations compared to SHIP WT mice after DSS treatment. Since tuft cells are the predominant source of IEC-derived IL-25 in the intestine, this suggests that SHIP deficiency increases (or maintains higher) tuft cell activity during DSS challenge.

IL-25 activates ILC2s to produce IL-4, IL-5, and IL-13. Thus, the concentrations of these cytokines were assessed in full thickness colon homogenates from SHIP WT and SHIP def mice. At baseline, colon homogenates from SHIP WT and SHIP def mice had similar concentrations of IL-4 (Fig 3.6B). Similar to our observations for IL-25, there was a trend to lower IL-4 concentrations in full thickness colon homogenates from SHIP WT mice after DSS treatment, whereas no differences were observed for SHIP def mice. There was a trend to higher IL-4 concentrations in full thickness colon homogenates from SHIP def mice compared to SHIP WT mice after DSS treatment, but the difference between groups of 8 and 6 mice did not reach statistical significance.

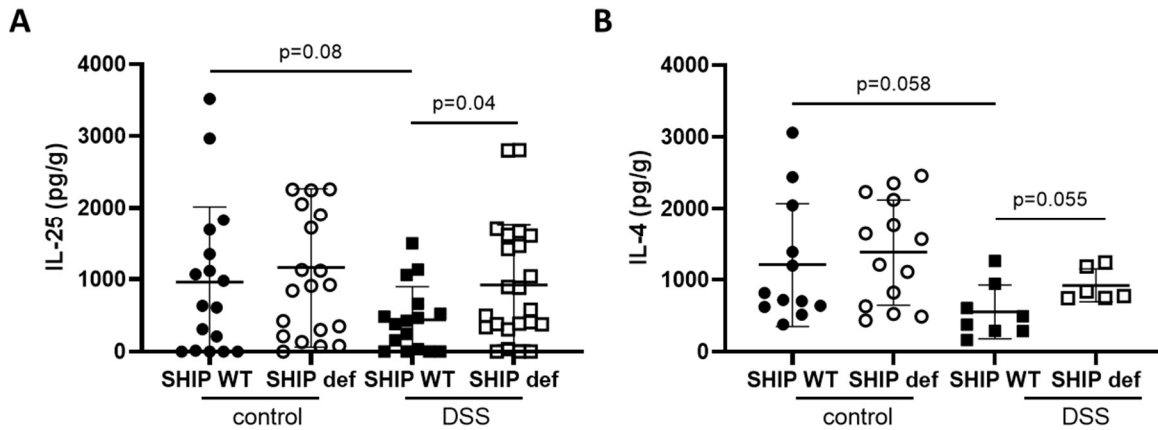


Fig 3.6. SHIP deficiency in tuft cells leads to higher IL-25 concentrations after DSS treatment.

Full thickness colonic tissue homogenates from SHIP WT and SHIP def mice that were untreated (control) or treated with DSS were assayed for (A) IL-25 and (B) IL-4. Points represent individual mice and lines show mean \pm SD for each group. For IL-25, $n = 17$ SHIP WT and 20 SHIP def mice that were not treated with DSS. $n = 16$ SHIP WT and 23 SHIP def DSS-treated mice. For IL-4, $n = 12$ SHIP WT and 14 SHIP def mice that were not treated with DSS. $n = 8$ SHIP WT and 6 SHIP def DSS-treated mice. Circle data points represent control mice and square data points represent DSS-treated mice. Closed and open points represent SHIP WT and SHIP def mice, respectively. p values are for comparisons indicated and were determined using an unpaired two-tailed t -test. Comparisons not indicated were not significantly different.

To determine whether higher IL-25 concentrations lead to higher concentrations of the type 2 cytokines IL-5 and IL-13, I assayed full thickness colon homogenates from SHIP WT and SHIP def mice that were untreated or treated with DSS. IL-33 concentrations were also measured, as it has been reported to drive colonic ILC2 activation during *C. difficile* infection, which induces intestinal inflammation¹⁷⁴. Concentrations of IL-5, IL-13, and IL-33 in SHIP WT and SHIP def mice were similar at baseline and after DSS treatment (Fig 3.7). IL-5 and IL-13 concentrations were lower in both SHIP WT and SHIP def mice after DSS treatment. These data suggest that these cytokines do not contribute to the exacerbated DSS-induced colitis in tuft cell-specific SHIP-deficient mice.

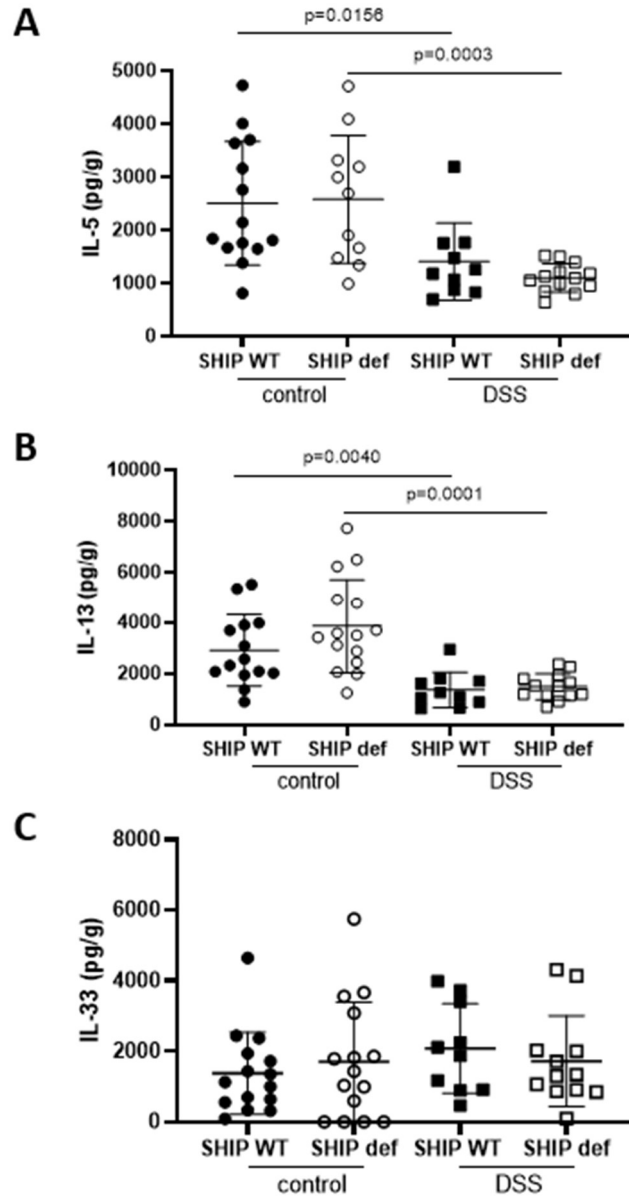


Fig 3.7. Colonic IL-5, IL-13, and IL-33 concentrations are not higher in tuft cell-specific SHIP-deficient mice.

Full thickness colonic tissue homogenates from SHIP WT and SHIP def mice that were untreated (control) or treated with DSS were assayed for (A) IL-5, (B) IL-13, and (C) IL-33. Points represent individual mice and lines show mean \pm SD for each group. For IL-5, n = 14 SHIP WT and 11 SHIP def mice that were not treated with DSS. n = 10 SHIP WT and 13 SHIP def DSS-treated mice. For IL-13, n = 14 SHIP WT and 15 SHIP def mice that were not treated with DSS. n = 10 SHIP WT and 13 SHIP def DSS-treated mice. For IL-33, n = 15 SHIP WT and 15 SHIP def mice that were not treated with DSS. n = 10 SHIP WT and 12 SHIP def DSS-treated mice. Circle data points represent control mice and square data points represent DSS-treated mice. Closed and open points represent SHIP WT and SHIP def mice, respectively. p values are for

comparisons indicated and were determined using an unpaired two-tailed *t*-test. Comparisons not indicated were not significantly different.

In the absence of overt increases (and instead, decreases) in predicted up-regulated type 2 cytokines after DSS treatment, I next asked whether type 1 cytokines that have been associated with inflammation in DSS-induced colitis were higher in SHIP def mice with more severe pathology. Cytokines associated with increased type 1 immune responses and DSS-induced colitis, IL-1 β , TNF, and IL-6, were measured by ELISA in full thickness colon homogenates from SHIP WT and SHIP def mice at baseline and after DSS treatment. Colon homogenates from SHIP WT and SHIP def mice had similar IL-1 β , TNF, and IL-6 concentrations at baseline and after DSS treatment (Fig 3.8). Both SHIP WT and SHIP def mice had significantly higher IL-1 β concentrations after DSS treatment. In contrast, both SHIP WT and SHIP def mice had lower TNF concentrations after DSS treatment compared to that measured in untreated mice. No significant differences in IL-6 concentrations were observed for SHIP WT and SHIP def mice after DSS treatment compared to control mice.

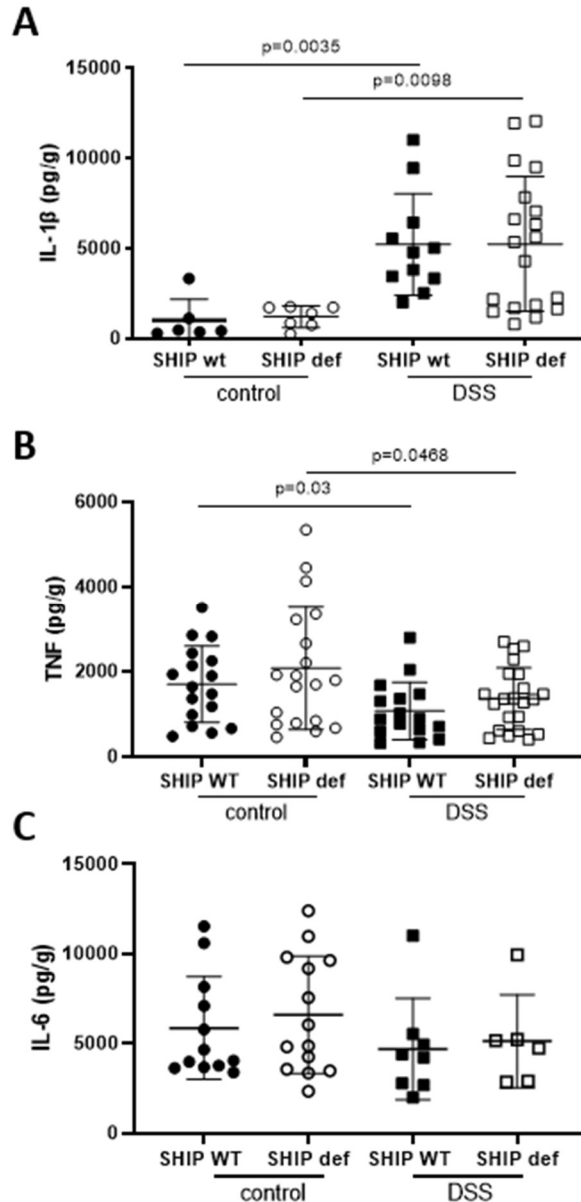


Fig 3.8. Type 1 pro-inflammatory cytokine concentrations are not higher due to tuft cell-specific SHIP deficiency after DSS treatment.

Full thickness colonic tissue homogenates from SHIP WT and SHIP def mice that were untreated (control) or treated with DSS were assayed for type 1 pro-inflammatory cytokines (A) IL-1 β , (B) TNF, and (C) IL-6. Points represent individual mice and lines show mean \pm SD for each group. For IL-1 β , n = 6 SHIP WT and 7 SHIP def mice that were not treated with DSS. n = 11 SHIP WT and 19 SHIP def DSS-treated mice. For TNF, n = 17 SHIP WT and 19 SHIP def mice that were not treated with DSS. n = 16 SHIP WT and 22 SHIP def DSS-treated mice. For IL-6, n = 12 SHIP WT and 14 SHIP def mice that were not treated with DSS. n = 8 SHIP WT and 6 SHIP def DSS-treated mice. Circle data points represent control mice and square data points represent DSS-treated mice. Closed and open points represent SHIP WT and SHIP def mice, respectively.

p values are for comparisons indicated and were determined using an unpaired two-tailed *t*-test. Comparisons not indicated were not significantly different.

McGinty *et al.* (2020) suggested that signals in addition to IL-25 may regulate the tuft cell-ILC2 circuit¹¹⁵. Specifically, their results indicate that cysteinyl leukotrienes have a role in activating type 2 immunity during helminth infection and may cooperate with IL-25 in context-specific regulation of tuft cell-ILC2 circuits within the small intestine¹¹⁵. Thus, I evaluated whether SHIP deficiency in tuft cells affects concentrations of cysteinyl leukotrienes during DSS-induced colitis. The cysteinyl leukotriene assay kit used included a pre-coated goat anti-mouse plate, so the colon homogenates from SHIP WT and def mice could contain antibodies that interfere with the assay. Only samples with strong correlation ($\leq 20\%$ difference) between two different dilutions were included in my analyses. Full thickness colon homogenates from untreated and DSS-treated SHIP WT and SHIP def mice had similar concentrations of cysteinyl leukotrienes (Fig 3.9). This suggests that cysteinyl leukotrienes do not contribute to exacerbated pathology in tuft cell-specific SHIP def mice during DSS-induced colitis.

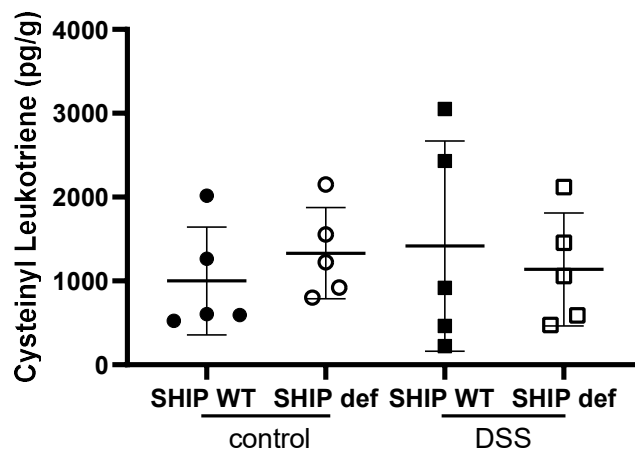


Fig 3.9. Cysteinyl leukotrienes concentrations are not higher due to tuft cell-specific SHIP deficiency.

Cysteinyl leukotriene concentrations in full thickness colonic tissue homogenates from control and DSS-treated SHIP WT and SHIP def mice. Points represent individual mice and lines show mean \pm SD for each group. $n = 5$ mice per group. Circle data points represent control mice and

square data points represent DSS-treated mice. Closed and open points represent SHIP WT and SHIP def mice, respectively. No statistically significant differences were found by an unpaired two-tailed *t*-test between untreated or DSS-treated SHIP WT and SHIP def mice.

3.3 SHIP deficiency causes reduced COX activity during DSS-induced colitis

Tuft cells produce COX1 and COX2, which convert arachidonic acid to prostaglandins that regulate inflammation and tissue repair. Since tuft cell activity (as suggested by IL-25 concentrations) is higher in SHIP def mice, COX activity levels may be higher, promoting more inflammation. To determine whether tuft cell-derived COX contributes to DSS-induced colitis, I performed COX activity assays on full thickness colonic tissue homogenates from SHIP WT and SHIP def mice. There was no significant difference in COX activity in the colon homogenates of untreated SHIP WT and SHIP def mice (Fig 3.10). After DSS treatment, COX activity was lower in both SHIP WT and SHIP def mice, and there was significantly lower COX activity in SHIP def mice compared to SHIP WT mice.

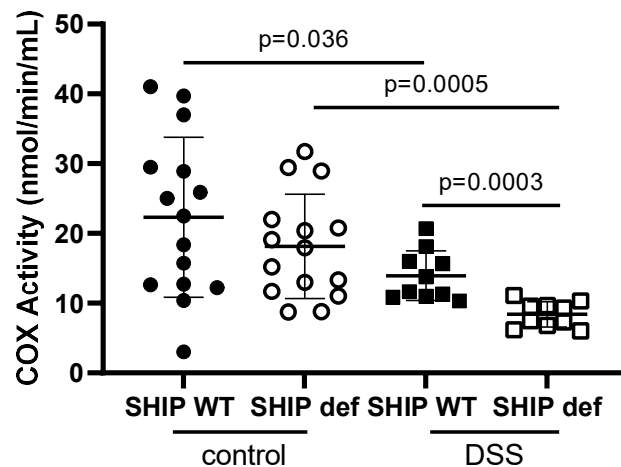


Fig 3.10. COX activity is reduced in mice with SHIP-deficient tuft cells after DSS treatment.

COX activity in full thickness colonic tissue homogenates from control and DSS-treated SHIP WT and SHIP def mice. Points represent individual mice and lines show mean \pm SD for each group. *n* = 15 for both SHIP WT and SHIP def mice that were not treated with DSS. *n* = 10 for both SHIP WT and SHIP def DSS-treated mice. Circle data points represent control mice and square data points represent DSS-treated mice. Closed and open points represent SHIP WT and

SHIP def mice, respectively. *p* values were determined using an unpaired two-tailed *t*-test. Comparisons not indicated were not significantly different.

These data suggest that higher COX activity does not contribute to inflammation or exacerbated colitis in SHIP def mice. Instead, reduced COX activity correlated with worsened disease, so COX may be protective. However, during DSS-induced colitis, increased inflammation in SHIP def mice may result in increased loss of epithelial cells, including tuft cells. Consequently, COX activity may be lower due to loss of COX-expressing tuft cells. To address this, I stained tuft cells for DCLK1 to quantify the percentage of tuft cells in total epithelial cells and normalize COX activity to tuft cell percentage (Fig 3.11). Tuft cell percentages were determined to account for differences in cross-section sizes between mice (Fig 3.11B). Crypt length did not differ significantly between untreated or DSS-treated SHIP WT and SHIP def mice.

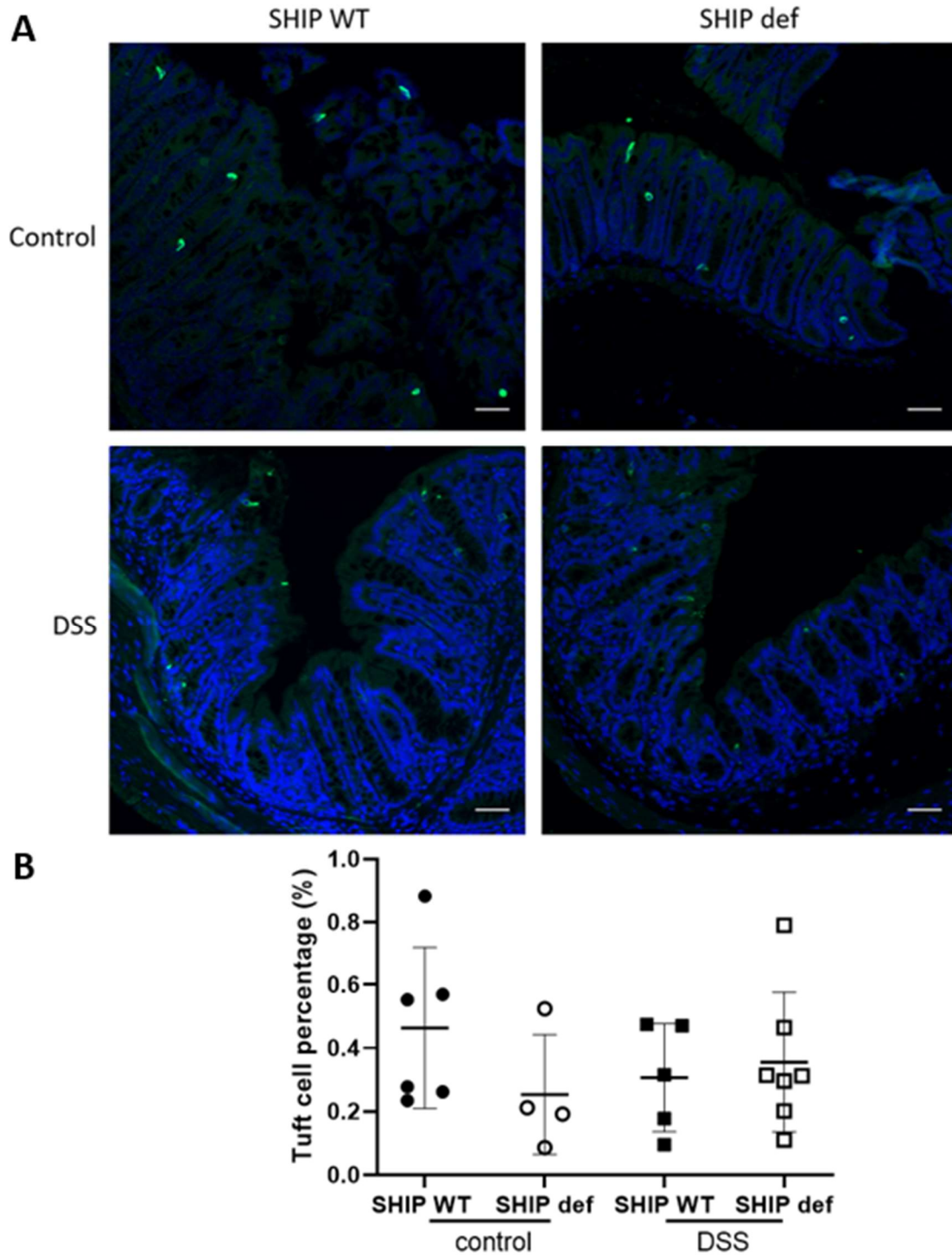


Fig 3.11. SHIP deficiency in tuft cells does not change colonic tuft cell percentage after DSS treatment.

A) Immunofluorescent staining of DCLK1 (green) and DAPI (blue) in colonic cross-sections from 8-week-old control and DSS-treated SHIP WT and SHIP def mice. Photographs were taken at a magnification of 20 \times . Scale bars = 50 μ m. Images shown are representative of 11-16 mice

per group. (B) Percentage of tuft cells in total epithelial cells in the colonic cross-sections from control and DSS-treated SHIP WT and SHIP def mice. Averaged totals from 4-6 representative fields in 1 cross-section per mouse. Points represent individual mice and lines show mean \pm SD for each group. $n = 6$ SHIP WT and 4 SHIP def mice that were not treated with DSS. $n = 5$ SHIP WT and 7 SHIP def DSS-treated mice. Circle data points represent control mice and square data points represent DSS-treated mice. Closed and open points represent SHIP WT and SHIP def mice, respectively. No statistically significant differences were found by an unpaired two-tailed *t*-test between untreated or DSS-treated SHIP WT and SHIP def mice.

Tuft cell percentage in total epithelial cells was similar for untreated and DSS-treated SHIP WT and SHIP def mice, with means ranging from 0.25-0.46% (Fig 3.11B). This suggests that SHIP deficiency in tuft cells does not cause tuft cell hyperplasia. Similarly, tuft cell percentages were not significantly affected after DSS treatment for SHIP WT or SHIP def mice. By normalizing COX activity according to tuft cell percentage in each mouse, I determined that SHIP WT and SHIP def mice had similar COX activity without and after DSS treatment (Fig 3.12). However, SHIP def mice had significantly lower COX activity after DSS treatment compared to untreated mice (Fig 3.12), as observed for COX activity prior to normalization (Fig 3.10).

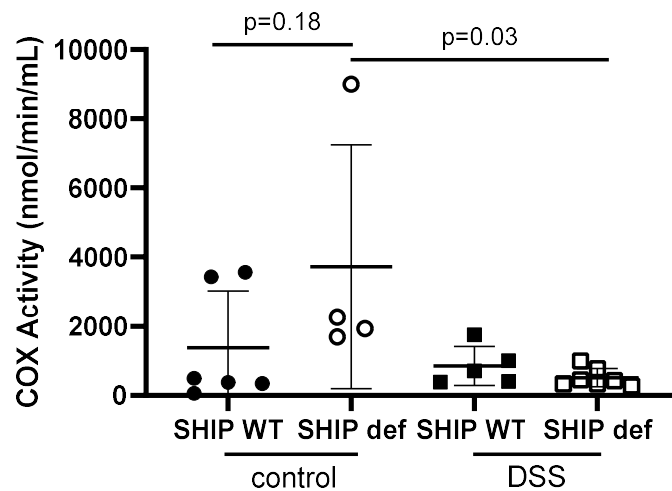


Fig 3.12. COX activity is lower after DSS treatment when normalized to tuft cell percentage in mice with SHIP-deficient tuft cells.

COX activity in full thickness colonic tissue homogenates normalized to tuft cell percentage in total epithelial cells from control and DSS-treated SHIP WT and SHIP def mice. Points represent

individual mice and lines show mean \pm SD for each group. n = 6 SHIP WT and 4 SHIP def mice that were not treated with DSS. n = 5 SHIP WT and 7 SHIP def DSS-treated mice. Circle data points represent control mice and square data points represent DSS-treated mice. Closed and open points represent SHIP WT and SHIP def mice, respectively. p values are for comparisons indicated and were determined using an unpaired two-tailed *t*-test. Comparisons not indicated were not significantly different.

3.4 Comparison of SHIP WT and SHIP def mice after 5 days of DSS treatment

To evaluate COX activity at an earlier timepoint prior to loss of epithelial cells and establish a timepoint with similar disease activity for use in DSS-induced colitis recovery experiments, I assessed the same parameters in SHIP WT and SHIP def mice after 5 days of DSS treatment, when divergence of disease activity was first seen.

SHIP WT and SHIP def mice were harvested after 5 days of DSS treatment. The gross pathology of colons for SHIP WT and SHIP def mice on day 5 were similar, with minimal shortening (Fig 3.13A). The colon lengths of SHIP WT and SHIP def mice were similar (Fig 3.13B), suggesting that there is no difference in disease on day 5. Further supporting this, weight loss indicated by percentage and weight scores on Days 0-5 of DSS treatment for both SHIP WT and SHIP def mice was minimal (Fig 3.14). Additionally, rectal bleeding, stool consistency, and DAI scores were similar between SHIP WT and SHIP def mice (Fig 3.15).

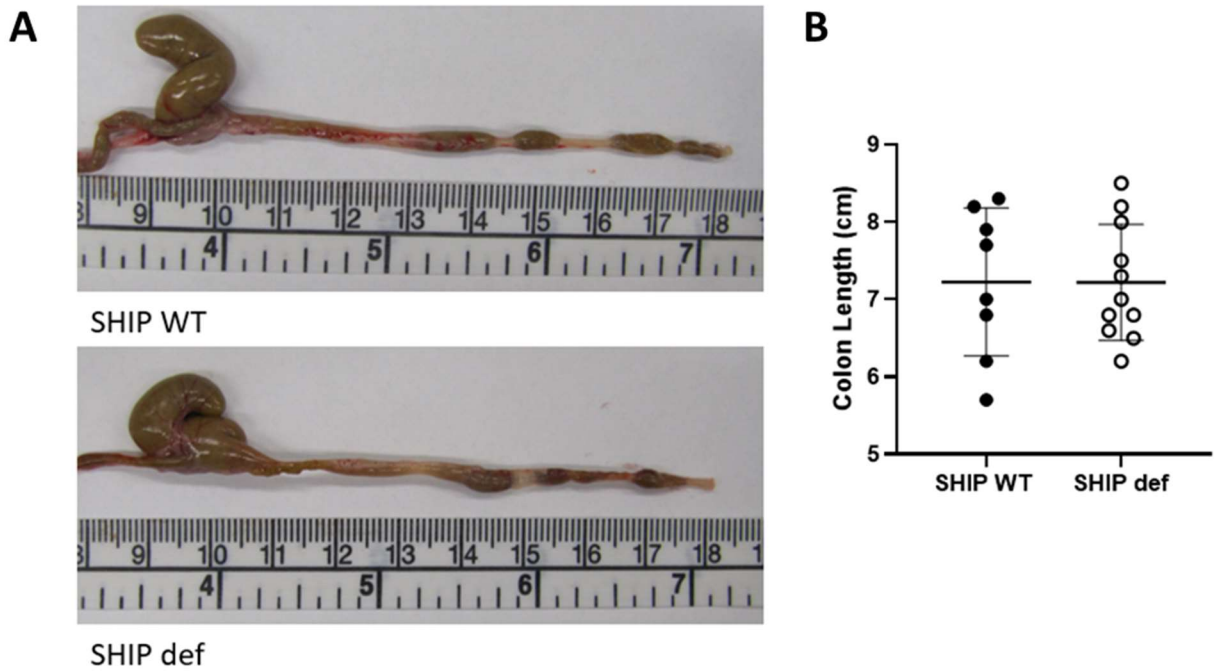


Fig 3.13. SHIP deficiency in tuft cells causes minimal colon shortening after 5 days of DSS treatment.

(A) Gross pathology of colons from SHIP WT and SHIP def mice after 5 days of DSS treatment. Images shown are representative of 8 SHIP WT and 11 SHIP def mice. (B) Colon lengths for SHIP WT and SHIP def mice that received DSS for 5 days. Points represent individual mice and lines show mean \pm SD for each group. No statistically significant differences were found by an unpaired two-tailed *t*-test between SHIP WT and SHIP def mice.

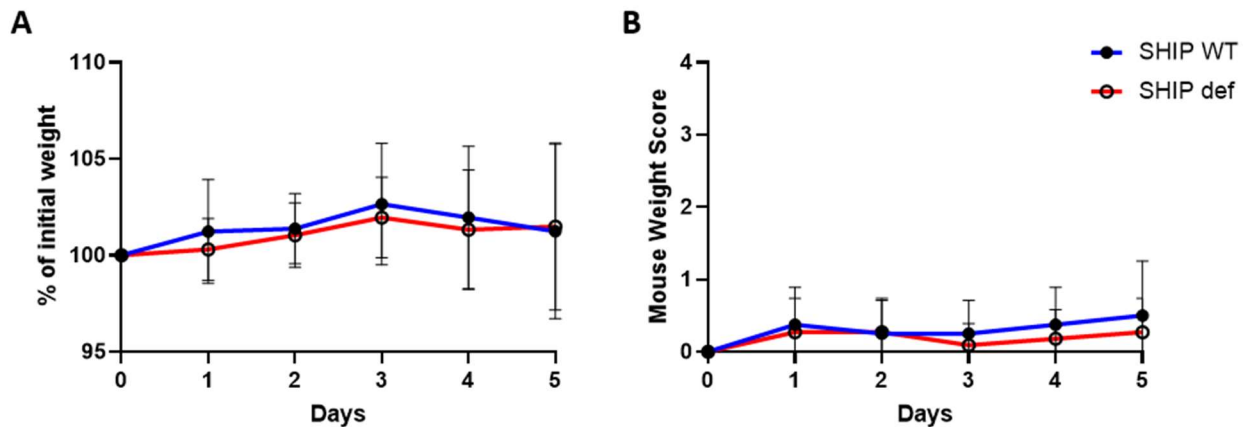


Fig 3.14. SHIP deficiency in tuft cells does not exacerbate weight loss within 5 days of DSS treatment.

(A) Weight indicated by percentage of initial weight. (B) Weight loss scores assigned on a scale of 0-4. 0 = 0% weight loss; 1 = 1-5% weight loss; 2 = 5-10% weight loss; 3 = 10-15% weight loss; 4 = >15% weight loss. Points represent the average of all mice in each group with error bars

representing \pm SD. $n = 8$ SHIP WT and 11 SHIP def mice. SHIP WT and SHIP def mice are represented by the blue and red lines, respectively. No statistically significant differences were found by multiple unpaired t -tests between SHIP WT and SHIP def mice with correction for multiple comparisons by the two-stage step-up method of Benjamini, Krieger and Yekutieli.

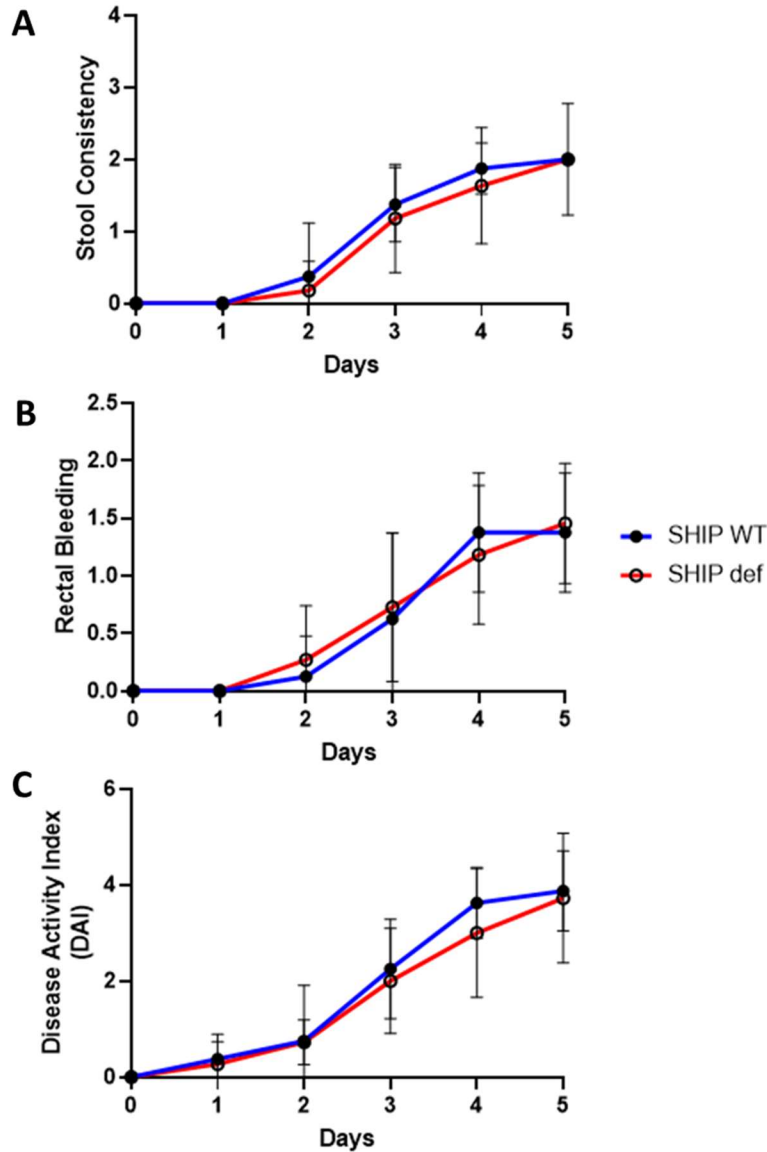


Fig 3.15. SHIP deficiency in tuft cells does not exacerbate disease activity within 5 days of DSS treatment.

(A) Stool consistency scores assigned on a scale of 0-4. 0 = normal stool in pellet form; 1 = loose stool; 2 = very loose stool; 3 = diarrhea; 4 = no formed stool. (B) Rectal bleeding scores assigned on a scale of 0-4. 0 = no blood in stool; 1 = blood detectable on hemocult paper; 2 = blood visible in stool; 3 = extensive blood in stool; 4 = extensive blood in stool and around anus. (C) DAI summing scores for stool consistency, rectal bleeding, and weight loss. Points represent the

average of all mice in each group with error bars representing \pm SD. $n = 8$ SHIP WT and 11 SHIP def mice. SHIP WT and SHIP def mice are represented by the blue and red lines, respectively. No statistically significant differences were found by multiple unpaired t -tests between SHIP WT and SHIP def mice with correction for multiple comparisons by the two-stage step-up method of Benjamini, Krieger and Yekutieli.

To determine if differences in disease activity were location-dependent in the colons of SHIP WT and SHIP def mice after 5 days of DSS treatment, swiss rolls of colons were assessed for histological damage (Fig 3.16). There was moderate histological damage throughout the colons of SHIP WT and SHIP def mice. No significant differences in histological damage were observed between the proximal and distal colon for DSS-treated SHIP WT and SHIP def mice. Thus, cross-sections from the distal colon were used in histological damage assessments. Additionally, homogenates of entire colons were used in cytokine assays.

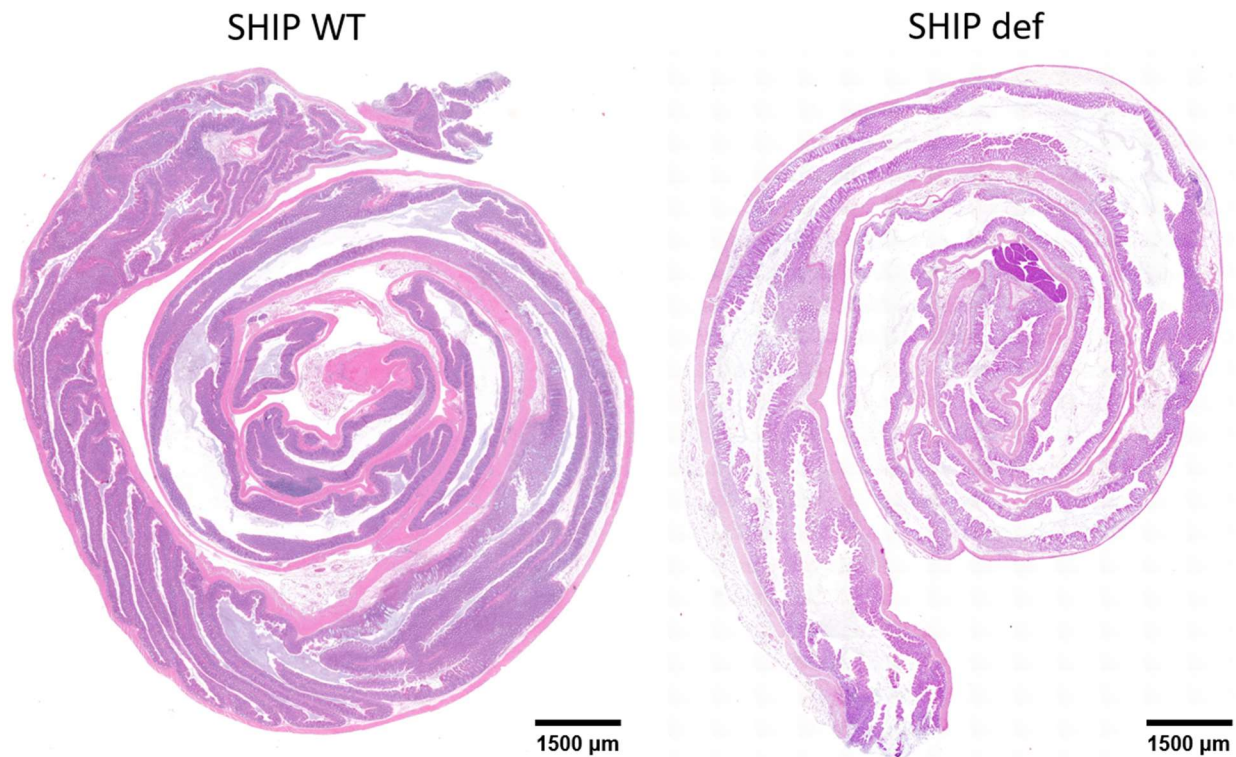


Fig 3.16. Histological damage after 5 days of DSS treatment does not significantly differ across the length of the colon due to SHIP deficiency in tuft cells.

H&E-stained colonic tissue cross-sections of Swiss rolls from SHIP WT and SHIP def mice that were treated with DSS for 5 days. The distal end of the colon is in the center of the roll. Photographs were taken at 10× magnification. Scale bars = 1500 μm.

After 5 days of DSS treatment, cross-sections of the colons of SHIP WT and SHIP def mice were collected and H&E-stained (Fig 3.17A). As described in Section 3.1, the composite score of goblet cell loss, muscle thickening, edema, ulceration, and immune cell infiltration was calculated to quantify histological damage. There was moderate histological damage for both SHIP WT and SHIP def mice after 5 days of DSS treatment (Fig 3.17A). SHIP WT and SHIP def mice had similar histological damage scores, suggesting that there is no significant difference in disease severity after 5 days of DSS treatment (Fig 3.17B).

was a trend to higher IL-5 levels in SHIP def mice after 5 days of DSS treatment, but the difference between groups of 7 and 10 mice did not reach statistical significance (Fig 3.19A).

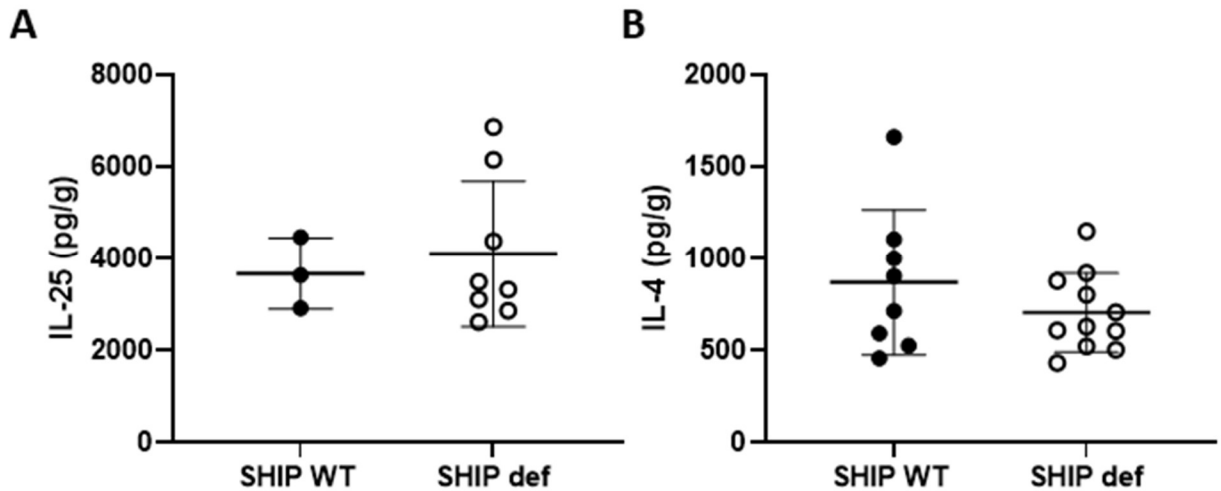


Fig 3.18. IL-25 and IL-4 concentrations are not higher in mice with SHIP-deficient tuft cells after 5 days of DSS treatment.

Full thickness colonic tissue homogenates from SHIP WT and SHIP def mice after 5 days of DSS treatment were assayed for (A) IL-25 and (B) IL-4. Points represent individual mice and lines show mean \pm SD for each group. For IL-25, n = 3 SHIP WT and 9 SHIP def mice. For IL-4, n = 8 SHIP WT and 11 SHIP def mice. No statistically significant differences were found by an unpaired two-tailed *t*-test between SHIP WT and SHIP def mice.

To determine if type 1 pro-inflammatory cytokines may be involved in disease activity after 5 days of DSS treatment, I assayed IL-1 β , TNF, and IL-6 in full thickness colon homogenates from SHIP WT and SHIP def mice. SHIP WT and SHIP def mice had similar IL-1 β , TNF, and IL-6 concentrations after 5 days of DSS treatment (Fig 3.20). This follows the similar disease severity in SHIP WT and SHIP def mice suggested by disease scores, histological damage, and gross pathology.

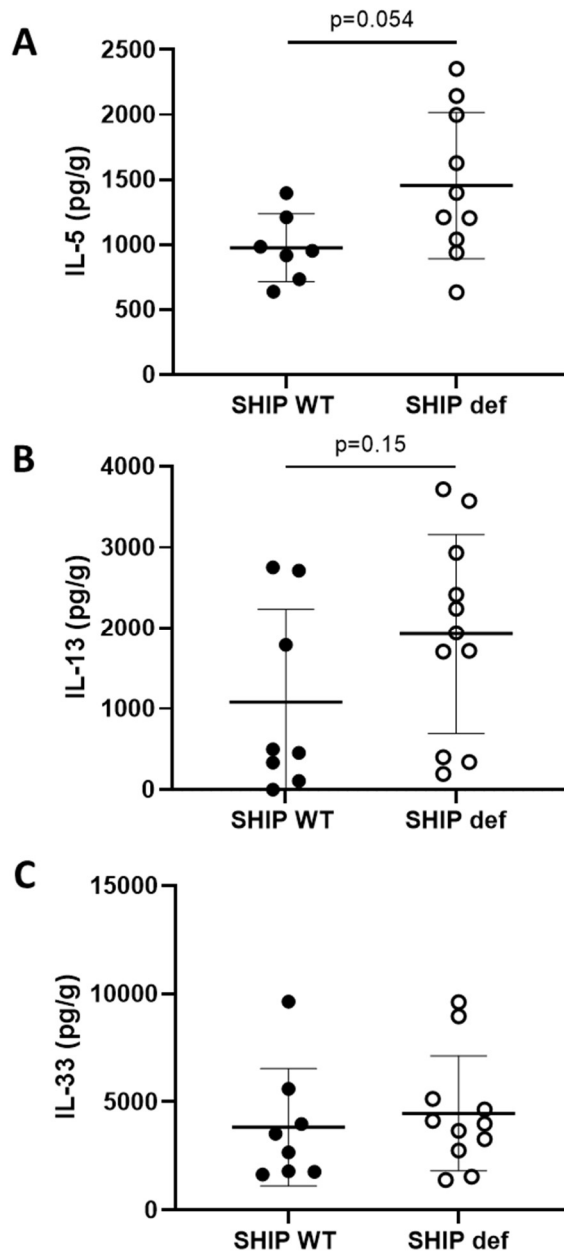


Fig 3.19. IL-5, IL-13, and IL-33 concentrations are not significantly higher due to SHIP deficiency in tuft cells in mice treated with DSS for 5 days.

Full thickness colonic tissue homogenates from SHIP WT and SHIP def mice after 5 days of DSS treatment were assayed for (A) IL-5, (B) IL-13, and (C) IL-33. Points represent individual mice and lines show mean \pm SD for each group. For IL-5, $n = 7$ SHIP WT and 10 SHIP def mice. For IL-13, $n = 8$ SHIP WT and 11 SHIP def control mice. $n = 10$ SHIP WT and 13 SHIP def DSS-treated mice. For IL-33, $n = 8$ SHIP WT and 11 SHIP def control mice. $n = 10$ SHIP WT and 12 SHIP def DSS-treated mice. p values are for comparisons indicated and were determined using an unpaired two-tailed t -test. No statistically significant difference in IL-33 was found by an unpaired two-tailed t -test between SHIP WT and SHIP def mice.

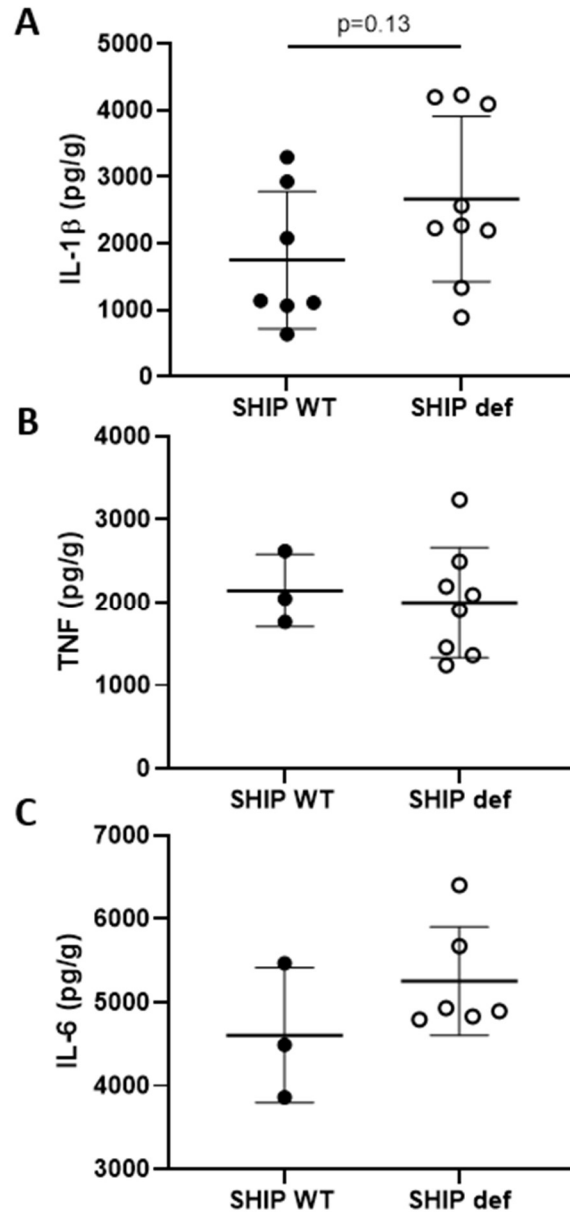


Fig 3.20. Type 1 pro-inflammatory cytokines are not higher due to SHIP deficiency in tuft cells after 5 days of DSS treatment.

Full thickness colonic tissue homogenates from SHIP WT and SHIP def mice harvested after 5 days of DSS treatment were assayed for type 1 pro-inflammatory cytokines (A) IL-1 β , (B) TNF, and (C) IL-6. Points represent individual mice and lines show mean \pm SD for each group. For IL-1 β , $n = 7$ SHIP WT and 9 SHIP def mice. For TNF, $n = 3$ SHIP WT and 8 SHIP def mice. For IL-6, $n = 3$ SHIP WT and 6 SHIP def mice. Closed and open points represent SHIP WT and SHIP def mice, respectively. $p = 0.13$ was determined using an unpaired two-tailed t -test. No statistically significant differences were found by an unpaired two-tailed t -test between SHIP WT and SHIP def mice.

Finally, full thickness colon homogenates from SHIP WT and SHIP def mice had similar COX activity after 5 days of DSS treatment (Fig 3.21). This further suggests that higher COX activity at an earlier timepoint (preceding loss of epithelial cells) does not contribute to inflammation or the exacerbated colitis in SHIP def mice that is seen after 7 days of DSS treatment.

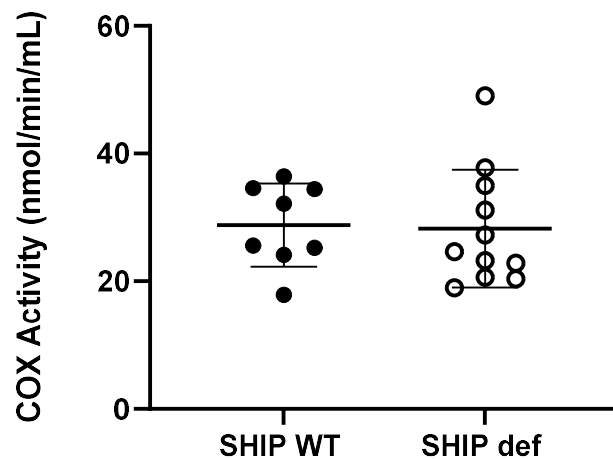


Fig 3.21. SHIP deficiency in tuft cells does not affect COX activity after 5 days of DSS treatment.

COX activity in full thickness colonic tissue homogenates from control and DSS-treated SHIP WT and SHIP def mice. Points represent individual mice and lines show mean \pm SD for each group. $n = 8$ SHIP WT and 11 SHIP def mice. No statistically significant differences were found by an unpaired two-tailed t -test between SHIP WT and SHIP def mice.

3.5 Examining a potential role for SHIP deficiency in tuft cells during recovery from DSS-induced colitis

In addition to inflammation, type 2 immunity and prostaglandins are involved in restoration of homeostasis post-injury. Given that there are higher IL-25 concentrations and lower COX activity in full thickness colonic tissue homogenates from SHIP def mice after 7 days of DSS treatment, type 2 immune activity and COX activity may impact recovery in mice

after DSS-induced colitis. To address this hypothesis, I examined recovery after 5 days of treatment with DSS. The results of Section 3.4 demonstrated that SHIP WT and SHIP def mice had similar disease severity after 5 days of DSS treatment. Thus, I induced colitis for 5 days using DSS and harvested colons from SHIP WT and SHIP def mice after 5 days of recovery. The gross pathology of colons for SHIP WT and SHIP def mice after 5 days of recovery were similar, with minimal colon shortening (Fig 3.22A). Furthermore, the colon lengths of SHIP WT and SHIP def mice were similar (Fig 3.22B), suggesting that there is no difference in disease severity.

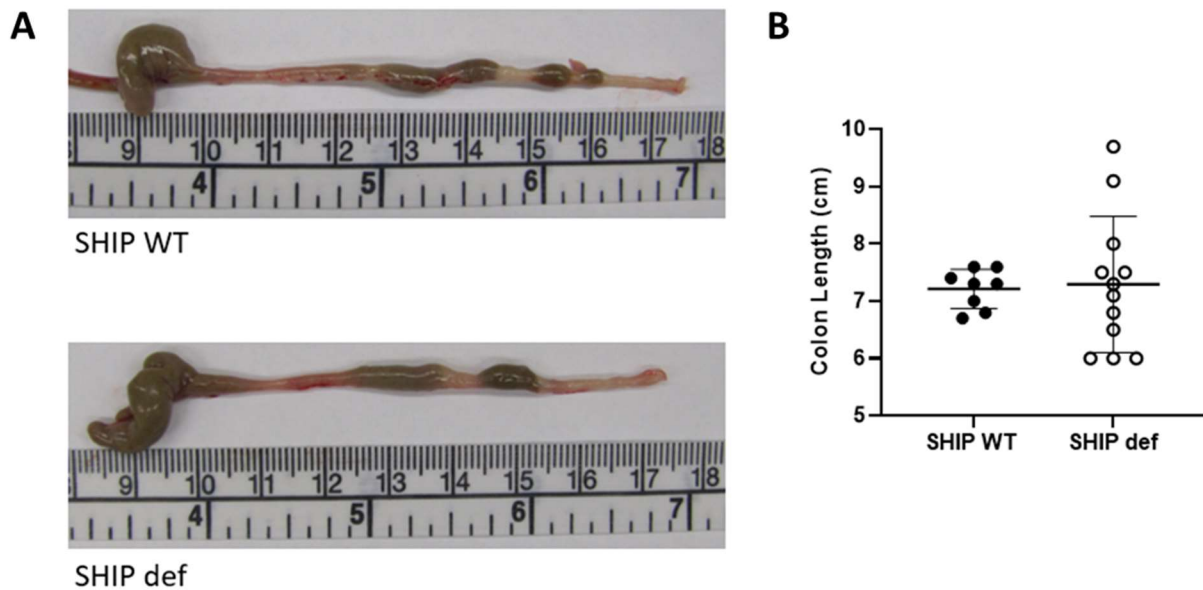


Fig 3.22. SHIP deficiency in tuft cells does not cause differences in colon length after 5 days of recovery from DSS-induced colitis.

(A) Gross pathology of colons of SHIP WT and SHIP def mice after 5 days of recovery from DSS-induced colitis. Images shown are representative of the average of 8 SHIP WT and 11 SHIP def mice. (B) Colon lengths (cm) for SHIP WT and SHIP def mice after 5 days of recovery from DSS-induced colitis. Points represent individual mice and lines show mean \pm SD for each group. $n = 8$ SHIP WT and 12 SHIP def mice. No statistically significant differences were found by an unpaired two-tailed t -test between SHIP WT and SHIP def mice.

There was no significant difference in weight measured as percentage of initial mouse weight or weight scores between SHIP WT and SHIP def mice throughout 5 days of recovery from DSS-induced colitis (Fig 3.23). SHIP def mice had increased stool consistency scores on Day 3 and rectal bleeding scores on Day 2 of recovery from DSS-induced colitis (Fig 3.24A and Fig 3.24B). There was no significant difference in DAI on any day during DSS-induced colitis recovery. However, there was a trend to higher DAI on Day 2 of recovery for SHIP def mice that did not reach statistical significance (Fig 3.24C).

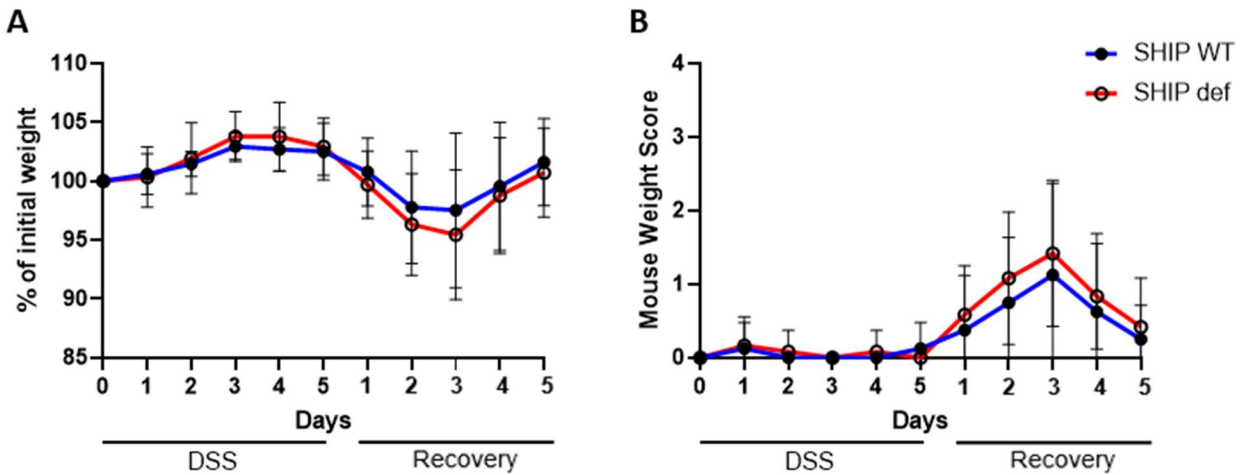


Fig 3.23. SHIP deficiency in tuft cells does not improve weight gain during recovery from DSS-induced colitis.

(A) Weight indicated by percentage of initial weight. (B) Weight loss scores assigned on a scale of 0-4. 0 = 0% weight loss; 1 = 1-5% weight loss; 2 = 5-10% weight loss; 3 = 10-15% weight loss; 4 = >15% weight loss. Points represent the average of all mice in each group with error bars representing \pm SD. $n = 8$ SHIP WT and 12 SHIP def mice. SHIP WT and SHIP def mice are represented by the blue and red lines, respectively. No statistically significant differences were found by multiple unpaired t -tests between SHIP WT and SHIP def mice with correction for multiple comparisons by the two-stage step-up method of Benjamini, Krieger and Yekutieli.

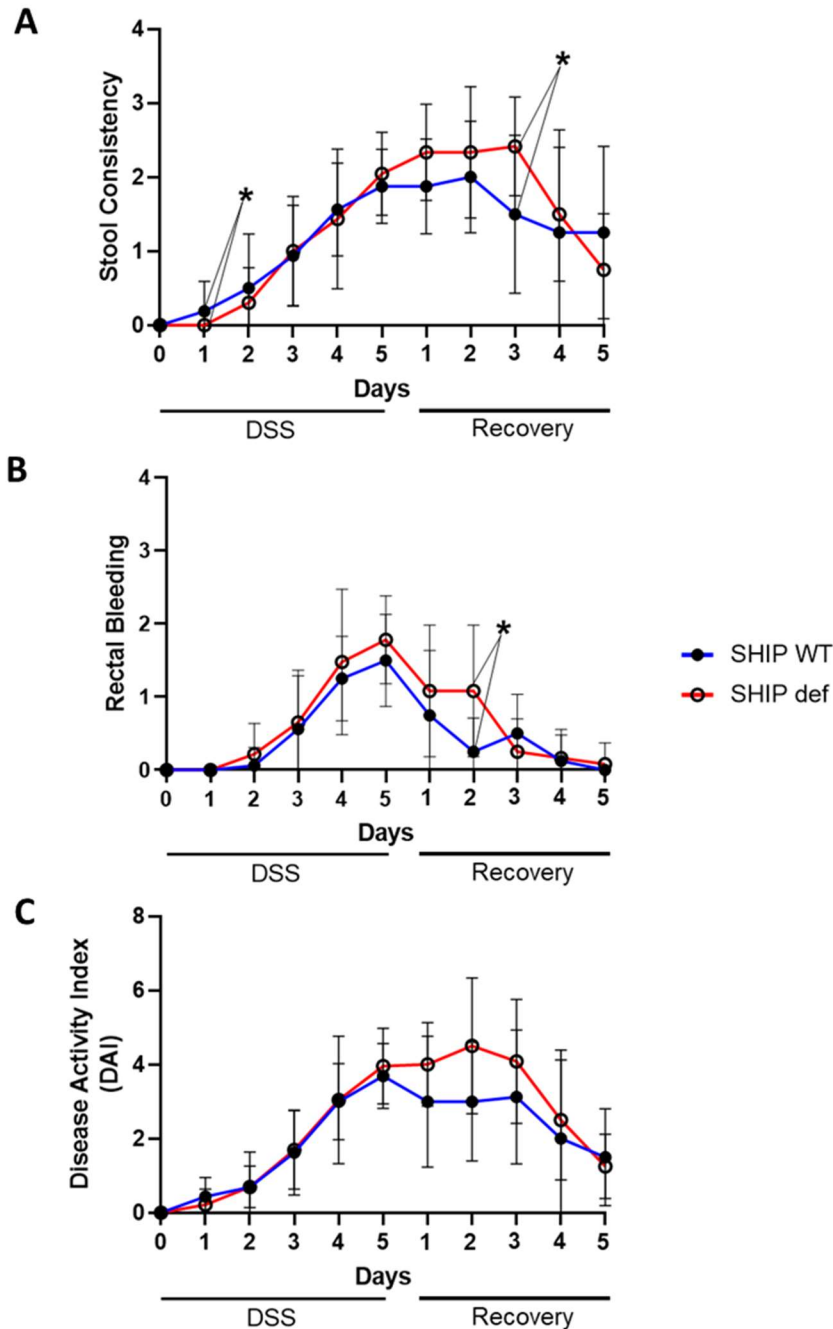


Fig 3.24. SHIP deficiency in tuft cells worsens stool consistency and rectal bleeding during recovery from DSS-induced colitis.

(A) Stool consistency scores assigned on a scale of 0-4. 0 = normal stool in pellet form; 1 = loose stool; 2 = very loose stool; 3 = diarrhea; 4 = no formed stool. (B) Rectal bleeding scores assigned on a scale of 0-4. 0 = no blood in stool; 1 = blood detectable on hemocult paper; 2 = blood visible in stool; 3 = extensive blood in stool; 4 = extensive blood in stool and around anus. (C) DAI summing scores for stool consistency, rectal bleeding, and weight loss. Points represent the average of all mice in each group with error bars representing \pm SD. n = 8 SHIP WT and 12

SHIP def mice. SHIP WT and SHIP def mice are represented by the blue and red lines, respectively. p values are for comparisons indicated and were determined using multiple unpaired *t*-tests with correction for multiple comparisons by the two-stage step-up method of Benjamini, Krieger and Yekutieli. * $p < 0.05$. Comparisons not indicated were not significantly different.

After 5 days of recovery, cross-sections of the colons from SHIP WT and SHIP def mice were collected and H&E-stained (Fig 3.25A). As described in Section 3.1, the composite score for goblet cell loss, muscle thickening, edema, ulceration, and immune cell infiltration was used to quantify histological damage. There was minimal histological damage for both SHIP WT and SHIP def mice (Fig 3.25B). SHIP WT and SHIP def mice had similar composite histological damage scores, suggesting that there was no significant difference in disease severity after 5 days of recovery from DSS-induced colitis (Fig 3.25B). However, there were trends to decreased immune cell infiltration and increased muscle thickness in SHIP def mice that did not reach statistical significance (Fig 3.26).

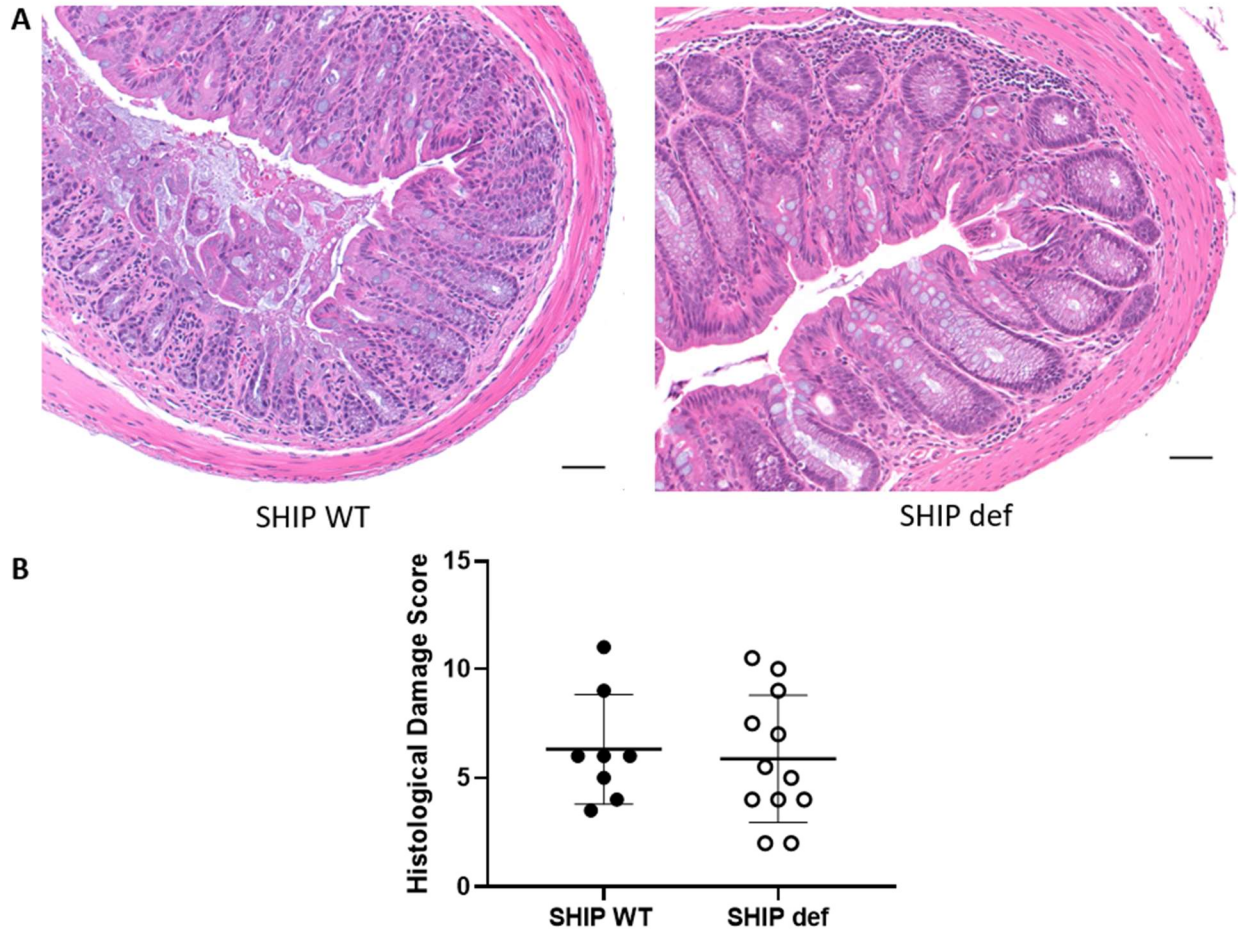


Fig 3.25. SHIP deficiency in tuft cells does not improve histological damage during DSS-induced colitis recovery.

(A) H&E-stained colon cross-sections of SHIP WT and SHIP def mice after 5 days of recovery from DSS-induced colitis. Photographs were taken at a magnification of 20 \times . Scale bars = 50 μ m. (B) Histological damage scores summing scores for crypt architecture loss, ulceration, goblet cell loss, immune cell infiltration, edema, and muscle thickening for SHIP WT and SHIP def mice. Points represent individual mice and lines show mean \pm SD for each group. n = 8 SHIP WT and 12 SHIP def mice. No statistically significant differences were found by an unpaired two-tailed *t*-test between SHIP WT and SHIP def mice.

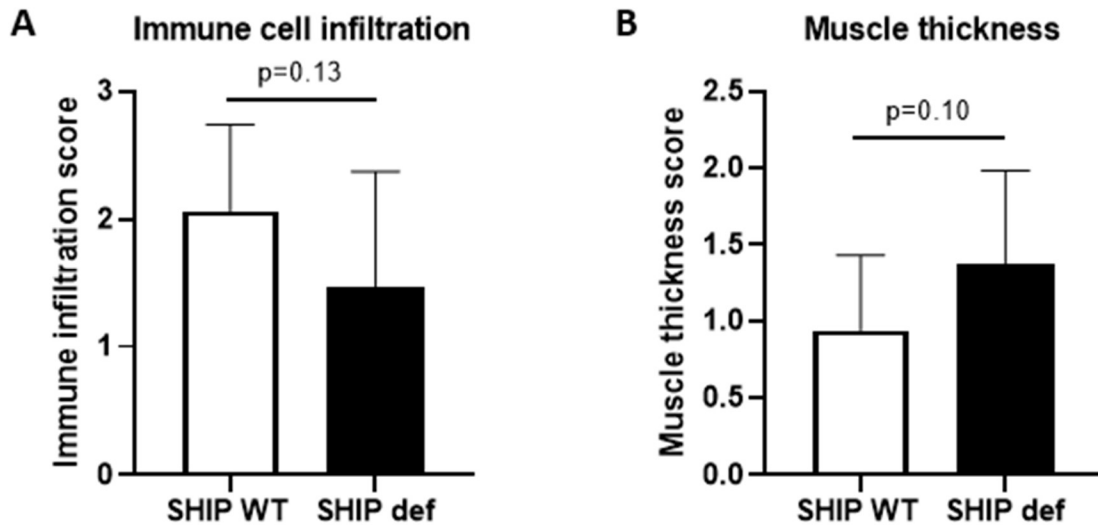


Fig 3.26. SHIP deficiency in tuft cells may lead to reduced immune cell infiltration and increased muscle thickness after 5 days of recovery from DSS-induced colitis.

(A) Immune cell infiltration scores for colon cross-sections from SHIP WT and SHIP def mice after 5 days of recovery from DSS-induced colitis. (B) Muscle thickness scores for colon cross-sections from SHIP WT and SHIP def mice following 5 days of DSS-induced colitis recovery. Bars represent means and lines show \pm SD for each group. $n = 8$ SHIP WT and 12 SHIP def mice. p values were determined using an unpaired two-tailed t -test.

Type 2 cytokine concentrations were measured in full thickness colon homogenates from SHIP WT and SHIP def mice after 5 days of recovery from DSS-induced colitis. Colon homogenates from SHIP WT and SHIP def mice had similar concentrations of IL-25 and IL-4 (Fig 3.27A, Fig 3.27B), which is consistent with the lack of difference in disease activity. Concentrations of IL-5, IL-13 and IL-33 were also similar (Fig 3.28).

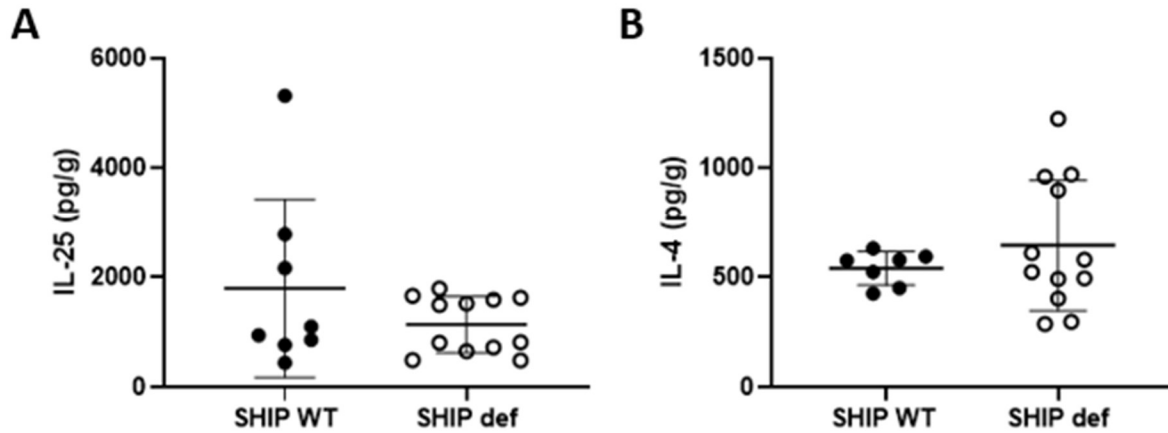


Fig 3.27. IL-25 and IL-4 concentrations are not higher in mice with SHIP-deficient tuft cells after 5 days of recovery from DSS-induced colitis.

Full thickness colonic tissue homogenates from SHIP WT and SHIP def mice after 5 days of recovery from DSS-induced colitis were assayed for (A) IL-25 and (B) IL-4. Points represent individual mice and lines show mean \pm SD for each group. $n = 8$ SHIP WT and 12 SHIP def mice. No statistically significant differences were found by an unpaired two-tailed t -test between SHIP WT and SHIP def mice.

To determine if type 1 pro-inflammatory cytokines are involved in disease activity after 5 days of DSS-induced colitis recovery, I assayed IL-1 β , TNF, and IL-6. SHIP WT and SHIP def mice had similar levels of IL-1 β , TNF, and IL-6 after 5 days of recovery from DSS-induced colitis (Fig 3.29). This is consistent with the similar disease severity indicated by disease scores, histological damage, and gross pathology.

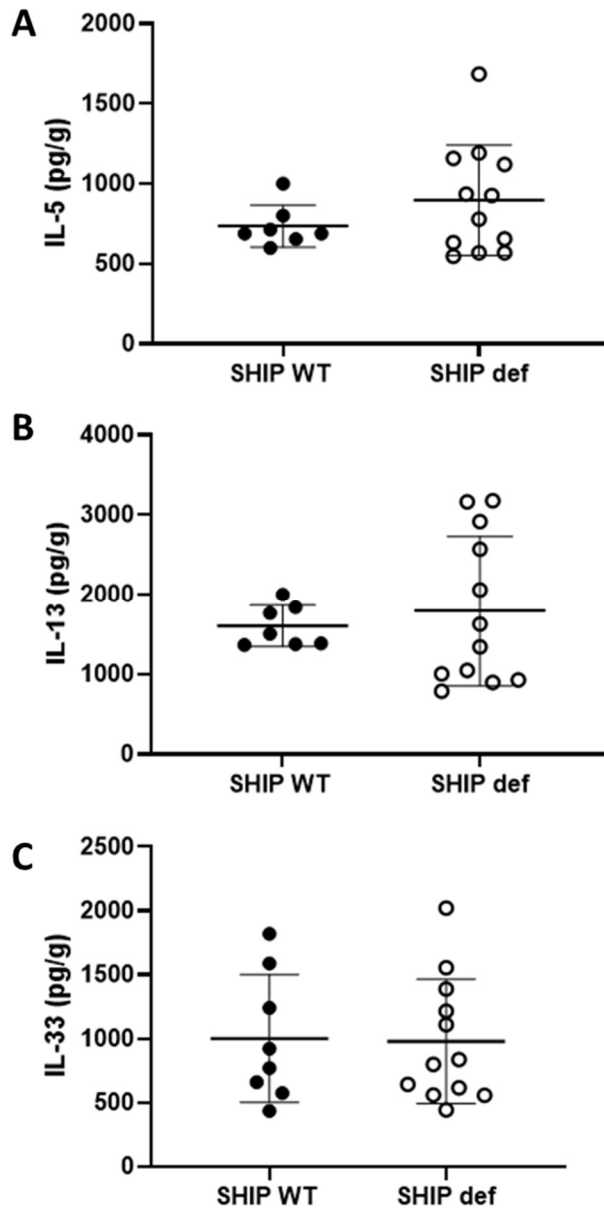


Fig 3.28. IL-5, IL-13, and IL-33 concentrations are not higher due to SHIP deficiency after 5 days of recovery from DSS-induced colitis.

Full thickness colonic tissue homogenates from SHIP WT and SHIP def mice after 5 days of recovery from DSS-induced colitis were assayed for (A) IL-5, (B) IL-13, and (C) IL-33. Points represent individual mice and lines show mean \pm SD for each group. For IL-5 and IL-13, $n = 7$ SHIP WT and 12 SHIP def mice. For IL-33, $n = 8$ SHIP WT and 12 SHIP def control mice. No statistically significant differences were found by an unpaired two-tailed t -test between SHIP WT and SHIP def mice.

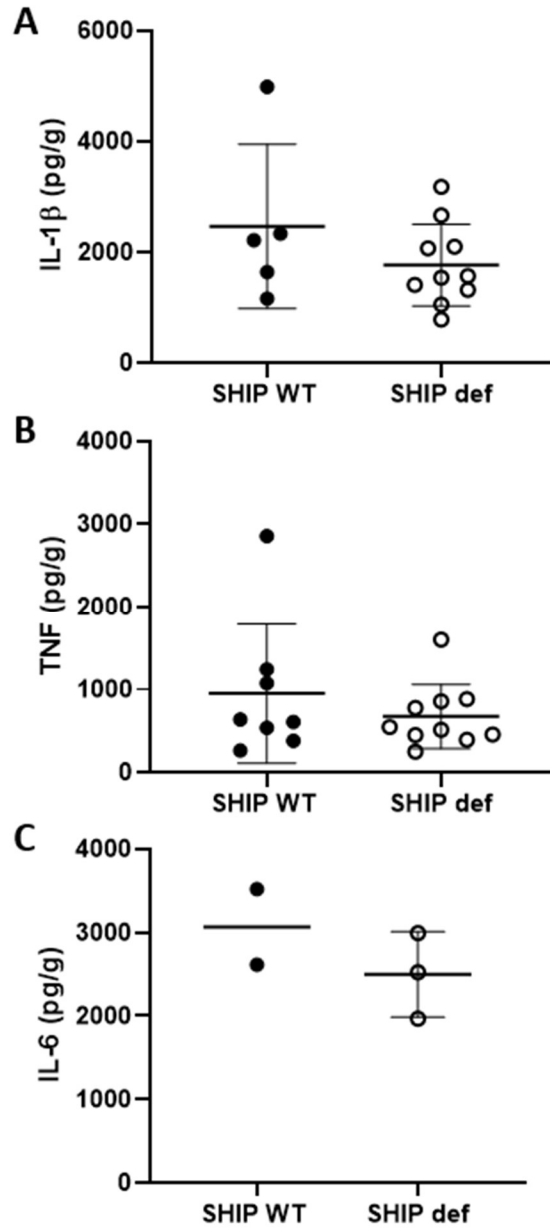


Fig 3.29. Type 1 pro-inflammatory cytokines are not higher due to SHIP deficiency after 5 days of recovery from DSS-induced colitis.

Full thickness colonic tissue homogenates from SHIP WT and SHIP def mice after 5 days of recovery from DSS-induced colitis were assayed for type 1 pro-inflammatory cytokines (A) IL-1 β , (B) TNF, and (C) IL-6. Points represent individual mice and lines show mean \pm SD for each group. For TNF, n = 8 SHIP WT and 9 SHIP def mice. For IL-6, n = 2 SHIP WT and 3 SHIP def mice. Closed and open points represent SHIP WT and SHIP def mice, respectively. No statistically significant differences were found by an unpaired two-tailed *t*-test between SHIP WT and SHIP def mice.

Finally, SHIP WT and SHIP def mice had similar COX activity after 5 days of recovery from DSS-induced colitis (Fig 3.30). This suggests that COX does not exacerbate or protect from colitis after 5 days of recovery.

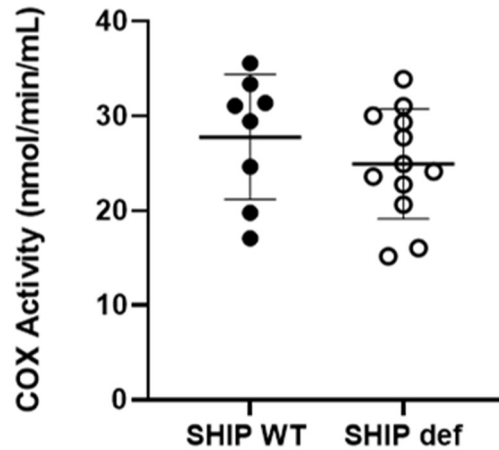


Fig 3.30. SHIP deficiency does not affect COX activity after 5 days of recovery from DSS-induced colitis.

COX activity in full thickness colonic tissue homogenates from control and DSS-treated SHIP WT and SHIP def mice. Points represent individual mice and lines show mean \pm SD for each group. $n = 8$ SHIP WT and 12 SHIP def mice. No statistically significant differences were found by an unpaired two-tailed t -test between SHIP WT and SHIP def mice.

Overall, my DSS-induced colitis recovery experiments suggested modest differences in recovery from DSS-induced colitis between SHIP WT and SHIP def mice. Mice with SHIP-deficient tuft cells had increased rectal bleeding and stool consistency scores during recovery, while displaying trends to less immune cell infiltration and increased muscle thickness.

Chapter 4: Discussion

Tuft cells in the GI tract have a role in chemo-sensing, promoting epithelial cell proliferation and barrier integrity, and activating immune responses⁸⁰. Tuft cell-deficient (*DCLK1* deletion) mice have exacerbated weight loss, barrier dysfunction, fewer proliferating cells, and higher concentrations of pro-inflammatory cytokines IL-1 β and IL-17 during DSS-induced colitis¹²⁸. Similarly, Yi *et al.* (2018) found that intestinal epithelial ablation of *DCLK1* worsened a genetically engineered model of spontaneous microbiota-dependent colitis, including symptoms of reduced body weight, stool loosening, colon thickening, and inflammatory cell infiltrates¹²⁷. Furthermore, *DCLK1* epithelial ablation worsens disease outcome after radiation-induced small intestinal injury due to dysfunctional epithelial regeneration¹⁷⁵. These results suggest that tuft cells have a critical role in regulating colonic inflammation and epithelial integrity in DSS-induced colitis¹²⁸. The effects of hyperresponsive tuft cells have not been studied. The tuft cell-specific SHIP-deficient mouse that we have generated is the first putative gain-of-function model for tuft cells that has been described. I showed that mice with SHIP deficiency in tuft cells had exacerbated colitis after 7 days of DSS challenge. In particular, they had greater weight loss, colon shortening, and histological damage. Taken together, these findings suggest that, like tuft cell deficiency, hyperresponsive tuft cells may worsen inflammation in DSS-induced colitis.

Sensitivity to DSS-induced colitis has been linked to Th1 and Th17 immune responses due to the induction of IL-1 β , TNF- α , IFN- γ production, and IL-17A^{167, 176-179}. As observed in previous studies, I found that DSS challenge caused an increase in IL-1 β concentrations within colon tissue homogenates^{177, 180}. However, I also showed that higher concentrations of IL-1 β did not drive exacerbated colitis in SHIP def mice. This is in contrast to the observations of Ngoh *et*

al. (2016) that IL-1 β contributes to spontaneous ileal inflammation in germ-line SHIP^{-/-} mice¹⁶⁷. My results suggest that a different pro-inflammatory molecule or mechanism is involved in the exacerbation of inflammation for mice with SHIP-deficient tuft cells during DSS-induced colitis.

Another key pro-inflammatory mediator is TNF- α , which is a major target for biologics in IBD therapy. Previously, targeting of TNF reduced colonic inflammation in DSS-induced colitis for wild-type mice¹⁸¹. Another study found that DSS treatment leads to higher serum levels of IL-6 and TNF- α , and antibodies against these cytokines reduce DSS-induced intestinal permeability¹⁸². Overall, the pro-inflammatory function of TNF and the therapeutic effects of its neutralization are well-established in colitis models and IBD¹⁸³. In contrast, I found that DSS challenge caused lower TNF concentrations for wild-type and SHIP def mice. This may have resulted from induction of negative regulatory cytokines during DSS-induced colitis, such as IL-10 or TGF- β ¹⁸⁴, which I did not measure. However, there is also some evidence supporting a dual role for TNF that is dependent on differential signaling. For example, mice deficient in TNF receptor 1 (*TNFR1*) were found to have more severe TNBS colitis^{183, 185}. Additionally, Naito *et al.* (2003) found that acute DSS-induced colitis was exacerbated in TNF- α -deficient mice compared to wild-type mice¹⁸⁶. In acute DSS-induced colitis, Noti *et al.* (2010) found that the absence of TNF exacerbated inflammation due to a lack of local colonic synthesis of glucocorticoids, which are steroid hormones that negatively regulate inflammatory responses¹⁸³. Furthermore, they determined that therapeutic administration of TNF partially improved disease outcomes in type 2-mediated inflammation in oxazolone-induced colitis¹⁸³. Thus, they proposed that the pro-inflammatory functions of TNF are critical for initiating inflammation, whereas its anti-inflammatory functions help to resolve disease¹⁸³. Collectively, these observations suggest that TNF may have an anti-inflammatory role in some colitis models.

Herein, I showed that DSS challenge reduced IL-25 concentrations in wild-type mice. Previous studies have described an anti-inflammatory role for IL-25 in intestinal inflammation. However, the exact mechanisms of IL-25 protection have not been described completely¹⁸⁷. For example, IL-25 has been shown to inhibit the development of acute DSS-induced colitis¹⁸⁸. In particular, mice treated with DSS and rIL-25-treated have elevated levels of IL-23 and the anti-inflammatory cytokine TGF- β ¹⁸⁸. Additionally, IL-25-deficient mice develop severe intestinal inflammation during *Trichuris muris* infection, correlating with elevated levels of Th1/Th17 cytokines^{187, 189}. Moreover, the administration of exogenous IL-25 improves clinical symptoms, histopathology, and type 2 inflammation in oxazolone-induced colitis^{190, 191}. These anti-inflammatory effects were associated with expansion of alternatively-activated macrophages (a subset of macrophages that can promote tissue repair)^{190, 191}. These studies support an important protective function of IL-25 in intestinal inflammation in type 1 and type 2-mediated mouse colitis models¹⁸⁷. In cultures of CD4⁺ T cells isolated from people with IBD, IL-25 has been found to downregulate the production of Th1/Th17 cytokines, TNF, IFN- γ , and IL-17A, while enhancing IL-10 production¹¹⁴. IL-25 also decreases the synthesis of pro-inflammatory cytokines IL-12 and IL-23 in macrophages from inflamed mucosa of people with CD¹⁹⁰. Furthermore, the intestinal mucosa of people with IBD have fewer IL-25 expressing cells and lower IL-25 concentrations during active disease^{114, 190}. These results suggest that people with IBD may have reduced tuft cell numbers and/or activity; however, people with IBD often have severe loss of intestinal epithelium that may account for loss of IL-25, which is IEC-derived¹¹⁴. Taken together, these findings characterize a potential anti-inflammatory, protective role of IL-25 in intestinal inflammation in colitis models and people with IBD.

I showed that mice with SHIP deficiency in tuft cells maintained similar IL-25 concentrations after DSS treatment. As such, they have higher IL-25 concentrations than wild-type controls, suggesting that SHIP deficiency increases or maintains tuft cell activity during DSS challenge. I found that elevated IL-25 concentrations caused by SHIP deficiency correlated with exacerbated DSS-induced colitis. Thus, IL-25 may have a pro-inflammatory role in DSS-induced colitis. This contrasts with the studies mentioned previously. Studies have reported disparate results on the role of exogenous IL-25 in colonic inflammation¹⁹². In contrast to the study by McHenga *et al.* (2008)¹⁸⁸, Wang *et al.* (2014) reported that genetic deletion of IL-25 protects mice from inflammation in DSS-induced colitis¹⁹². Thus, endogenous IL-25 acts as a pro-inflammatory factor in DSS-induced colitis¹⁹². Interestingly, McHenga *et al.* (2010) later reported that only high doses of exogenous IL-25 ameliorate inflammation, whereas low doses aggravate DSS-induced colitis^{192, 193}. Additionally, overexpression of IL-25 causes epithelial cell hyperplasia, increased mucus secretion, and increases in IL-4, IL-5, IgE, eosinophils, lymphocytes, and neutrophils in peripheral blood of transgenic mice, leading to type 2-mediated multiorgan inflammation^{187, 194, 195}. Consistent with this, Camelo *et al.* (2012) blocked IL-25 (and its IL-17 receptor B) to ameliorate type 2-mediated inflammation in oxazolone-induced colitis¹⁸⁷. Altogether, these studies describe a pro-inflammatory function for IL-25 in type 1 and type 2-mediated colitis. In line with this, my findings suggest that constitutive IL-25 is a pro-inflammatory factor in mice with SHIP deficiency in tuft cells during DSS-induced colitis.

As mentioned previously, tuft cells are the predominant IEC-derived source of IL-25, which recruits eosinophils and initiates type 2 immune responses via activation of ILC2s^{80, 85}. This involves IL-4, IL-5, and IL-13 production. IL-4 and IL-13 induce tuft and goblet cell hyperplasia, forming a feedforward loop that is referred to as the tuft cell-ILC2 circuit.^{56, 80} In

the small intestine, the role of this circuit in helminth defense and allergic inflammation has been well-established⁸⁵. Recent studies suggest that type 2 immune responses may either exacerbate or protect in different types of colitis¹¹⁶. When type 2 immunity becomes dysregulated, type 2 cytokines may cause persistent inflammation (seen in UC-like chronic inflammation) and fibrogenesis that leads to fibrosis and stricture formations (seen more commonly in CD)¹¹⁶. Following reduced IL-25 concentrations, I found lower concentrations of the type 2 cytokines, IL-4, IL-5 and IL-13, in wild-type mice after DSS challenge. The downregulation of type 2 cytokines may be due to acute DSS-induced colitis being a type 1-mediated disease^{167, 176}. IL-4 displayed a similar trend to that of IL-25, where SHIP deficiency increased or maintained baseline concentrations after DSS challenge. Thus, IL-25 may activate ILC2s to produce IL-4, as expected. However, this did not reach statistical significance. Previously, Weisser *et al.* (2011) found that germ-line SHIP^{-/-} were protected from DSS-induced colitis because of hyperactive IL-4-secreting basophils that skew macrophages to a wound healing and tissue modeling phenotype¹⁹⁶. These macrophages have low production of pro-inflammatory cytokines and high levels of anti-inflammatory cytokines IL-10 and TGF- β in response to stimulation^{196, 197}. In contrast, I showed that SHIP deficiency in tuft cells exacerbated DSS-induced colitis despite a trend to higher IL-4 concentrations. This suggests that the protective effect of IL-4-activated macrophages may have been underestimated because SHIP-deficient tuft cells may have been exacerbating disease. My results are consistent with studies showing that IL-4 can exacerbate inflammation directly or via its effects on other pro-inflammatory mediators. For example, DSS-induced colitis is ameliorated in IL-4-deficient mice, which have higher numbers of IgG2a, IgG2b and IgG3-producing B cells, reduced IgE levels, impaired peripheral eosinophilia, and lower concentrations of IL-5¹⁹⁸.

Despite higher concentrations of IL-25 (and a similar trend for IL-4), I found that IL-5 and IL-13 concentrations were similar in wild-type controls and SHIP def mice after DSS challenge. Thus, my observations suggest that the type 2 cytokines IL-5 and IL-13 did not exacerbate DSS-induced colitis in mice with SHIP-deficient tuft cells. Furthermore, there was no evidence of eosinophilia, which is induced by type 2 cytokines, associated with SHIP deficiency in tuft cells. These results are consistent with those of Stevceva *et al.* (2000), who demonstrated that while IL-5 has a role in eosinophil recruitment in acute colonic inflammation, IL-5 deficiency does not affect disease severity¹⁹⁹. Thus, IL-5 and eosinophils do not significantly exacerbate or protect mice from DSS-induced colitis¹⁹⁹. Previously, IL-13 was reported to drive intestinal inflammation in DSS-induced colitis²⁰⁰. However, IL-13 has also been proposed to have a critical role in promoting anti-inflammatory activity and recovery from DSS-induced colitis²⁰¹. Even so, studies have shown similar IL-13 production in mucosal explants and activated lamina propria mononuclear cells from people with CD and UC compared to healthy controls, suggesting an absence of a role for IL-13 in IBD²⁰². This may explain the lack of a therapeutic effect of anti-IL-13 antibody in people with UC^{116, 203}. Given these findings, it is clear that the role of type 2 cytokines in the colon and IBD require further study.

In addition to IL-25, ILC2s react to other activating signals, including IL-33 and leukotrienes⁸⁵. IL-33 has been found to drive ILC2 activation, leading to type 2-mediated protection during *C. difficile* infection in mice¹⁷⁴. In DSS-induced colitis, inflammation is ameliorated in IL-33-deficient mice and by blocking IL-33 signaling¹¹⁷. Consistent with this, rIL-33 treatment exacerbates DSS-induced colitis via induction of type 2 immunity²⁰⁴. In contrast, my results indicate that IL-33 did not drive inflammation during DSS-induced colitis in wild-type and SHIP def mice. Leukotrienes have also been implicated in ILC2 activation⁸⁵. Recently,

small intestinal tuft cells were reported to secrete cysteinyl leukotrienes that cooperate with IL-25 to activate type 2 immunity against helminth infections¹¹⁵. My findings indicate that cysteinyl leukotriene concentrations were similar before and after DSS challenge. Furthermore, SHIP deficiency in tuft cells did not affect cysteinyl leukotriene concentrations. Thus, I did not identify a role for cysteinyl leukotrienes in DSS-induced colitis¹¹⁷.

Most studies have focused on IL-25 regulating intestinal homeostasis through its ability to activate type 2 immunity. As mentioned above, I found that IL-5 and IL-13 concentrations did not follow higher IL-25 concentrations in SHIP def mice during DSS-induced colitis. Additionally, I did not observe changes in tuft cell percentage due to SHIP deficiency or during DSS-induced colitis. If the tuft cell-ILC2 circuit functions as expected, higher IL-25 concentrations should activate the feedforward loop that leads to abundant type 2 cytokines and tuft cell hyperplasia. Thus, my findings suggest that the tuft cell-ILC2 circuit may not function during DSS-induced colitis as it does in the small intestine. Indeed, while the tuft cell-ILC2 circuit is well-established in the small intestine, evidence thus far suggests that it does not operate in the colon⁷⁹. Small intestinal ILC2s constitutively express the IL-25 receptor, which is negatively regulated by A20 (encoded by TNF- α -induced protein 3, *TNFAIP3*)²⁰⁵. A20 deficiency in ILC2s spontaneously activates the tuft cell-ILC2 circuit in the small intestine, as suggested by increased frequency of DCLK1⁺ tuft cells, but not in other parts of the GI tract (i.e. the colon)^{79, 205}. Additionally, systemic delivery of rIL-4 drives tuft cell hyperplasia in the small intestine only⁷⁹, which is consistent with my observation of unchanged tuft cell percentages in colon cross-sections. However, small and transient changes in tuft cell frequency occur in the colon when germ-free mice are colonized with bacteria via unknown mechanisms^{79, 206}. Thus,

while the tuft cell-ILC2 circuit does not appear to function in tissues outside the small intestine, tuft cell-ILC2 interactions may still exist⁷⁹.

There are three potential mechanisms by which tuft cells and IL-25 may exacerbate DSS-induced colitis if not through activation of type 2 immunity. Previously, stimulation of a colonic epithelial cell line with IL-25 increased IL-6, TNF- α , IL-8, and chemokine ligand 2 (CCL2) expression¹⁹². I did not see increased pro-inflammatory cytokines IL-6 and TNF due to SHIP deficiency in tuft cells; however, I did not measure concentrations of CCL2 and murine homologues of IL-8, which recruit inflammatory cells¹⁹². IL-25 overexpression in mice also leads to B cell hyperplasia and altered antibody production, which may disrupt intestinal homeostasis, thereby contributing to intestinal inflammation^{194, 207}. Additionally, tuft cells promote IEC proliferation²⁰⁸. Defective epithelial differentiation is a central factor in the development of intestinal inflammation, as undifferentiated colonic epithelium produces high levels of pro-inflammatory cytokines and chemokines²⁰⁸. Increased tuft cell activity due to SHIP deficiency may lead to hyperproliferative and undifferentiated colonic epithelium that promotes inflammation and impairs barrier function²⁰⁸. These three proposed mechanisms highlight the complex role that tuft cells have in regulating intestinal homeostasis.

Tuft cells are the only epithelial cells in the uninfamed intestine that express COX1 and COX2, which form prostaglandins, including PGD₂ and PGE₂⁹². The two isoforms operate in different conditions: COX1 expression is constitutive in most tissues, while COX2 is induced in response to stimuli such as inflammation, wound healing, and neoplasia²⁰⁹. COX1 expression is unchanged in IBD, while COX2 is undetectable in normal ileum or colon and induced in epithelial cells of inflamed foci in IBD²¹⁰. Prostaglandins play a central role in intestinal

homeostasis, regulating mucosal protection, gastrointestinal secretion and motility, epithelial barrier integrity, inflammation, and tissue repair^{92, 211}. During intestinal inflammation, there are rapid increases in mucosal prostaglandin synthesis that correlate with disease activity in mouse models and people with IBD¹⁰³. Previously, Sauv e (2019) showed that tuft cells are the only COX1-expressing epithelial cell type in the absence of inflammation in the ilea of SHIP^{-/-} mice⁹⁰. COX activity levels are higher in the inflamed ileal tissue of SHIP^{-/-} mice, and inflammation can be prophylactically treated using the COX inhibitor piroxicam⁹⁰. COX is thereby involved in initiating spontaneous ileal inflammation in SHIP^{-/-} mice⁹⁰. In the colonic epithelium, COX1 is also localized in tuft cells²¹². Studies have similarly shown a pro-inflammatory function for COX in the colons of people with IBD^{210, 213}. In contrast to these observations, I showed that SHIP deficiency in tuft cells caused reduced COX activity during DSS-induced colitis, which was associated with exacerbated inflammation. Thus, my findings indicate that COX may be protective in DSS-induced colitis. This is consistent with a study by Tessner *et al.* (1998), which indicated that DSS treatment downregulates COX1 expression in the epithelium²¹⁴. COX1 has been shown to have a protective role against small intestinal and colonic mucosal injury through prostaglandin synthesis that mediates epithelial regeneration^{103, 214, 215}. COX2 deficiency leads to increased epithelial permeability and reduced expression of tight junction proteins²¹⁶. In DSS-induced colitis, COX1^{-/-} mice and COX2^{-/-} mice have increased susceptibility due to impaired intestinal barrier function^{103, 213}. COX inhibition has also been found to cause increased colonic injury and delayed gastric ulcer healing^{108, 216-218}. Moreover, COX inhibition decreases prostaglandin levels and is responsible for NSAID-dependent exacerbation of DSS-induced colitis²¹⁹. Prostaglandins also have protective functions against gastrointestinal injury¹⁰³. For example, experimental colitis can be ameliorated by pretreatment with prostaglandins^{103, 220}. DSS

treatment reduces epithelial cell proliferation, which can be reversed by exogenous PGE₂²¹⁴. Additionally, PGE₂ and its receptor, EP4, have been reported to be downregulated in people with UC and mice during DSS-induced colitis²²¹. COX, PGE₂, and EP4 have been proposed to partially exert their protective effects during mucosal injury by enhancing β -arrestin1 (a scaffold protein)/AKT signaling that promotes epithelial proliferation in the colon²²¹. Accumulating evidence supports a protective role for COX and prostaglandins during experimental colitis due to their function in maintenance of intestinal epithelial barrier function²¹⁶. My findings suggest that SHIP deficiency in tuft cells leads to reduced COX activity that exacerbates DSS-induced colitis, which may be due to increased barrier dysfunction (e.g. permeability and epithelial cell proliferation).

Sauvé (2019) reported that inflammation (and not SHIP deficiency in tuft cells) drives tuft cell hyperplasia⁹⁰. There is no tuft cell hyperplasia in the non-inflamed tissues (e.g. colon) of SHIP^{-/-} mice⁹⁰. Similarly, I did not observe an effect of SHIP deficiency on tuft cell percentages in the colon. However, I did not find a higher tuft cell percentage in the colons of mice with SHIP-deficient tuft cells during DSS-induced colitis, which we expected to be an inflammatory state that induces tuft cell hyperplasia. This may reflect the lack of elevated type 2 cytokines, which induce tuft cell hyperplasia. In contrast, the inflamed ilea of SHIP^{-/-} mice have increased type 2 cytokines IL-4 and IL-13¹⁷¹. Interestingly, COX activity is higher in the uninflamed SHIP^{-/-} ileum at 4 weeks of age, but there is no accompanying tuft cell hyperplasia⁹⁰. Similarly, I did not find a correlation in COX activity and IL-25 concentrations, which were higher in SHIP def mice during DSS-induced colitis. Taken together, these findings suggest that SHIP does not directly regulate COX activity.

To evaluate the potential protective activity of COX, I examined the effect of SHIP deficiency in tuft cells on recovery from DSS-induced colitis. It was first necessary to choose a time for DSS challenge that would sufficiently induce colitis but not bias recovery against mice with SHIP-deficient tuft cells because of higher disease activity. Previous studies have induced colitis over 5 days of DSS challenge^{119, 222, 223}. I determined that there was no significant exacerbation of colitis due to SHIP deficiency in tuft cells after 5 days of DSS challenge. Consistent with this, there were similar concentrations of IL-25 and IL-4 in the colon homogenates of wild-type and SHIP def mice after 5 days of DSS challenge. Interestingly, there was a trend to higher concentrations of IL-1 β , IL-5, and IL-13 associated with SHIP deficiency in tuft cells. There is a possibility that the presence of elevated levels of these pro-inflammatory mediators may contribute to later exacerbated colitis that is seen after 7 days of DSS challenge. There was no difference in COX activity due to SHIP deficiency in tuft cells after 5 days of DSS challenge, which is consistent with the lack of difference in disease activity. Additionally, mean COX activity was significantly higher after 5 days of DSS challenge compared to after 7 days for wild-type and SHIP def mice. This further supports a protective role of COX in DSS-induced colitis. Because disease activity was similar, the recovery period was started at the same timepoint for wild-type and SHIP def mice.

I found that SHIP deficiency in tuft cells did not affect body weight during recovery from DSS-induced colitis. Mice with SHIP-deficient tuft cells had increased rectal bleeding and stool consistency early in the recovery period, but they resembled wild-type mice by day 4 of recovery. Colon lengths and total histological damage measured after 5 days of recovery did not differ significantly. Consistent with the lack of difference in disease activity after 5 days of recovery, there was no difference in the concentrations of IL-25, IL-4, IL-5, IL-13, IL-33, type 1

pro-inflammatory cytokines IL-1 β , TNF, IL-6, or COX activity. This is in line with previous associations of normal COX1 expression with recovery from DSS-induced colitis²¹⁴. In contrast to my results, previous studies of recovery from DSS-induced colitis have identified IL-33 as a factor promoting recovery. In particular, Lopetuso *et al.* (2018) reported upregulated IL-33 in a 2-week recovery experiment¹¹⁹. Furthermore, IL-33-deficient mice have impaired recovery, and exogenous IL-33 promotes recovery by accelerating epithelial restitution and repair¹¹⁹.

Interestingly, there is a trend to less immune cell infiltration and greater muscle thickness in colon cross-sections due to SHIP deficiency in tuft cells, which suggests that recovery may be associated with an exacerbated type 2 immune response. This has been associated with pathological wound healing and fibrosis in germ-line SHIP^{-/-} mice¹⁷¹. This may also follow the trends of higher IL-5 and IL-13 concentrations measured after 5 days of DSS challenge. IL-5 stimulates B cell growth, increases IgA secretion, and mediates eosinophil activation, while IL-13 is pro-inflammatory and promotes apoptosis of IECs, causing mucosal barrier dysfunction⁴⁷. However, IL-5 and IL-13 are also upregulated in response to tissue injury and are critical for the resolution of inflammation and promoting tissue repair²⁰¹. Persistent type 2 inflammation may also be the cause of increased rectal bleeding and stool consistency early in recovery. At this point, the mechanisms of the tuft cell-ILC2 circuit and type 2 cytokines in DSS-induced colitis and recovery are unclear. In future studies, one could assay these molecules on additional days throughout recovery from DSS-induced colitis, particularly on Days 2 and 3 when disease activity differs, to determine their role in tissue repair and pathological healing.

In summary, my findings suggest that SHIP deficiency in tuft cells exacerbates DSS-induced colitis, which may be mediated, in part, by pro-inflammatory IL-25 activity and reduced COX activity, leading to impaired barrier function. I have also evaluated the role of type 2

immunity and protective COX activity in recovery from DSS-induced colitis. A common pattern I observed was wide variation in the outputs I measured, which may reflect biological variation and the complexity of the immunological pathways that underlie intestinal inflammation. My work has provided insight into the effects of SHIP deficiency in tuft cells in the complex environment of the gut during DSS-induced colitis.

Chapter 5: Concluding remarks

5.1 Conclusions

Tuft cells are a unique epithelial cell type that have pro-inflammatory and protective functions in the intestine. The effects of their activity and products in different contexts remain understudied. Herein, I focused on the role of SHIP in tuft cell responses during DSS-induced colitis and recovery by examining IL-25, activation of type 2 immunity, and COX activity. COX activity is higher in the inflamed ileal tissues of germ-line SHIP^{-/-} mice⁹⁰. Prophylactic treatment with the COX inhibitor piroxicam prevents the development of spontaneous ileal inflammation in SHIP^{-/-} mice⁹⁰. Based on this, I hypothesized that mice with SHIP deficiency in tuft cells will have exacerbated DSS-induced colitis because SHIP blocks COX-mediated inflammation. Tuft cells also promote IEC proliferation and type 2 immune responses^{79, 128}. Previously, the role of type 2 cytokines, which can be activated through the small intestinal tuft cell-ILC2 circuit, has been well-established in inflammation and repair during helminth infections and allergic inflammation⁷⁹. When dysregulated, type 2 immunity may lead to persistent inflammation and/or excessive tissue repair that causes fibrosis and stricture formation that are associated with IBD¹¹⁶. Thus, I hypothesized that tuft cell-specific SHIP-deficient mice will have impaired recovery from DSS-induced colitis because SHIP-deficient tuft cells will activate ILC2s to produce excessive type 2 cytokines that cause persistent inflammation and pathological healing. To investigate these hypotheses, I had three aims: 1) to determine the role of SHIP in tuft cell responses to commensal microbes during DSS-induced colitis, 2) to determine if ILC2s and COX-mediated inflammation contribute to pathological inflammation during DSS-induced colitis in tuft cell-specific SHIP-deficient mice, and 3) to determine the effect of SHIP deficiency in tuft cells on recovery after DSS-induced colitis.

There have been multiple studies of mice deficient in tuft cells or IL-25 in experimental colitis. To my knowledge, the tuft cell-specific SHIP-deficient mouse is the first gain-of-function murine model for tuft cells. I showed that SHIP deficiency in tuft cells exacerbated DSS-induced colitis and is associated with increased IL-25 concentrations and reduced COX activity. There are conflicting conclusions for the role of IL-25 in the gut, with several reports suggesting that IL-25 is anti-inflammatory^{114, 190}, whereas Wang *et al.* (2014) characterized a pro-inflammatory role by demonstrating that IL-25^{-/-} mice are protected from inflammation in DSS-induced colitis¹⁹². My results further support a pro-inflammatory function for IL-25 during DSS-induced colitis, as tuft cell-specific SHIP-deficient mice had exacerbated disease and higher IL-25 concentrations. Unexpectedly, increased inflammation in mice with SHIP-deficient tuft cells was not accompanied by changes in tuft cell percentage, whereas there is tuft cell hyperplasia in the inflamed ileal tissue of SHIP^{-/-} mice⁹⁰. Additionally, despite higher IL-25 concentrations, exacerbation of disease did not seem to be mediated by type 2 cytokines as has been described in the inflamed ileum of germ-line SHIP^{-/-} mice¹⁷¹ and during helminth infection²⁰⁵. This adds to accumulating evidence that suggests that the tuft cell-ILC2 circuit may not function in the colon as it does in the small intestine⁷⁹.

Contrary to my hypothesis, SHIP deficiency in tuft cells caused reduced COX activity during DSS-induced colitis. This finding is consistent with previous literature describing a protective function for COX in experimental colitis^{103, 213-215} but in contrast to previous work done by our research team, which suggested that COX-expressing tuft cells are involved in the initiation of ileal inflammation in germ-line SHIP^{-/-} mice⁹⁰. Overall, these observations support dual functions for COX that are context-specific.

Finally, SHIP deficiency in tuft cells leads to increased disease activity early in recovery from DSS-induced colitis. In particular, I observed increased rectal bleeding, stool loosening, and potential colonic muscle thickening. These features may stem from higher concentrations of type 2 cytokines that have dual effects: promoting inflammation and pathological healing¹¹⁶. However, these were transient effects after 5 days of DSS challenge that were not captured later after 5 days of recovery.

There are several limitations that I have considered. A common pattern I observed in my data was wide variation in cytokine concentrations and disease outcomes between samples within experimental groups. This may be partially explained by the observation that DSS-induced colitis develops more rapidly in males than females¹⁴⁰. However, I did not observe significant differences in my results when data was segregated by sex. A limitation of tuft cell-specific SHIP-deficient mice is the 50% cre-recombinase efficiency using the *Fabp1* promoter, which results in some tuft cells retaining SHIP expression in the colon. This may further impact the significance of results and explain the variation seen in the outputs measured. Villin-cre is a more efficient system to target specific gene expression in the gut that is more widely used. However, the mouse villin 1 promoter is located on the same chromosome (chromosome 1) as the mouse SHIP gene (*INPP5D*). Thus, the chance of a recombination event that would permit expression of both Villin-cre and floxed SHIP on chromosome 1 is low. In fact, our research team bred SHIP^{+/-} Villin^{+/-cre} mice for two years and were unable to achieve a cross-over event. Finally, a limitation of the DSS-induced colitis model is that it relies on acute exposure to DSS that causes sudden epithelial injury, which differs from the spontaneous inflammation that occurs in people with IBD¹⁴⁰. Rather, the DSS-induced colitis model allows for the study of potential

pathogenic factors in rapid and controlled conditions that would be difficult to assess in the complicated context of human IBD.

The direct effects of tuft cells in human IBD are unknown⁸⁰. It is clear that tuft cells are highly heterogeneous, expressing varying levels of markers, such as COX1 and COX2, and having different effector functions in different tissues and conditions⁷⁹. By examining the role of SHIP in tuft cell activity, these studies contribute to our understanding of the role of tuft cells in the colon during type 1 inflammation. In particular, they provide insight into the effect of SHIP deficiency on the functions of tuft cell-derived COX, tuft cell-ILC2 interactions in the colon, and type 2 cytokines in DSS-induced colitis. Thus, this work may help characterize some of the basic biological processes involved in intestinal inflammation that may be pertinent to IBD. Moreover, tuft cell functions may be relevant to pathology in people with IBD who also have low expression of SHIP. Based on my findings, SHIP deficiency in tuft cells may lead to changes in tuft cell-derived COX and IL-25 that exacerbate intestinal inflammation and impair recovery.

5.2 Future directions

I have identified overproduction of IL-25 and reduced COX activity as potential disease mechanisms in DSS-treated mice with SHIP-deficient tuft cells. As such, treating these mice with neutralizing antibodies to IL-25 or its receptor, IL-17BR, during DSS treatment could ameliorate inflammation. Previously, blocking IL-25 signaling via this method protected against inflammation in the type 2-mediated oxazolone-induced colitis model¹⁸⁷. Though I did not observe a significant role for type 2 cytokines in the exacerbation of DSS-induced colitis, the effects of blocking IL-25 on type 2 immunity could be evaluated. Additionally, IL-25 may inhibit Th1/Th17 pathways; exogenous IL-25 downregulates IL-12, IL-23, TNF, IFN- γ , and IL-17A production while enhancing IL-10 production in cultures of CD4⁺ T cells isolated from

people with IBD¹¹⁴. Furthermore, overexpression of IL-25 causes epithelial cell hyperplasia, increased mucus secretion, and increases in IL-4, IL-5, IgE, eosinophils, lymphocytes, and neutrophils in peripheral blood of transgenic mice^{187, 194, 195}. Concentrations of these pro-inflammatory mediators, type 2 cytokines, inhibitory cytokines (IL-10 and TGF- β), and IgE can be measured after DSS challenge +/- IL-25 blockade. Immunophenotyping could be done via flow cytometry to investigate the populations of tuft cells, eosinophils, lymphocytes, and neutrophils in tuft cell-specific SHIP-deficient mice during DSS-induced colitis, recovery, and after anti-IL-25 treatment. Moreover, intestinal barrier integrity could be assessed via the fluorescein isothiocyanate (FITC)-dextran permeability assay as described by Qu *et al.* (2015)¹²⁸. To further investigate reduced COX activity in mice with SHIP-deficient tuft cells, the effects of PGE₂ treatment on DSS-induced colitis could be examined. This would also include measuring the same outputs mentioned for anti-IL-25 or anti-IL-17BR antibody blockade. In addition, the effects of PGE₂ on epithelial cell proliferation and apoptosis could be evaluated by quantifying levels of Lgr5 (stem cells), proliferating cell nuclear antigen (PCNA)-positive cells, and staining apoptotic cells by terminal deoxynucleotidyl transferase dUTP nick end labeling (TUNEL)^{128, 221}.

The effects of SHIP deficiency in tuft cells on tuft cell activity could also be studied in a high-throughput, comprehensive (omics) approach to identify potential disease mechanisms. Global gene expression analysis (RNA sequencing) could be done to compare gene expression in organoids generated from wild-type and germ-line SHIP-deficient mice (SHIP wild-type and SHIP knockout cultures). Tuft cells are not normally present in organoids but can be induced by addition of IL-4 or IL-13 to cultures^{224, 225}. Thus, gene expression could be compared between 3 groups of ileal epithelial cells: organoids without tuft cells, organoids with tuft cells, and organoids with SHIP-deficient tuft cells. Furthermore, stimulating cultures with different

concentrations of IL-4 and/or IL-13 could control tuft cell numbers, which would allow correlation of changes in gene expression with tuft cell numbers. Single-cell RNA sequencing could also be used to study the effects of SHIP deficiency in tuft cells. Gene expression profiles of cells in colon homogenates from wild-type and tuft cell-specific SHIP-deficient mice after 7 days of DSS challenge could also be analyzed. Together with the data generated from organoid experiments, the cell-extrinsic effects of SHIP deficiency in tuft cells in the complex gut environment could be assessed.

Finally, tuft cell-specific SHIP-deficient mice are a unique gain-of-function model that can be used in other disease models. For example, the role of SHIP and tuft cell activity in type 2-mediated oxazolone-induced colitis would provide further insight into the role of tuft cells in type 2 immunity within the colon, including interactions with IL-33 and cysteinyl leukotrienes. In the small intestine, the effect of SHIP deficiency in tuft cells on tuft cell-ILC2 circuits could be studied in the context of helminth infection. For example, *T. spiralis* is a helminth known to induce tuft cell hyperplasia²²⁶. In this experiment, I would hypothesize that increased tuft cell activity due to SHIP deficiency would lead to abundant type 2 immune responses and tuft cell hyperplasia, which may allow these mice to clear helminth infection more effectively. Type 2 cytokines could be assayed as described earlier, and tuft cell and ILC2 numbers could be determined by immunohistochemistry or immunofluorescence.

The functions of tuft cell-derived IL-25 and COX and how they are impacted by SHIP deficiency require further investigation. Characterization of tuft cell activity in a variety of contexts, including DSS-induced colitis, will provide insight into potential mechanisms that contribute to the development of IBD, a disease of complex etiology.

References

1. Rosen MJ, Dhawan A, Saeed SA. Inflammatory Bowel Disease in Children and Adolescents. *JAMA Pediatr.* 2015;**169**(11):1053-1060.
2. Seyedian SS, Nokhostin F, Malamir MD. A review of the diagnosis, prevention, and treatment methods of inflammatory bowel disease. *J Med Life.* 2019;**12**(2):113-122.
3. Kaplan GG, Bernstein CN, Coward S, et al. The Impact of Inflammatory Bowel Disease in Canada 2018: Epidemiology. *J Can Assoc Gastroenterol.* 2019;**2**(Suppl 1):S6-s16.
4. The global, regional, and national burden of inflammatory bowel disease in 195 countries and territories, 1990-2017: a systematic analysis for the Global Burden of Disease Study 2017. *Lancet Gastroenterol Hepatol.* 2020;**5**(1):17-30.
5. Jairath V, Feagan BG. Global burden of inflammatory bowel disease. *Lancet Gastroenterol Hepatol.* 2020;**5**(1):2-3.
6. Park KT, Ehrlich OG, Allen JI, et al. The Cost of Inflammatory Bowel Disease: An Initiative From the Crohn's & Colitis Foundation. *Inflamm Bowel Dis.* 2020;**26**(1):1-10.
7. Kuenzig ME, Lee L, El-Matary W, et al. The Impact of Inflammatory Bowel Disease in Canada 2018: Indirect Costs of IBD Care. *Journal of the Canadian Association of Gastroenterology.* 2018;**2**(Supplement_1):S34-S41.
8. Kuenzig ME, Benchimol EI, Lee L, et al. The Impact of Inflammatory Bowel Disease in Canada 2018: Direct Costs and Health Services Utilization. *J Can Assoc Gastroenterol.* 2019;**2**(Suppl 1):S17-s33.
9. Hendrickson BA, Gokhale R, Cho JH. Clinical Aspects and Pathophysiology of Inflammatory Bowel Disease. *Clinical Microbiology Reviews.* 2002;**15**(1):79-94.
10. Fakhoury M, Negrulj R, Mooranian A, et al. Inflammatory bowel disease: clinical aspects and treatments. *J Inflamm Res.* 2014;**7**:113-120.
11. Guan Q. A Comprehensive Review and Update on the Pathogenesis of Inflammatory Bowel Disease. *J Immunol Res.* 2019;**2019**:7247238.
12. Molnár T, Tiszlavicz L, Gyulai C, et al. Clinical significance of granuloma in Crohn's disease. *World J Gastroenterol.* 2005;**11**(20):3118-3121.
13. Adegbola SO, Sahnun K, Warusavitarne J, et al. Anti-TNF Therapy in Crohn's Disease. *Int J Mol Sci.* 2018;**19**(8).
14. Shi HY, Ng SC. The state of the art on treatment of Crohn's disease. *J Gastroenterol.* 2018;**53**(9):989-998.
15. Hazel K, O'Connor A. Emerging treatments for inflammatory bowel disease. *Ther Adv Chronic Dis.* 2020;**11**:2040622319899297.
16. Chichlowski M, Hale LP. Bacterial-mucosal interactions in inflammatory bowel disease: an alliance gone bad. *Am J Physiol Gastrointest Liver Physiol.* 2008;**295**(6):G1139-1149.
17. Lee SH, Kwon JE, Cho ML. Immunological pathogenesis of inflammatory bowel disease. *Intest Res.* 2018;**16**(1):26-42.
18. Uhlig HH, Schwerd T, Koletzko S, et al. The diagnostic approach to monogenic very early onset inflammatory bowel disease. *Gastroenterology.* 2014;**147**(5):990-1007.e1003.
19. Loddo I, Romano C. Inflammatory Bowel Disease: Genetics, Epigenetics, and Pathogenesis. *Front Immunol.* 2015;**6**:551.

20. Liu JZ, van Sommeren S, Huang H, et al. Association analyses identify 38 susceptibility loci for inflammatory bowel disease and highlight shared genetic risk across populations. *Nat Genet.* 2015;**47**(9):979-986.
21. Ramos GP, Papadakis KA. Mechanisms of Disease: Inflammatory Bowel Diseases. *Mayo Clinic Proceedings.* 2019;**94**(1):155-165.
22. Lauro ML, D'Ambrosio EA, Bahnson BJ, et al. Molecular Recognition of Muramyl Dipeptide Occurs in the Leucine-rich Repeat Domain of Nod2. *ACS Infect Dis.* 2017;**3**(4):264-270.
23. Ogura Y, Bonen DK, Inohara N, et al. A frameshift mutation in NOD2 associated with susceptibility to Crohn's disease. *Nature.* 2001;**411**(6837):603-606.
24. Magalhaes JG, Sorbara MT, Girardin SE, et al. What is new with Nods? *Curr Opin Immunol.* 2011;**23**(1):29-34.
25. Palomino-Morales RJ, Oliver J, Gómez-García M, et al. Association of ATG16L1 and IRGM genes polymorphisms with inflammatory bowel disease: a meta-analysis approach. *Genes & Immunity.* 2009;**10**(4):356-364.
26. McCole DF. IBD candidate genes and intestinal barrier regulation. *Inflamm Bowel Dis.* 2014;**20**(10):1829-1849.
27. Khor B, Gardet A, Xavier RJ. Genetics and pathogenesis of inflammatory bowel disease. *Nature.* 2011;**474**(7351):307-317.
28. McGovern DP, Kugathasan S, Cho JH. Genetics of Inflammatory Bowel Diseases. *Gastroenterology.* 2015;**149**(5):1163-1176.e1162.
29. Halme L, Paavola-Sakki P, Turunen U, et al. Family and twin studies in inflammatory bowel disease. *World J Gastroenterol.* 2006;**12**(23):3668-3672.
30. Ananthakrishnan AN, Bernstein CN, Iliopoulos D, et al. Environmental triggers in IBD: a review of progress and evidence. *Nat Rev Gastroenterol Hepatol.* 2018;**15**(1):39-49.
31. Hou JK, Abraham B, El-Serag H. Dietary intake and risk of developing inflammatory bowel disease: a systematic review of the literature. *Am J Gastroenterol.* 2011;**106**(4):563-573.
32. Khalili H, Higuchi LM, Ananthakrishnan AN, et al. Oral contraceptives, reproductive factors and risk of inflammatory bowel disease. *Gut.* 2013;**62**(8):1153-1159.
33. Ananthakrishnan AN, Higuchi LM, Huang ES, et al. Aspirin, nonsteroidal anti-inflammatory drug use, and risk for Crohn disease and ulcerative colitis: a cohort study. *Ann Intern Med.* 2012;**156**(5):350-359.
34. Abegunde AT, Muhammad BH, Bhatti O, et al. Environmental risk factors for inflammatory bowel diseases: Evidence based literature review. *World J Gastroenterol.* 2016;**22**(27):6296-6317.
35. Dominguez-Bello MG, Blaser MJ, Ley RE, et al. Development of the human gastrointestinal microbiota and insights from high-throughput sequencing. *Gastroenterology.* 2011;**140**(6):1713-1719.
36. Nell S, Suerbaum S, Josenhans C. The impact of the microbiota on the pathogenesis of IBD: lessons from mouse infection models. *Nat Rev Microbiol.* 2010;**8**(8):564-577.
37. Nishida A, Inoue R, Inatomi O, et al. Gut microbiota in the pathogenesis of inflammatory bowel disease. *Clin J Gastroenterol.* 2018;**11**(1):1-10.
38. Ahmed I, Roy BC, Khan SA, et al. Microbiome, Metabolome and Inflammatory Bowel Disease. *Microorganisms.* 2016;**4**(2).

39. Silva FAR, Rodrigues BL, Ayrizono MdLS, et al. The Immunological Basis of Inflammatory Bowel Disease. *Gastroenterology Research and Practice*. 2016;**2016**:2097274.
40. Sartor RB. Microbial influences in inflammatory bowel diseases. *Gastroenterology*. 2008;**134**(2):577-594.
41. Mowat AM, Agace WW. Regional specialization within the intestinal immune system. *Nature Reviews Immunology*. 2014;**14**(10):667-685.
42. Ince MN, Elliott DE. Immunologic and molecular mechanisms in inflammatory bowel disease. *Surg Clin North Am*. 2007;**87**(3):681-696.
43. Shi N, Li N, Duan X, et al. Interaction between the gut microbiome and mucosal immune system. *Military Medical Research*. 2017;**4**(1):14.
44. Ng SC, Kamm MA, Stagg AJ, et al. Intestinal dendritic cells: their role in bacterial recognition, lymphocyte homing, and intestinal inflammation. *Inflamm Bowel Dis*. 2010;**16**(10):1787-1807.
45. Maroilley T, Berri M, Lemonnier G, et al. Immunome differences between porcine ileal and jejunal Peyer's patches revealed by global transcriptome sequencing of gut-associated lymphoid tissues. *Scientific Reports*. 2018;**8**(1):9077.
46. Steinbach EC, Plevy SE. The role of macrophages and dendritic cells in the initiation of inflammation in IBD. *Inflamm Bowel Dis*. 2014;**20**(1):166-175.
47. Okumura R, Takeda K. Maintenance of intestinal homeostasis by mucosal barriers. *Inflamm Regen*. 2018;**38**:5.
48. van Lierop PP, Samsom JN, Escher JC, et al. Role of the innate immune system in the pathogenesis of inflammatory bowel disease. *J Pediatr Gastroenterol Nutr*. 2009;**48**(2):142-151.
49. Rescigno M, Di Sabatino A. Dendritic cells in intestinal homeostasis and disease. *J Clin Invest*. 2009;**119**(9):2441-2450.
50. Travers J, Rothenberg ME. Eosinophils in mucosal immune responses. *Mucosal Immunology*. 2015;**8**(3):464-475.
51. Al-Haddad S, Riddell RH. The role of eosinophils in inflammatory bowel disease. *Gut*. 2005;**54**(12):1674-1675.
52. Lampinen M, Rönblom A, Amin K, et al. Eosinophil granulocytes are activated during the remission phase of ulcerative colitis. *Gut*. 2005;**54**(12):1714-1720.
53. Bischoff SC, Barbara G, Buurman W, et al. Intestinal permeability--a new target for disease prevention and therapy. *BMC Gastroenterol*. 2014;**14**:189.
54. Wright RD, Cooper D. Glycobiology of leukocyte trafficking in inflammation. *Glycobiology*. 2014;**24**(12):1242-1251.
55. Zhu J, Paul WE. Peripheral CD4+ T-cell differentiation regulated by networks of cytokines and transcription factors. *Immunol Rev*. 2010;**238**(1):247-262.
56. Gerbe F, Sidot E, Smyth DJ, et al. Intestinal epithelial tuft cells initiate type 2 mucosal immunity to helminth parasites. *Nature*. 2016;**529**(7585):226-230.
57. Maloy KJ, Powrie F. Intestinal homeostasis and its breakdown in inflammatory bowel disease. *Nature*. 2011;**474**(7351):298-306.
58. Bouma G, Strober W. The immunological and genetic basis of inflammatory bowel disease. *Nat Rev Immunol*. 2003;**3**(7):521-533.

59. Strober W, Fuss IJ. Proinflammatory cytokines in the pathogenesis of inflammatory bowel diseases. *Gastroenterology*. 2011;**140**(6):1756-1767.
60. Fuss IJ, Neurath M, Boirivant M, et al. Disparate CD4+ lamina propria (LP) lymphokine secretion profiles in inflammatory bowel disease. Crohn's disease LP cells manifest increased secretion of IFN-gamma, whereas ulcerative colitis LP cells manifest increased secretion of IL-5. *J Immunol*. 1996;**157**(3):1261-1270.
61. Roda G, Marocchi M, Sartini A, et al. Cytokine Networks in Ulcerative Colitis. *Ulcers*. 2011;**2011**:391787.
62. Acharya S, Timilshina M, Jiang L, et al. Amelioration of Experimental autoimmune encephalomyelitis and DSS induced colitis by NTG-A-009 through the inhibition of Th1 and Th17 cells differentiation. *Scientific Reports*. 2018;**8**(1):7799.
63. Múzes G, Molnár B, Tulassay Z, et al. Changes of the cytokine profile in inflammatory bowel diseases. *World J Gastroenterol*. 2012;**18**(41):5848-5861.
64. Curciarello R, Docena GH, MacDonald TT. The Role of Cytokines in the Fibrotic Responses in Crohn's Disease. *Front Med (Lausanne)*. 2017;**4**:126.
65. Choy MC, Visvanathan K, De Cruz P. An Overview of the Innate and Adaptive Immune System in Inflammatory Bowel Disease. *Inflamm Bowel Dis*. 2017;**23**(1):2-13.
66. Darsigny M, Babeu JP, Dupuis AA, et al. Loss of hepatocyte-nuclear-factor-4alpha affects colonic ion transport and causes chronic inflammation resembling inflammatory bowel disease in mice. *PLoS One*. 2009;**4**(10):e7609.
67. Irvine EJ, Marshall JK. Increased intestinal permeability precedes the onset of Crohn's disease in a subject with familial risk. *Gastroenterology*. 2000;**119**(6):1740-1744.
68. Muise AM, Walters TD, Glowacka WK, et al. Polymorphisms in E-cadherin (CDH1) result in a mis-localised cytoplasmic protein that is associated with Crohn's disease. *Gut*. 2009;**58**(8):1121-1127.
69. Söderholm JD, Olaison G, Peterson KH, et al. Augmented increase in tight junction permeability by luminal stimuli in the non-inflamed ileum of Crohn's disease. *Gut*. 2002;**50**(3):307-313.
70. Buhner S, Buning C, Genschel J, et al. Genetic basis for increased intestinal permeability in families with Crohn's disease: role of CARD15 3020insC mutation? *Gut*. 2006;**55**(3):342-347.
71. Van der Sluis M, De Koning BA, De Bruijn AC, et al. Muc2-deficient mice spontaneously develop colitis, indicating that MUC2 is critical for colonic protection. *Gastroenterology*. 2006;**131**(1):117-129.
72. Salzman NH, Underwood MA, Bevins CL. Paneth cells, defensins, and the commensal microbiota: a hypothesis on intimate interplay at the intestinal mucosa. *Semin Immunol*. 2007;**19**(2):70-83.
73. Kucharzik T, Maaser C, Lügering A, et al. Recent understanding of IBD pathogenesis: implications for future therapies. *Inflamm Bowel Dis*. 2006;**12**(11):1068-1083.
74. Kong S, Zhang YH, Zhang W. Regulation of Intestinal Epithelial Cells Properties and Functions by Amino Acids. *BioMed Research International*. 2018;**2018**:2819154.
75. Gerbe F, Legraverend C, Jay P. The intestinal epithelium tuft cells: specification and function. *Cell Mol Life Sci*. 2012;**69**(17):2907-2917.
76. Antoni L, Nuding S, Wehkamp J, et al. Intestinal barrier in inflammatory bowel disease. *World J Gastroenterol*. 2014;**20**(5):1165-1179.

77. Travassos LH, Carneiro LA, Ramjeet M, et al. Nod1 and Nod2 direct autophagy by recruiting ATG16L1 to the plasma membrane at the site of bacterial entry. *Nat Immunol.* 2010;**11**(1):55-62.
78. Johansson ME, Ambort D, Pelaseyed T, et al. Composition and functional role of the mucus layers in the intestine. *Cell Mol Life Sci.* 2011;**68**(22):3635-3641.
79. Ting H-A, von Moltke J. The Immune Function of Tuft Cells at Gut Mucosal Surfaces and Beyond. *The Journal of Immunology.* 2019;**202**(5):1321-1329.
80. Steele SP, Melchor SJ, Petri WA, Jr. Tuft Cells: New Players in Colitis. *Trends Mol Med.* 2016;**22**(11):921-924.
81. Sato A. Tuft cells. *Anat Sci Int.* 2007;**82**(4):187-199.
82. Jarvi O, Keyrilainen O. On the cellular structures of the epithelial invasions in the glandular stomach of mice caused by intramural application of 20-methylcholantren. *Acta Pathol Microbiol Scand Suppl.* 1956;**39**(Suppl 111):72-73.
83. Sato A, Hamano M, Miyoshi S. Increasing frequency of occurrence of tuft cells in the main excretory duct during postnatal development of the rat submandibular gland. *Anat Rec.* 1998;**252**(2):276-280.
84. Hewitt RJ, Lloyd CM. Regulation of immune responses by the airway epithelial cell landscape. *Nat Rev Immunol.* 2021;**21**(6):347-362.
85. Schneider C, O'Leary CE, Locksley RM. Regulation of immune responses by tuft cells. *Nature Reviews Immunology.* 2019;**19**(9):584-593.
86. von Moltke J, Ji M, Liang HE, et al. Tuft-cell-derived IL-25 regulates an intestinal ILC2-epithelial response circuit. *Nature.* 2016;**529**(7585):221-225.
87. Westphalen CB, Asfaha S, Hayakawa Y, et al. Long-lived intestinal tuft cells serve as colon cancer-initiating cells. *J Clin Invest.* 2014;**124**(3):1283-1295.
88. Ushima S, Ishimaru Y, Narukawa M, et al. Catecholamines Facilitate Fuel Expenditure and Protect Against Obesity via a Novel Network of the Gut-Brain Axis in Transcription Factor Skn-1-deficient Mice. *EBioMedicine.* 2016;**8**:60-71.
89. Sly LM, Ho V, Antignano F, et al. The role of SHIP in macrophages. *Front Biosci.* 2007;**12**:2836-2848.
90. Sauvé JP. COX-expressing tuft cells initiate Crohn's disease-like intestinal inflammation in SHIP^{-/-} mice. University of British Columbia 2019.
91. Moxey PC, Trier JS. Specialized cell types in the human fetal small intestine. *Anat Rec.* 1978;**191**(3):269-285.
92. Gerbe F, van Es JH, Makrini L, et al. Distinct ATOH1 and Neurog3 requirements define tuft cells as a new secretory cell type in the intestinal epithelium. *J Cell Biol.* 2011;**192**(5):767-780.
93. Saqui-Salces M, Keeley TM, Grosse AS, et al. Gastric tuft cells express DCLK1 and are expanded in hyperplasia. *Histochem Cell Biol.* 2011;**136**(2):191-204.
94. Mulvaney J, Dabdoub A. Atoh1, an essential transcription factor in neurogenesis and intestinal and inner ear development: function, regulation, and context dependency. *J Assoc Res Otolaryngol.* 2012;**13**(3):281-293.
95. Sureban SM, May R, Qu D, et al. DCLK1 regulates pluripotency and angiogenic factors via microRNA-dependent mechanisms in pancreatic cancer. *PLoS One.* 2013;**8**(9):e73940.

96. Miyata N, Morris LL, Chen Q, et al. Microbial Sensing by Intestinal Myeloid Cells Controls Carcinogenesis and Epithelial Differentiation. *Cell Rep.* 2018;**24**(9):2342-2355.
97. Bankova LG, Dwyer DF, Yoshimoto E, et al. The cysteinyl leukotriene 3 receptor regulates expansion of IL-25-producing airway brush cells leading to type 2 inflammation. *Sci Immunol.* 2018;**3**(28).
98. Holzer P. Opioid receptors in the gastrointestinal tract. *Regul Pept.* 2009;**155**(1-3):11-17.
99. Iizuka M, Konno S. Wound healing of intestinal epithelial cells. *World J Gastroenterol.* 2011;**17**(17):2161-2171.
100. Dey I, Lejeune M, Chadee K. Prostaglandin E2 receptor distribution and function in the gastrointestinal tract. *Br J Pharmacol.* 2006;**149**(6):611-623.
101. Ricciotti E, FitzGerald GA. Prostaglandins and inflammation. *Arterioscler Thromb Vasc Biol.* 2011;**31**(5):986-1000.
102. Nakanishi M, Rosenberg DW. Multifaceted roles of PGE2 in inflammation and cancer. *Semin Immunopathol.* 2013;**35**(2):123-137.
103. Morteau O, Morham SG, Sellon R, et al. Impaired mucosal defense to acute colonic injury in mice lacking cyclooxygenase-1 or cyclooxygenase-2. *J Clin Invest.* 2000;**105**(4):469-478.
104. O'Banion MK, Miller JC, Chang JW, et al. Interleukin-1 beta induces prostaglandin G/H synthase-2 (cyclooxygenase-2) in primary murine astrocyte cultures. *J Neurochem.* 1996;**66**(6):2532-2540.
105. Bachwich PR, Chensue SW, Larrick JW, et al. Tumor necrosis factor stimulates interleukin-1 and prostaglandin E2 production in resting macrophages. *Biochem Biophys Res Commun.* 1986;**136**(1):94-101.
106. Masferrer JL, Isakson PC, Seibert K. Cyclooxygenase-2 inhibitors: a new class of anti-inflammatory agents that spare the gastrointestinal tract. *Gastroenterol Clin North Am.* 1996;**25**(2):363-372.
107. Zidar N, Odar K, Glavac D, et al. Cyclooxygenase in normal human tissues--is COX-1 really a constitutive isoform, and COX-2 an inducible isoform? *J Cell Mol Med.* 2009;**13**(9b):3753-3763.
108. Mizuno H, Sakamoto C, Matsuda K, et al. Induction of cyclooxygenase 2 in gastric mucosal lesions and its inhibition by the specific antagonist delays healing in mice. *Gastroenterology.* 1997;**112**(2):387-397.
109. Connors J, Dawe N, Van Limbergen J. The Role of Succinate in the Regulation of Intestinal Inflammation. *Nutrients.* 2018;**11**(1).
110. Banerjee A, Herring CA, Chen B, et al. Succinate Produced by Intestinal Microbes Promotes Specification of Tuft Cells to Suppress Ileal Inflammation. *Gastroenterology.* 2020;**159**(6):2101-2115.e2105.
111. Gieseck RL, 3rd, Wilson MS, Wynn TA. Type 2 immunity in tissue repair and fibrosis. *Nat Rev Immunol.* 2018;**18**(1):62-76.
112. Lee CG, Homer RJ, Zhu Z, et al. Interleukin-13 induces tissue fibrosis by selectively stimulating and activating transforming growth factor beta(1). *J Exp Med.* 2001;**194**(6):809-821.
113. Noor Z, Burgess SL, Watanabe K, et al. Interleukin-25 Mediated Induction of Angiogenin-4 Is Interleukin-13 Dependent. *PLoS One.* 2016;**11**(4):e0153572.

114. Su J, Chen T, Ji XY, et al. IL-25 downregulates Th1/Th17 immune response in an IL-10-dependent manner in inflammatory bowel disease. *Inflamm Bowel Dis*. 2013;**19**(4):720-728.
115. McGinty JW, Ting HA, Billipp TE, et al. Tuft-Cell-Derived Leukotrienes Drive Rapid Anti-helminth Immunity in the Small Intestine but Are Dispensable for Anti-protist Immunity. *Immunity*. 2020;**52**(3):528-541.e527.
116. Bamias G, Cominelli F. Role of type 2 immunity in intestinal inflammation. *Curr Opin Gastroenterol*. 2015;**31**(6):471-476.
117. Sedhom MA, Pichery M, Murdoch JR, et al. Neutralisation of the interleukin-33/ST2 pathway ameliorates experimental colitis through enhancement of mucosal healing in mice. *Gut*. 2013;**62**(12):1714-1723.
118. Pushparaj PN, Li D, Komai-Koma M, et al. Interleukin-33 exacerbates acute colitis via interleukin-4 in mice. *Immunology*. 2013;**140**(1):70-77.
119. Lopetuso LR, De Salvo C, Pastorelli L, et al. IL-33 promotes recovery from acute colitis by inducing miR-320 to stimulate epithelial restitution and repair. *Proc Natl Acad Sci U S A*. 2018;**115**(40):E9362-e9370.
120. Howitt MR, Lavoie S, Michaud M, et al. Tuft cells, taste-chemosensory cells, orchestrate parasite type 2 immunity in the gut. *Science*. 2016;**351**(6279):1329-1333.
121. Buonomo EL, Cowardin CA, Wilson MG, et al. Microbiota-Regulated IL-25 Increases Eosinophil Number to Provide Protection during *Clostridium difficile* Infection. *Cell Rep*. 2016;**16**(2):432-443.
122. Gagliardi G, Goswami M, Passera R, et al. DCLK1 immunoreactivity in colorectal neoplasia. *Clin Exp Gastroenterol*. 2012;**5**:35-42.
123. Nakanishi Y, Seno H, Fukuoka A, et al. Delk1 distinguishes between tumor and normal stem cells in the intestine. *Nat Genet*. 2013;**45**(1):98-103.
124. Kang Z, Swaidani S, Yin W, et al. Epithelial cell-specific Act1 adaptor mediates interleukin-25-dependent helminth expulsion through expansion of Lin(-)c-Kit(+) innate cell population. *Immunity*. 2012;**36**(5):821-833.
125. Gerbe F, Jay P. Intestinal tuft cells: epithelial sentinels linking luminal cues to the immune system. *Mucosal Immunology*. 2016;**9**(6):1353-1359.
126. Urban JF, Jr., Noben-Trauth N, Donaldson DD, et al. IL-13, IL-4Ralpha, and Stat6 are required for the expulsion of the gastrointestinal nematode parasite *Nippostrongylus brasiliensis*. *Immunity*. 1998;**8**(2):255-264.
127. Yi J, Bergstrom K, Fu J, et al. Delk1 in tuft cells promotes inflammation-driven epithelial restitution and mitigates chronic colitis. *Cell Death Differ*. 2019;**26**(9):1656-1669.
128. Qu D, Weygant N, May R, et al. Ablation of Doublecortin-Like Kinase 1 in the Colonic Epithelium Exacerbates Dextran Sulfate Sodium-Induced Colitis. *PLoS One*. 2015;**10**(8):e0134212.
129. Rieder F, Brenmoehl J, Leeb S, et al. Wound healing and fibrosis in intestinal disease. *Gut*. 2007;**56**(1):130-139.
130. Heller F, Florian P, Bojarski C, et al. Interleukin-13 is the key effector Th2 cytokine in ulcerative colitis that affects epithelial tight junctions, apoptosis, and cell restitution. *Gastroenterology*. 2005;**129**(2):550-564.
131. Sturm A, Dignass AU. Epithelial restitution and wound healing in inflammatory bowel disease. *World J Gastroenterol*. 2008;**14**(3):348-353.

132. Kiesler P, Fuss IJ, Strober W. Experimental Models of Inflammatory Bowel Diseases. *Cell Mol Gastroenterol Hepatol*. 2015;**1**(2):154-170.
133. Pizarro TT, Pastorelli L, Bamias G, et al. SAMP1/YitFc mouse strain: a spontaneous model of Crohn's disease-like ileitis. *Inflamm Bowel Dis*. 2011;**17**(12):2566-2584.
134. Cominelli F, Arseneau KO, Rodriguez-Palacios A, et al. Uncovering Pathogenic Mechanisms of Inflammatory Bowel Disease Using Mouse Models of Crohn's Disease-Like Ileitis: What is the Right Model? *Cell Mol Gastroenterol Hepatol*. 2017;**4**(1):19-32.
135. Wilk JN, Bilsborough J, Viney JL. The *mdr1a*^{-/-} mouse model of spontaneous colitis: a relevant and appropriate animal model to study inflammatory bowel disease. *Immunol Res*. 2005;**31**(2):151-159.
136. Elson CO, Cong Y, Sundberg J. The C3H/HeJBir mouse model: a high susceptibility phenotype for colitis. *Int Rev Immunol*. 2000;**19**(1):63-75.
137. Eden K. Adoptive Transfer Colitis. *Methods Mol Biol*. 2019;**1960**:207-214.
138. Mizoguchi A, Takeuchi T, Himuro H, et al. Genetically engineered mouse models for studying inflammatory bowel disease. *J Pathol*. 2016;**238**(2):205-219.
139. Bamias G, Arseneau KO, Cominelli F. Mouse models of inflammatory bowel disease for investigating mucosal immunity in the intestine. *Curr Opin Gastroenterol*. 2017;**33**(6):411-416.
140. Chassaing B, Aitken JD, Malleshappa M, et al. Dextran sulfate sodium (DSS)-induced colitis in mice. *Curr Protoc Immunol*. 2014;**104**:15.25.11-15.25.14.
141. Eichele DD, Kharbanda KK. Dextran sodium sulfate colitis murine model: An indispensable tool for advancing our understanding of inflammatory bowel diseases pathogenesis. *World J Gastroenterol*. 2017;**23**(33):6016-6029.
142. Viernes DR, Choi LB, Kerr WG, et al. Discovery and development of small molecule SHIP phosphatase modulators. *Med Res Rev*. 2014;**34**(4):795-824.
143. Le Coq J, Camacho-Artacho M, Velázquez JV, et al. Structural basis for interdomain communication in SHIP2 providing high phosphatase activity. *Elife*. 2017;**6**.
144. Fruman DA, Meyers RE, Cantley LC. Phosphoinositide kinases. *Annu Rev Biochem*. 1998;**67**:481-507.
145. Jean S, Kiger AA. Classes of phosphoinositide 3-kinases at a glance. *J Cell Sci*. 2014;**127**(Pt 5):923-928.
146. Yang J, Nie J, Ma X, et al. Targeting PI3K in cancer: mechanisms and advances in clinical trials. *Molecular Cancer*. 2019;**18**(1):26.
147. Yu X, Long YC, Shen HM. Differential regulatory functions of three classes of phosphatidylinositol and phosphoinositide 3-kinases in autophagy. *Autophagy*. 2015;**11**(10):1711-1728.
148. Hawkins PT, Stephens LR. PI3K signalling in inflammation. *Biochimica et biophysica acta*. 2015;**1851**(6):882-897.
149. Iershov A, Nemazanyy I, Alkhoury C, et al. The class 3 PI3K coordinates autophagy and mitochondrial lipid catabolism by controlling nuclear receptor PPAR α . *Nature Communications*. 2019;**10**(1):1566.
150. Vanhaesebroeck B, Guillermet-Guibert J, Graupera M, et al. The emerging mechanisms of isoform-specific PI3K signalling. *Nature reviews Molecular cell biology*. 2010;**11**(5):329-341.

151. Cantley LC. The phosphoinositide 3-kinase pathway. *Science*. 2002;**296**(5573):1655-1657.
152. Vanhaesebroeck B, Leevers SJ, Ahmadi K, et al. Synthesis and function of 3-phosphorylated inositol lipids. *Annual review of biochemistry*. 2001;**70**:535-602.
153. Taylor V, Wong M, Brandts C, et al. 5' phospholipid phosphatase SHIP-2 causes protein kinase B inactivation and cell cycle arrest in glioblastoma cells. *Mol Cell Biol*. 2000;**20**(18):6860-6871.
154. Veillette A, Latour S, Davidson D. Negative regulation of immunoreceptor signaling. *Annu Rev Immunol*. 2002;**20**:669-707.
155. Dobranowski P, Sly LM. SHIP negatively regulates type II immune responses in mast cells and macrophages. *J Leukoc Biol*. 2018.
156. Franke TF, Kaplan DR, Cantley LC, et al. Direct regulation of the Akt proto-oncogene product by phosphatidylinositol-3,4-bisphosphate. *Science*. 1997;**275**(5300):665-668.
157. Ma K, Cheung SM, Marshall AJ, et al. PI(3,4,5)P3 and PI(3,4)P2 levels correlate with PKB/akt phosphorylation at Thr308 and Ser473, respectively; PI(3,4)P2 levels determine PKB activity. *Cell Signal*. 2008;**20**(4):684-694.
158. Sewell GW, Marks DJ, Segal AW. The immunopathogenesis of Crohn's disease: a three-stage model. *Curr Opin Immunol*. 2009;**21**(5):506-513.
159. Krystal G, Damen JE, Helgason CD, et al. SHIPs ahoy. *Int J Biochem Cell Biol*. 1999;**31**(10):1007-1010.
160. Erneux C, Govaerts C, Communi D, et al. The diversity and possible functions of the inositol polyphosphate 5-phosphatases. *Biochim Biophys Acta*. 1998;**1436**(1-2):185-199.
161. Kerr WG. Inhibitor and activator: dual functions for SHIP in immunity and cancer. *Ann N Y Acad Sci*. 2011;**1217**:1-17.
162. Miletic AV, Anzelon-Mills AN, Mills DM, et al. Coordinate suppression of B cell lymphoma by PTEN and SHIP phosphatases. *J Exp Med*. 2010;**207**(11):2407-2420.
163. Sleeman MW, Wortley KE, Lai KM, et al. Absence of the lipid phosphatase SHIP2 confers resistance to dietary obesity. *Nat Med*. 2005;**11**(2):199-205.
164. Fernandes S, Srivastava N, Sudan R, et al. SHIP1 Deficiency in Inflammatory Bowel Disease Is Associated With Severe Crohn's Disease and Peripheral T Cell Reduction. *Front Immunol*. 2018;**9**:1100.
165. Barrett JC, Hansoul S, Nicolae DL, et al. Genome-wide association defines more than 30 distinct susceptibility loci for Crohn's disease. *Nat Genet*. 2008;**40**(8):955-962.
166. Ngoh EN, Brugger HK, Monajemi M, et al. The Crohn's disease-associated polymorphism in ATG16L1 (rs2241880) reduces SHIP gene expression and activity in human subjects. *Genes Immun*. 2015;**16**(7):452-461.
167. Ngoh EN, Weisser SB, Lo Y, et al. Activity of SHIP, Which Prevents Expression of Interleukin 1 β , Is Reduced in Patients With Crohn's Disease. *Gastroenterology*. 2016;**150**(2):465-476.
168. Somasundaram R, Fernandes S, Deuring JJ, et al. Analysis of SHIP1 expression and activity in Crohn's disease patients. *PLoS One*. 2017;**12**(8):e0182308.
169. Helgason CD, Damen JE, Rosten P, et al. Targeted disruption of SHIP leads to hemopoietic perturbations, lung pathology, and a shortened life span. *Genes Dev*. 1998;**12**(11):1610-1620.

170. Haddon DJ, Antignano F, Hughes MR, et al. SHIP1 is a repressor of mast cell hyperplasia, cytokine production, and allergic inflammation in vivo. *J Immunol*. 2009;**183**(1):228-236.
171. McLarren KW, Cole AE, Weisser SB, et al. SHIP-deficient mice develop spontaneous intestinal inflammation and arginase-dependent fibrosis. *Am J Pathol*. 2011;**179**(1):180-188.
172. Kerr WG, Park MY, Maubert M, et al. SHIP deficiency causes Crohn's disease-like ileitis. *Gut*. 2011;**60**(2):177-188.
173. Saam JR, Gordon JI. Inducible gene knockouts in the small intestinal and colonic epithelium. *J Biol Chem*. 1999;**274**(53):38071-38082.
174. Frisbee AL, Saleh MM, Young MK, et al. IL-33 drives group 2 innate lymphoid cell-mediated protection during *Clostridium difficile* infection. *Nature Communications*. 2019;**10**(1):2712.
175. May R, Qu D, Weygant N, et al. Brief report: Dclk1 deletion in tuft cells results in impaired epithelial repair after radiation injury. *Stem Cells*. 2014;**32**(3):822-827.
176. Wei B, Zhang R, Zhai J, et al. Suppression of Th17 Cell Response in the Alleviation of Dextran Sulfate Sodium-Induced Colitis by Ganoderma lucidum Polysaccharides. *J Immunol Res*. 2018;**2018**:2906494.
177. Arai Y, Takanashi H, Kitagawa H, et al. Involvement of interleukin-1 in the development of ulcerative colitis induced by dextran sulfate sodium in mice. *Cytokine*. 1998;**10**(11):890-896.
178. Yang F, Wang D, Li Y, et al. Th1/Th2 Balance and Th17/Treg-Mediated Immunity in relation to Murine Resistance to Dextran Sulfate-Induced Colitis. *J Immunol Res*. 2017;**2017**:7047201.
179. Zhu J, Wang Y, Yang F, et al. IL-33 alleviates DSS-induced chronic colitis in C57BL/6 mice colon lamina propria by suppressing Th17 cell response as well as Th1 cell response. *Int Immunopharmacol*. 2015;**29**(2):846-853.
180. Yan Y, Kolachala V, Dalmaso G, et al. Temporal and spatial analysis of clinical and molecular parameters in dextran sodium sulfate induced colitis. *PLoS One*. 2009;**4**(6):e6073.
181. CHO O, Jeong Y-J, Heo T-H. TNF targeting small molecule attenuates colonic inflammation in acute DSS-induced colitis mice. *The Journal of Immunology*. 2019;**202**(1 Supplement):52.11-52.11.
182. Xiao YT, Yan WH, Cao Y, et al. Neutralization of IL-6 and TNF- α ameliorates intestinal permeability in DSS-induced colitis. *Cytokine*. 2016;**83**:189-192.
183. Noti M, Corazza N, Mueller C, et al. TNF suppresses acute intestinal inflammation by inducing local glucocorticoid synthesis. *J Exp Med*. 2010;**207**(5):1057-1066.
184. Li B, Alli R, Vogel P, et al. IL-10 modulates DSS-induced colitis through a macrophage-ROS-NO axis. *Mucosal Immunol*. 2014;**7**(4):869-878.
185. Wang K, Han G, Dou Y, et al. Opposite role of tumor necrosis factor receptors in dextran sulfate sodium-induced colitis in mice. *PLoS One*. 2012;**7**(12):e52924.
186. Naito Y, Takagi T, Handa O, et al. Enhanced intestinal inflammation induced by dextran sulfate sodium in tumor necrosis factor-alpha deficient mice. *J Gastroenterol Hepatol*. 2003;**18**(5):560-569.

187. Camelo A, Barlow JL, Drynan LF, et al. Blocking IL-25 signalling protects against gut inflammation in a type-2 model of colitis by suppressing nuocyte and NKT derived IL-13. *J Gastroenterol*. 2012;**47**(11):1198-1211.
188. McHenga SS, Wang D, Li C, et al. Inhibitory effect of recombinant IL-25 on the development of dextran sulfate sodium-induced experimental colitis in mice. *Cell Mol Immunol*. 2008;**5**(6):425-431.
189. Owyang AM, Zaph C, Wilson EH, et al. Interleukin 25 regulates type 2 cytokine-dependent immunity and limits chronic inflammation in the gastrointestinal tract. *J Exp Med*. 2006;**203**(4):843-849.
190. Caruso R, Sarra M, Stolfi C, et al. Interleukin-25 inhibits interleukin-12 production and Th1 cell-driven inflammation in the gut. *Gastroenterology*. 2009;**136**(7):2270-2279.
191. Rizzo A, Monteleone I, Fina D, et al. Inhibition of colitis by IL-25 associates with induction of alternatively activated macrophages. *Inflamm Bowel Dis*. 2012;**18**(3):449-459.
192. Wang A-J, Smith A, Li Y, et al. Genetic deletion of IL-25 (IL-17E) confers resistance to dextran sulfate sodium-induced colitis in mice. *Cell & Bioscience*. 2014;**4**(1):72.
193. McHenga SS, Wang D, Janneh FM, et al. Differential dose effects of recombinant IL-25 on the development of dextran sulfate sodium-induced colitis. *Inflamm Res*. 2010;**59**(10):879-887.
194. Kim MR, Manoukian R, Yeh R, et al. Transgenic overexpression of human IL-17E results in eosinophilia, B-lymphocyte hyperplasia, and altered antibody production. *Blood*. 2002;**100**(7):2330-2340.
195. Pan G, French D, Mao W, et al. Forced expression of murine IL-17E induces growth retardation, jaundice, a Th2-biased response, and multiorgan inflammation in mice. *J Immunol*. 2001;**167**(11):6559-6567.
196. Weisser SB, Brugger HK, Voglmaier NS, et al. SHIP-deficient, alternatively activated macrophages protect mice during DSS-induced colitis. *J Leukoc Biol*. 2011;**90**(3):483-492.
197. Kuroda E, Ho V, Ruschmann J, et al. SHIP Represses the Generation of IL-3-Induced M2 Macrophages by Inhibiting IL-4 Production from Basophils. *The Journal of Immunology*. 2009;**183**(6):3652.
198. Stevceva L, Pavli P, Husband A, et al. Dextran sulphate sodium-induced colitis is ameliorated in interleukin 4 deficient mice. *Genes Immun*. 2001;**2**(6):309-316.
199. Stevceva L, Pavli P, Husband A, et al. Eosinophilia is attenuated in experimental colitis induced in IL-5 deficient mice. *Genes Immun*. 2000;**1**(3):213-218.
200. Shajib MS, Wang H, Kim JJ, et al. Interleukin 13 and serotonin: linking the immune and endocrine systems in murine models of intestinal inflammation. *PLoS One*. 2013;**8**(8):e72774.
201. Karnele EP, Pasricha TS, Ramalingam TR, et al. Anti-IL-13R α 2 therapy promotes recovery in a murine model of inflammatory bowel disease. *Mucosal Immunology*. 2019;**12**(5):1174-1186.
202. Biancheri P, Di Sabatino A, Ammoscato F, et al. Absence of a role for interleukin-13 in inflammatory bowel disease. *Eur J Immunol*. 2014;**44**(2):370-385.
203. Tilg H, Kaser A. Failure of interleukin 13 blockade in ulcerative colitis. *Gut*. 2015;**64**(6):857-858.

204. Zhu J, Yang F, Sang L, et al. IL-33 Aggravates DSS-Induced Acute Colitis in Mouse Colon Lamina Propria by Enhancing Th2 Cell Responses. *Mediators Inflamm.* 2015;**2015**:913041.
205. Schneider C, O'Leary CE, von Moltke J, et al. A Metabolite-Triggered Tuft Cell-ILC2 Circuit Drives Small Intestinal Remodeling. *Cell.* 2018;**174**(2):271-284.e214.
206. McKinley ET, Sui Y, Al-Kofahi Y, et al. Optimized multiplex immunofluorescence single-cell analysis reveals tuft cell heterogeneity. *JCI Insight.* 2017;**2**(11).
207. Castro-Dopico T, Colombel JF, Mehandru S. Targeting B cells for inflammatory bowel disease treatment: back to the future. *Curr Opin Pharmacol.* 2020;**55**:90-98.
208. Lyons J, Ghazi PC, Starchenko A, et al. The colonic epithelium plays an active role in promoting colitis by shaping the tissue cytokine profile. *PLoS Biol.* 2018;**16**(3):e2002417.
209. Gonzalez-Angulo AM, Fuloria J, Prakash O. Cyclooxygenase 2 inhibitors and colon cancer. *Ochsner J.* 2002;**4**(3):176-179.
210. Singer, II, Kawka DW, Schloemann S, et al. Cyclooxygenase 2 is induced in colonic epithelial cells in inflammatory bowel disease. *Gastroenterology.* 1998;**115**(2):297-306.
211. Miyoshi H, VanDussen KL, Malvin NP, et al. Prostaglandin E2 promotes intestinal repair through an adaptive cellular response of the epithelium. *Embo j.* 2017;**36**(1):5-24.
212. Jensen TSR, Mahmood B, Damm MB, et al. Combined activity of COX-1 and COX-2 is increased in non-neoplastic colonic mucosa from colorectal neoplasia patients. *BMC Gastroenterology.* 2018;**18**(1):31.
213. Wang D, Dubois RN. The role of COX-2 in intestinal inflammation and colorectal cancer. *Oncogene.* 2010;**29**(6):781-788.
214. Tessner TG, Cohn SM, Schloemann S, et al. Prostaglandins prevent decreased epithelial cell proliferation associated with dextran sodium sulfate injury in mice. *Gastroenterology.* 1998;**115**(4):874-882.
215. Cohn SM, Schloemann S, Tessner T, et al. Crypt stem cell survival in the mouse intestinal epithelium is regulated by prostaglandins synthesized through cyclooxygenase-1. *J Clin Invest.* 1997;**99**(6):1367-1379.
216. Fredenburgh LE, Velandia MM, Ma J, et al. Cyclooxygenase-2 deficiency leads to intestinal barrier dysfunction and increased mortality during polymicrobial sepsis. *J Immunol.* 2011;**187**(10):5255-5267.
217. Reuter BK, Asfaha S, Buret A, et al. Exacerbation of inflammation-associated colonic injury in rat through inhibition of cyclooxygenase-2. *J Clin Invest.* 1996;**98**(9):2076-2085.
218. Okayama M, Hayashi S, Aoi Y, et al. Aggravation by Selective COX-1 and COX-2 Inhibitors of Dextran Sulfate Sodium (DSS)-Induced Colon Lesions in Rats. *Digestive Diseases and Sciences.* 2007;**52**(9):2095-2103.
219. Tanaka K-I, Suemasu S, Ishihara T, et al. Inhibition of both COX-1 and COX-2 and resulting decrease in the level of prostaglandins E2 is responsible for non-steroidal anti-inflammatory drug (NSAID)-dependent exacerbation of colitis. *European Journal of Pharmacology.* 2009;**603**(1):120-132.
220. Allgayer H, Deschryver K, Stenson WF. Treatment with 16,16'-dimethyl prostaglandin E2 before and after induction of colitis with trinitrobenzenesulfonic acid in rats decreases inflammation. *Gastroenterology.* 1989;**96**(5 Pt 1):1290-1300.

221. Peng X, Li J, Tan S, et al. COX-1/PGE2/EP4 alleviates mucosal injury by upregulating β -arr1-mediated Akt signaling in colitis. *Scientific Reports*. 2017;**7**(1):1055.
222. Lo Sasso G, Phillips BW, Sewer A, et al. The reduction of DSS-induced colitis severity in mice exposed to cigarette smoke is linked to immune modulation and microbial shifts. *Scientific Reports*. 2020;**10**(1):3829.
223. Lu J, Dong B, Chen A, et al. Escherichia coli promotes DSS-induced murine colitis recovery through activation of the TLR4/NF- κ B signaling pathway. *Mol Med Rep*. 2019;**19**(3):2021-2028.
224. Aladegbami B, Barron L, Bao J, et al. Epithelial cell specific Raptor is required for initiation of type 2 mucosal immunity in small intestine. *Scientific Reports*. 2017;**7**(1):5580.
225. Lindholm HT, Parmar N, Drurey C, et al. Developmental pathways regulate cytokine-driven effector and feedback responses in the intestinal epithelium. *bioRxiv*. 2020:2020.2006.2019.160747.
226. Luo X-C, Chen Z-H, Xue J-B, et al. Infection by the parasitic helminth *Trichinella spiralis* activates a Tas2r-mediated signaling pathway in intestinal tuft cells. *Proceedings of the National Academy of Sciences*. 2019;**116**(12):5564.